



Final Technical Report for USGS Award No. G14AP00031

**Development and Evaluation of Simplified Performance-Based Procedures for
the Estimation of Liquefaction-Induced Lateral Spread Displacements and
Seismic Slope Displacements**

**Kevin W. Franke
Levi T. Ekstrom
Lucy Astorga**

**Brigham Young University
368P Clyde Building
Provo, UT 84602
Ph: 801-422-1349
Fax: 801-422-0159**

Period of Performance: March 1, 2014 to August 31, 2015

Report Date: January 8, 2015

DISCLAIMER

The authors alone are responsible for the preparation and accuracy of the information, data, analysis, discussions, recommendations, and conclusions presented herein. The contents do not necessarily reflect the views, opinions, endorsements, or policies of the United States Geological Survey (USGS). The USGS makes no representation or warranty of any kind, and assumes no liability therefore.

ACKNOWLEDGMENTS

The authors acknowledge the USGS for funding this. The views and opinions presented in this report represent those of its authors, and may not represent those of the agency funding this research.

TABLE OF CONTENTS

LIST OF TABLES	iv
LIST OF FIGURES	v
ABSTRACT.....	8
1.0 INTRODUCTION	10
1.1 Objectives	10
1.2 Scope.....	10
1.3 Outline of Report	10
2.0 DERIVATION OF THE SIMPLIFIED MODELS	11
2.1 Overview.....	11
2.2 Empirical Lateral Spread Displacement Models	11
2.2.1 Youd et al (2002) Empirical Model	11
2.2.2 Bardet et al (2002) Empirical Model	17
2.3 Empirical Seismic Slope Stability Models	19
2.3.1 Rathje and Saygili (2009) Model	19
2.3.2 Bray and Travararou (2007) Model	20
2.3.3 Performance-based Implementation of Seismic Slope Displacement Models	20
2.3.4 Simplified Performance-Based Seismic Slope Displacement Procedure	21
2.4 Summary	23
3.0 VALIDATION OF THE SIMPLIFIED MODELS	24
3.1 Overview.....	24
3.1.1 Sites used in the Analysis	24
3.2 Simplified Lateral Spread Displacement Model Validation.....	24
3.2.1 EZ-FRISK	25
3.2.2 Comparison of Results	25
3.3 Validation of the Seismic Slope Stability Models	28
3.4 Summary	32
4.0 EVALUATION OF GRID SPACING.....	38
4.1 Overview	38
4.2 Grid-Spacing Evaluation.....	38
4.2.1 Methodology	38

4.3 Summary	45
5.0 MAP DEVELOPMENT	46
5.1 Overview	46
5.2 Creating the Grid Points	46
5.3 Analysis of the Grid Points	47
5.3.1 Analysis of the Lateral Spread Displacement Model Grid Points	47
5.3.2 Analysis of the Seismic Slope Stability Model Grid Points	48
5.4 Creation of the Maps	48
5.5 Summary	49
6.0 COMPARISON OF PROBABILISTIC AND DETERMINISTIC ANALYSES	51
6.1 Overview	51
6.2 Methodology	51
6.2.1 Simplified Performance-Based Seismic Hazard Analysis	51
6.2.2 Deterministic Procedure	52
6.2.3 Pseudo-probabilistic Seismic Hazard Analysis	54
6.3 Results	55
6.3.1 Empirical Lateral Spread Displacement Model	55
6.3.2 Empirical Seismic Slope Displacement Model	57
6.4 Summary	59
7.0 CONCLUSIONS	61
7.1 Summary	61
7.2 Findings	61
7.2.1 Derivation of the Simplified Procedures	61
7.2.2 Validation of the Simplified Procedures	61
7.2.3 Evaluation of Grid Spacing	61
7.2.4 Map Development	62
7.2.5 Comparison with Deterministic Procedures	62
REFERENCES	63
APPENDIX A: Supplementary Validation Data	65
APPENDIX B: Sample Lateral Spread Parameter Maps	69
APPENDIX C: Sample Seismic Slope Displacement Maps	82

LIST OF TABLES

Table 2-1 Regression coefficients for the Youd et al. (2002) empirical lateral spread model	12
Table 2-2 Site-specific geometry coefficients for computing the adjustment factor, ΔD_H	17
Table 2-3 Regression coefficients for the Bardet et al. (2002) empirical lateral spread model	17
Table 2-4 Site-specific geometry coefficients for computing the adjustment factor, ΔD	19
Table 3-1 Locations used for the validation of the simplified models	24
Table 3-2 Lateral spread displacements (m) for the site specific analysis using the two models for the three desired return periods (Youd et al (2002)).	26
Table 3-3 Lateral spread displacements (m) for the site specific analysis using the two models for the three desired return periods (Bardet et al (2002)).	26
Table 3-4: Summary of Magnitude, PGA and f_a site used for each city used in the validation	29
Table 4-1 Proposed Grid Spacing for Lateral Spread Displacement Reference Parameter Maps Based on Mapped USGS <i>PGA</i>	43
Table 4-2 Proposed Grid Spacing for Seismic Slope Displacement Reference Parameter Maps Based on Mapped USGS <i>PGA</i>	45
Table 6-1 NGA model weights used in the deterministic procedure.....	53
Table 6-2 Input variables used in the deterministic models (a_{max} calculated using F_{pga} from AASHTO code).	53
Table 6-3 Input values found using USGS 2008 Deaggregation ($T_R = 475$ years).	54
Table 6-4 Input values found using USGS 2008 Deaggregation (TR = 2475 years).	55

LIST OF FIGURES

Figure 2-1 Schematic diagram of the fully probabilistic lateral spread model with Youd et al. (2002) (after Franke and Kramer 2014).....	13
Figure 2-2 Variations of lateral spread hazard curves as a function of the site term, \mathcal{S} (after Kramer et al. 2007)	14
Figure 2-3 Reference soil profile used to derive the simplified performance-based lateral spread approximation	15
Figure 3-1 Site-specific soil profile used in the simplified lateral spread displacement model validation.....	25
Figure 3-2 Comparison of lateral spread displacements for the simplified and full performance-based models for the Youd et al (2002) model.	27
Figure 3-3 Comparison of lateral spread displacements for the simplified and full performance-based models for the Bardet et al (2002) model.	28
Figure 3-4 Comparison of seismic slope displacements for the simplified and full performance-based models based on Rathje and Saygili (2009).....	30
Figure 3-5 Comparison of seismic slope displacements for the simplified and full performance-based models based on Bray and Travarasrou (2007).....	31
Figure 4-1 Layout of grid points centered on city's anchor point.	39
Figure 4-2 Range of PGA values for cities included in final grid spacing study.....	40
Figure 4-3 USGS 2008 PGA hazard map ($T_r = 2475$ years).....	41
Figure 4-4 Correlation between PGA and optimum grid spacing to achieve 5% maximum absolute percent error for predicted lateral spread displacement.....	42
Figure 4-5 Correlation between PGA and optimum grid spacing to achieve 5% maximum absolute percent error for predicted seismic slope displacement.....	44
Figure 5-1 Grid points for Utah combined with USGS 2008 PGA hazard map.....	47
Figure 5-2 a) Kriging raster and b) contours for Utah ($T_r = 2475$ yrs).....	48
Figure 5-3 D_H^{ref} for Utah ($T_r = 2475$ years).....	49
Figure 6-1 Soil profile used for the lateral spread displacement comparison study.	52
Figure 6-2 Comparison of Deterministic, Pseudo-probabilistic, and Simplified methods for Butte, MT (Latitude 46.033, Longitude -112.533).....	56

Figure 6-3 Comparison of Deterministic, Pseudo-probabilistic, and Simplified methods for Salt Lake City, UT (Latitude 40.755, Longitude -111.898).....	56
Figure 6-4 Comparison of Deterministic, Pseudo-probabilistic, and Simplified methods for San Francisco, CA (Latitude 37.775, Longitude -122.418).....	57
Figure 6-5 Comparison of Deterministic, Pseudo-probabilistic, and Simplified methods for Butte, MT (Latitude 46.033, Longitude -112.533).....	58
Figure 6-6 Comparison of Deterministic, Pseudo-probabilistic, and Simplified methods for Salt Lake City, UT (Latitude 40.755, Longitude -111.898).....	58
Figure 6-7 Comparison of Deterministic, Pseudo-probabilistic, and Simplified methods for San Francisco, CA (Latitude 37.775, Longitude -122.418).....	59
Figure B- 1 Lateral Spread Parameter (D_H^{ref}) Map for Montana (Tr = 475)	70
Figure B- 2 Lateral Spread Parameter (D_H^{ref}) Map for Montana (Tr = 2,475)	71
Figure B- 3 Lateral Spread Parameter (D_H^{ref}) Map for Montana (Tr = 475)	72
Figure B- 4 Lateral Spread Parameter (D_H^{ref}) Map for Montana (Tr = 2,475)	73
Figure B- 5 Lateral Spread Parameter (D_H^{ref}) Map for Utah (Tr = 475).....	74
Figure B- 6 Lateral Spread Parameter (D_H^{ref}) Map for Utah (Tr = 2,475).....	75
Figure B- 7 Lateral Spread Parameter (D_H^{ref}) Map for Utah (Tr = 475).....	76
Figure B- 8 Lateral Spread Parameter (D_H^{ref}) Map for Utah (Tr = 2,475).....	77
Figure B- 9 Lateral Spread Parameter (D_H^{ref}) Map for Northern California (Tr = 475).....	78
Figure B- 10 Lateral Spread Parameter (D_H^{ref}) Map for Northern California (Tr = 2,475).....	79
Figure B- 11 Lateral Spread Parameter (D_H^{ref}) Map for Northern California (Tr = 475).....	80
Figure B- 12 Lateral Spread Parameter (D_H^{ref}) Map for Northern California (Tr = 2,475).....	81
Figure C- 1 Seismic Slope Displacement (D^{ref}) Map for Montana (Tr = 475)	83
Figure C- 2 Seismic Slope Displacement (D^{ref}) Map for Montana (Tr = 2,475)	84
Figure C- 3 Seismic Slope Displacement (D^{ref}) Map for Montana (Tr = 475)	85
Figure C- 4 Seismic Slope Displacement (D^{ref}) Map for Montana (Tr = 2,475)	86
Figure C- 5 Seismic Slope Displacement (D^{ref}) Map for Utah (Tr = 475).....	87
Figure C- 6 Seismic Slope Displacement (D^{ref}) Map for Utah (Tr = 2,475).....	88

Figure C- 7 Seismic Slope Displacement (D^{ref}) Map for Utah (Tr = 475).....	89
Figure C- 8 Seismic Slope Displacement (D^{ref}) Map for Utah (Tr = 2,475).....	90
Figure C- 9 Seismic Slope Displacement (D^{ref}) Map for Northern California (Tr = 475)	91
Figure C- 10 Seismic Slope Displacement (D^{ref}) Map for Northern California (Tr = 2,475)	92
Figure C- 11 Seismic Slope Displacement (D^{ref}) Map for Northern California (Tr = 475)	93
Figure C- 12 Seismic Slope Displacement (D^{ref}) Map for Northern California (Tr = 2,475)	94

ABSTRACT

One of the 2013 research priorities for the Earthquake Effects (EE) research area is to “improve techniques for ground-failure susceptibility and hazard assessment...[and to] develop and apply methods for probabilistic mapping of liquefaction and other types of failure.” In response to this priority, the proposed research objective of this project is to create and evaluate simplified performance-based design procedures for the *a priori* prediction of lateral spread displacement and seismic slope displacement. To achieve this objective, the following tasks are proposed: (1) Derive multiple simplified models to approximate the results of full performance-based lateral spread and seismic slope displacement procedures at a targeted hazard level; (2) Evaluate the simplified performance-based models in three separate seismic environments: high seismicity (Northern California), moderate seismicity (Utah), and Low Seismicity (Montana) at two return periods; and (3) Test the simplified performance-based models against full performance-based, conventional (i.e. pseudo-probabilistic), and deterministic models to identify strengths and correct any significant weaknesses.

The potential for damage from lateral spread and seismic slope displacement is a major concern for geotechnical and structural engineers throughout seismically active areas of the United States. Liquefaction-induced lateral spread displacement and seismic slope displacement are earthquake effects that have significantly impacted critical components of infrastructure in the past including bridges, ports, roads, lifelines, and building foundations. Millions of dollars are spent annually to analyze and mitigate these hazards for both new construction and retrofit of existing structures, but these analyses are typically performed in a subjective deterministic or pseudo-probabilistic manner. Alternatively, the relatively recent development and continual refinement of the performance-based earthquake engineering (PBEE) concept provides engineers the tools and procedures necessary to make objective decisions based on anticipated structural performance and/or anticipated losses for a given level of risk. Recent advances in PBEE in geotechnical engineering have introduced risk-based procedures to evaluate liquefaction, lateral spread displacement, and seismic slope displacement in a performance-based framework from which the likelihood of exceeding various levels of hazard within a given time frame can be computed. However, the ability to apply these full performance-based procedures on everyday projects remains well beyond the capabilities of most practicing engineers due to the complex nature of the procedures, the engineers’ lack of familiarity with probabilistic methods, and the specialized computational tools required for proper implementation. Therefore, without additional resources and/or simplification, these and other future performance-based analysis procedures for evaluating various geotechnical-related seismic phenomena will largely remain unutilized by the geotechnical engineering community.

The simplified performance-based design procedures developed and tested through this research will provide the geotechnical engineering community with a user-friendly approach to develop uniform hazard estimates of liquefaction-induced lateral spread displacements and seismic slope displacements. Despite their simplicity, the performance-based procedures developed through this research will be powerful and will allow the average engineer to assess lateral spread and seismic slope displacement in terms of uniform hazard and probability. Such procedures would enhance the design engineer’s ability to make logical and objective decisions based on likelihoods, not just possibilities. Furthermore, this research is intended to serve as a pilot study for assessing the feasibility of implementing the simplified probabilistic lateral spread and seismic slope displacement procedures on a national scale through the USGS National Seismic Hazard Mapping Project (NSHMP). The simplified performance-based procedures will be designed to be compatible with modern seismic building codes, which are increasingly incorporating more and more aspects of PBEE and provide little to no specific guidance for geotechnical engineers who desire to assess seismic ground deformation hazard. The simplified performance-based procedures and associated design maps developed through this research could readily be incorporated into future revisions of seismic building codes such as NEHRP, ASCE 7, IBC, and/or AASHTO. Future research with the USGS could lead to development of lateral spread and/or seismic slope displacement

maps and online computational tools allowing geotechnical engineers the ability to efficiently and consistently incorporate these performance-based approaches into their everyday designs.

1.0 INTRODUCTION

1.1 Objectives

The objective of this report is to provide simplified performance-based procedures to the members of the USGS which closely approximates the results of full probabilistic analyses for liquefaction initiation and lateral spread displacement. This was done by performing the following steps:

- Introduce the original models used to determine lateral spread displacements and seismic slope stability and provide in-depth derivations that demonstrate the development of the simplified methods
- Validate the simplified models by performing a site-specific analysis for several different sites using the simplified and full models
- Assess proper grid spacing for map development
- Create the hazard-targeted lateral spread and seismic slope stability parameter maps
- Compare the simplified procedure with deterministic methods

1.2 Scope

The states included in this research were: Montana, Northern California, and Utah. Hazard-targeted liquefaction parameter maps were developed for these states only. However, the same principles used in the simplified procedure provided in this report should apply similarly to other states. The final products of this research are: 1) a final report describing the findings of the research, 2) liquefaction parameter maps for the states mentioned at the 475 and 2475 year return periods.

1.3 Outline of Report

The research conducted for this report will contain the following:

- Derivation of the Simplified Models
- Validation of the Simplified Models
- Grid Spacing Study
- Development of the Parameter Maps
- Comparison with Deterministic Analyses
- Conclusions
- Appendices

2.0 DERIVATION OF THE SIMPLIFIED MODELS

2.1 Overview

This section describes the derivation of the simplified liquefaction triggering and lateral spread displacement models. The original models will be introduced and the derivation process for the simplified models will be described in detail.

2.2 Empirical Lateral Spread Displacement Models

The simplified lateral spread displacement models used in the study were the Youd et al (2002) and Bardet et al (2002) empirical models. Both models will be described and then the derivation of the simplified procedures will be outlined.

2.2.1 Youd et al (2002) Empirical Model

The Youd et al model is derived from the widely-used empirical lateral spread model originally presented by Bartlett and Youd (1995). Their model was regressed from a large database of lateral spread case histories from Japan and the western United States, and a large number of parameters related to soil properties, slope geometry, and level of ground motion were statistically evaluated. Bartlett and Youd identified the parameters that produced the best regression, and from those parameters regressed their original empirical predictive relationship. Youd et al. (2002) later updated their original empirical model by using an expanded and corrected version of the 1995 database. The updated Bartlett and Youd empirical model has since been adopted as the state of practice in much of the world, and it is routinely applied on a wide variety of projects in all types of seismic environments. The Youd et al. (2002) updated empirical model is given as:

$$\begin{aligned} \overline{\log D_H} = & b_0 + b_1 M + b_2 \log R^* + b_3 R + b_4 \log W + b_5 \log S \\ & + b_6 \log T_{15} + b_7 \log (100 - F_{15}) + b_8 \log (D50_{15} + 0.1) \end{aligned} \quad (1)$$

where

D_H = median computed permanent lateral spread displacement (m)

M = earthquake moment magnitude

R = the closest horizontal distance from the site to the source (km)

W = the free-face ratio (%)

S = the ground slope (%)

T_{15} = the cumulative thickness (in upper 20 m) of all saturated soil layers with corrected Standard Penetration Test (SPT) blowcounts (i.e., $(N_1)_{60}$) less than 15 blows/foot (m)

F_{15} = the average fines content of the soil comprising T_{15} (%)

$D50_{15}$ = the average mean grain size of the soil comprising T_{15} (mm)

and R^* is computed as

$$R^* = R + 10^{0.89M - 5.64} \quad (2)$$

Model coefficients b_0 through b_8 are given in Table 2-1.

Table 2-1 Regression coefficients for the Youd et al. (2002) empirical lateral spread model

Model	b_0	b_1	b_2	b_3	b_4	b_5	b_6	b_7	b_8
Ground slope	-16.213	1.532	-1.406	-0.012	0	0.338	0.540	3.413	-0.795
Free Face	-16.713	1.532	-1.406	-0.012	0.592	0	0.540	3.413	-0.795

2.2.1.1 Full Performance-based Youd et al (2002) Model

Kramer et al. (2007) suggested that performance-based estimates of lateral spread displacement could be computed by modifying an empirical lateral spreading model in such a way so as to insert it directly into a probabilistic seismic hazard analysis (PSHA). Such a modification could be performed by separating the model terms associated with seismic loading (i.e. the Loading Parameter, \mathcal{L}) from the model terms associated with local site and geometry conditions (i.e. the Site Parameter, \mathcal{S}). Therefore, a modified form of any given empirical lateral spread model could be written as:

$$\mathcal{D} = \mathcal{L} - \mathcal{S} + \varepsilon \quad (3)$$

where \mathcal{D} is the transformed (e.g. log, ln, square root) lateral spread displacement, and \mathcal{L} , \mathcal{S} , and ε represent the apparent loading, site, and uncertainty terms.

Following the Kramer et al. (2007) framework, Franke and Kramer (2014) demonstrated how the Youd et al. (2002) empirical model for lateral spread displacement could be adapted to develop fully probabilistic estimates of lateral spread displacement. The performance-based form of the Youd et al. (2002) was shown to be:

$$\log D_H = \mathcal{L} - \mathcal{S} + \varepsilon \quad (4)$$

where

$$\mathcal{L} = b_1 M + b_2 \log R^* + b_3 R \quad (5)$$

$$\mathcal{S} = -(b_0 + b_4 \log W + b_5 \log S + b_6 \log T_{15} + b_7 \log (100 - F_{15}) + b_8 \log (D50_{15} + 0.1)) \quad (6)$$

$$\varepsilon = \sigma_{\log D_H} \Phi^{-1}[P] \quad (7)$$

$$\sigma_{\log D_H} = 0.197 \quad (8)$$

If computing the probability of exceeding some given displacement, d , Equation (8) can be incorporated as:

$$P[D_H > d] = 1 - \Phi \left[\frac{\log d - \overline{\log D_H}}{\sigma_{\log D_H}} \right] = 1 - \Phi \left[\frac{\log d - \log D_H}{0.197} \right] \quad (9)$$

Because a given site should produce a single value of \mathcal{S} to be used in design, the left side of Equation (4) can be thought of as a simple linear function of \mathcal{L} with a constant y-intercept equal to \mathcal{S} and a data spread characterized by ε , as shown in Figure 2-1. Because \mathcal{S} is considered a constant value in the performance-based analysis, multiple lateral spread hazard curves could be developed for a site for different values of \mathcal{S} (Figure 2-2). Thus, the effect of varying site and/or geometry conditions when computing probabilistic lateral spread displacements could be evaluated.

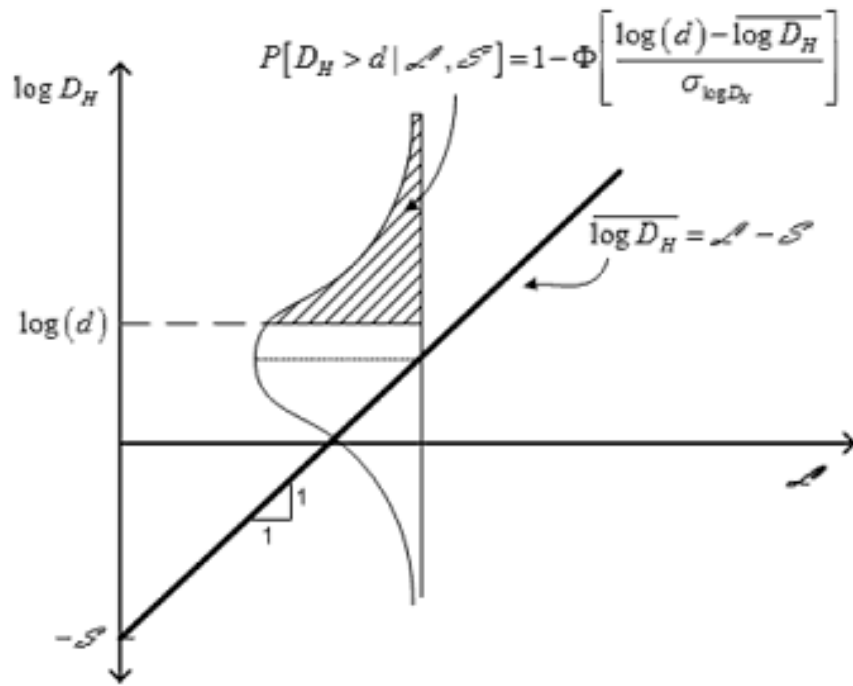


Figure 2-1 Schematic diagram of the fully probabilistic lateral spread model with Youd et al. (2002) (after Franke and Kramer 2014)

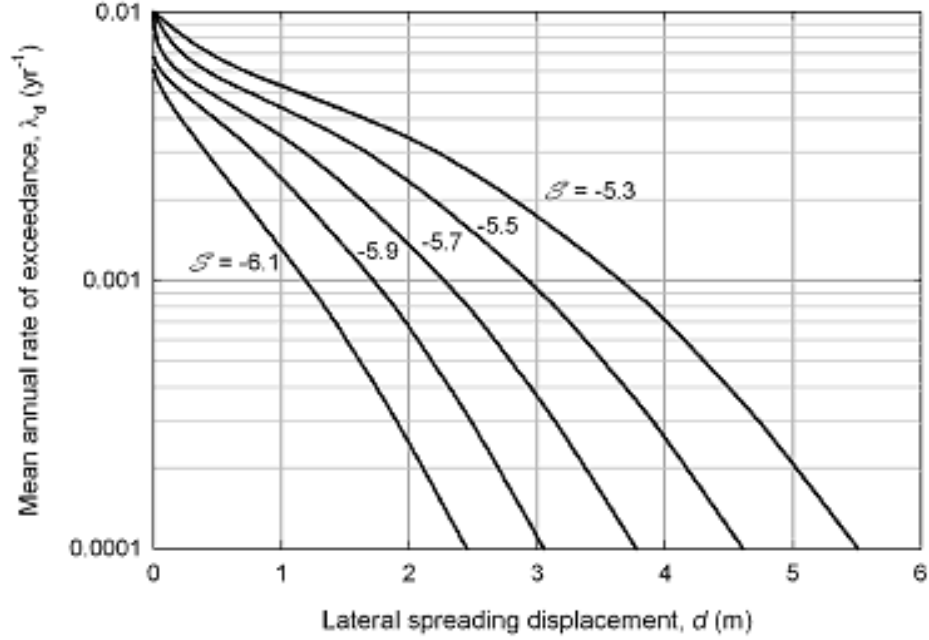


Figure 2-2 Variations of lateral spread hazard curves as a function of the site term, \mathcal{S} (after Kramer et al. 2007)

Though it is not an actual or measurable ground motion parameter, the apparent loading parameter in Equation (5) is a function of magnitude and distance and attenuates in a manner similar to measurable ground motion intensity measures described by traditional Ground Motion Prediction Equations (GMPEs). In the context of the Youd et al. (2002) model, the apparent loading term, therefore, acts in a manner analogous to an Intensity Measure (IM), the variation of whose median value with M and R is described by Equation (5).

By incorporating Equations (50) and (51) into the probabilistic framework presented in Equation (54) and assigning all of the uncertainty in the Youd et al. (2002) model to the conditional displacement calculation, a performance-based model can be expressed in terms of lateral spread displacement conditional upon the site parameter as:

$$\lambda_{D_H|\mathcal{S}}(d|\mathcal{S}) = \sum_{i=1}^{N_{\mathcal{L}}} P[D_H > d | \mathcal{S}, \mathcal{L}_i] \Delta\lambda_{\mathcal{L}_i} \quad (10)$$

where $\lambda_{D_H|\mathcal{S}}(d|\mathcal{S})$ is the mean annual rate of exceeding a displacement d conditional upon site conditions \mathcal{S} , $N_{\mathcal{L}}$ is the number of loading parameter increments required to span the range of possible \mathcal{L} values, and $\Delta\lambda_{\mathcal{L}_i}$ is the increment of the apparent loading parameter in hazard space. For a single source, Equation (10) can also be written as:

$$\lambda_{D_H|\mathcal{S}}(d|\mathcal{S}) = v \sum_{i=1}^{N_{\mathcal{L}}} P[D_H > d | \mathcal{S}, \mathcal{L}_i] P[\mathcal{L}_i] \quad (11)$$

where ν is the mean annual rate of exceeding a minimum magnitude of interest for a given seismic source. Because the loading parameter is a function of magnitude and distance (which are commonly assumed to be independent in PSHA work) and can be affected by multiple seismic sources, Equation (11) can be rewritten as:

$$\lambda_{D_H|\mathcal{S}}(d|\mathcal{S}) = \sum_{i=1}^{N_S} \nu_i \sum_{j=1}^{N_M} \sum_{k=1}^{N_R} P[D_H > d | \mathcal{S}, M = m_j, R = r_k] P[M = m_j, R = r_k] \quad (12)$$

which is very similar to the PSHA framework commonly used to compute uniform hazard estimates of ground motions. Therefore, Equations (4) through (9) can be incorporated into common seismic hazard analysis software such as EZ-FRISK or OpenSHA to develop uniform hazard estimates of lateral spread displacement and displacement hazard curves.

2.2.1.2 Simplified Performance-based Youd et al (2002) Model

If a generic reference site is used to compute \mathcal{S} , then a series of performance-based lateral spread analyses could be performed across a grid to develop contour maps of lateral spread displacement corresponding to various return periods of interest. These maps are called lateral spread reference maps. For example, a reference site for the derivation of the simplified performance-based lateral spread procedure is presented in Figure 2-3. This profile was chosen based on the profile used to develop the full performance-based method to be consistent. Values of 3.0m, 20%, and 0.2mm are computed for the lateral spread parameters T_{15} , F_{15} , and $D50_{15}$, respectively. As shown in Figure 2-3, the geometry of the site constitutes a ground slope condition with ground slope (i.e. S) equal to 1%. The resulting value of \mathcal{S} for the reference site, as computed from Equation (6), is therefore equal to 9.043.

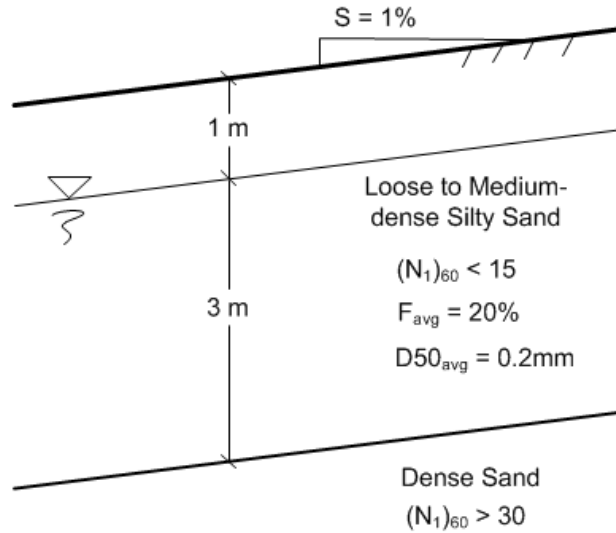


Figure 2-3 Reference soil profile used to derive the simplified performance-based lateral spread approximation

The lateral spread displacement corresponding to the generic reference site could therefore be obtained from the appropriate map and adjusted in order to provide site-specific

lateral spread displacements corresponding to the desired return period. The equation for this site-specific adjustment is given as:

$$[\log D_H]^{site} = [\log D_H]^{ref} + \Delta D_H \quad (13)$$

where $[\log D_H]^{site}$ is the logarithm of the lateral spread displacement adjusted for site-specific conditions, $[\log D_H]^{ref}$ is the logarithm of the lateral spread displacement corresponding to the reference site (obtained from the map), and ΔD_H is the adjustment factor computed by the engineer. By substituting Equation (4) into Equation (13), the adjustment factor can be written as:

$$\Delta D_H = (\mathcal{L} - \mathcal{S})^{site} - (\mathcal{L} - \mathcal{S})^{ref} = (\mathcal{L}^{site} - \mathcal{L}^{ref}) + (\mathcal{S}^{ref} - \mathcal{S}^{site}) \quad (14)$$

However, because $\mathcal{L}^{site} = \mathcal{L}^{ref}$, Equation (14) can be simplified as:

$$\Delta D_H = \mathcal{S}^{ref} - \mathcal{S}^{site} \quad (15)$$

If Equation (6) is substituted for \mathcal{S} , then Equation (15) can be rewritten as:

$$\begin{aligned} \Delta D_H = & - \left[b_0 + b_4 \log W + b_5 \log S + b_6 \log T_{15} + b_7 \log (100 - F_{15}) + b_8 \log (D50_{15} + 0.1) \right]^{ref} \\ & + \left[b_0 + b_4 \log W + b_5 \log S + b_6 \log T_{15} + b_7 \log (100 - F_{15}) + b_8 \log (D50_{15} + 0.1) \right]^{site} \end{aligned} \quad (16)$$

By simplifying Equation (16) and inserting model coefficients and parameters for the reference site, the adjustment factor can be computed as:

$$\begin{aligned} \Delta D_H = & b_0^{site} + b_4^{site} \log(W^{site}) + b_5^{site} \log(S^{site}) + 0.540 \log\left(\frac{T_{15}^{site}}{3}\right) \\ & + 3.413 \log\left(\frac{100 - F_{15}^{site}}{80}\right) - 0.795 \log\left(\frac{D50_{15}^{site} + 0.1}{0.3}\right) + 16.213 \end{aligned} \quad (17)$$

where b_4^{site} and b_5^{site} denote site-specific geometry coefficients dependent on the geometry model (i.e. ground slope or free-face) and are provided in Table 2-2. Parameters with the 'site' superscript denote site-specific soil and geometry parameters determined from the site-specific soil information provided by the engineer.

Table 2-2 Site-specific geometry coefficients for computing the adjustment factor, ΔD_H

Model	b_0^{site}	b_4^{site}	b_5^{site}
Ground Slope	-16.213	0	0.338
Free Face	-16.713	0.592	0

Once the reference lateral spread displacement is obtained from the appropriate (i.e. hazard-targeted) map and the adjustment factor is computed using Equation (17) and Table 2-2, the site-specific hazard-targeted lateral spread displacement (in meters) can be computed as:

$$D_H^{site} = 10^{([\log D_H]^{ref} + \Delta D_H)} \quad (18)$$

2.2.2 Bardet et al (2002) Empirical Model

The Bardet et al model was regressed from the same database used by the Youd et al model introduced in Bartlett and Youd (1995). Due to the difficulty in determining fines content (F_{15}) and mean grain size ($D_{50_{15}}$) for the liquefiable layers, the Bardet et al model proposed a four parameter model using moment magnitude (M_w), source-to-site distance (R), slope (S), free-face ratio (W), and cumulative thickness of the liquefiable layers (T_{15}). The Bardet et al. (2002) empirical model is given as:

$$\log(D + 0.01) = b_0 + b_{off} + b_1 M + b_2 \log(R) + b_3 R + b_4 \log(W) + b_5 \log(S) + b_6 \log(T_{15}) \quad (19)$$

where

D = median computed permanent lateral spread displacement (m)

M = earthquake moment magnitude

R = the closest horizontal distance from the site to the source (km)

W = the free-face ratio (%)

S = the ground slope (%)

T_{15} = the cumulative thickness (in upper 20 m) of all saturated soil layers with corrected Standard Penetration Test (SPT) blowcounts (i.e., $(N_1)_{60}$) less than 15 blows/foot (m)

Model coefficients b_0 through b_6 are given in Table 2-1.

Table 2-3 Regression coefficients for the Bardet et al. (2002) empirical lateral spread model

Model	b_0	b_{off}	b_1	b_2	b_3	b_4	b_5	b_6
Ground slope	-6.815	0	1.107	-0.278	-0.026	0	0.454	0.558
Free Face	-6.815	-0.465	1.107	-0.278	-0.026	0.497	0	0.558

2.2.2.1 Full Performance-based Bardet et al (2002) Model

The procedure outlines in section 2.2.1.1 for the Youd et al model can adapted to the Bardet et al model using the Kramer et al. (2007) framework in the same way. Both models used the same database and parameters, so the performance-based framework should apply in the same manner. The equations from the performance-based Youd et al model were modified for the Bardet et al model and are as follows:

$$\log(D + 0.01) = \mathcal{L} - \mathcal{S} + \varepsilon \quad (20)$$

where

$$\mathcal{L} = b_1 M + b_2 \log R + b_3 R \quad (21)$$

$$\mathcal{S} = -(b_0 + b_{off} + b_4 \log W + b_5 \log S + b_6 \log T_{15}) \quad (22)$$

$$\varepsilon = \sigma_{\log D_H} \Phi^{-1}[P] \quad (23)$$

$$\sigma_{\log D_H} = 0.290 \quad (24)$$

The rest of the procedure outlined in section 2.2.1.1 remains the same, except all the locations where D_H is written become D .

2.2.2.2 Simplified Performance-based Bardet et al (2002) Model

The simplified procedure for the development of the Bardet et al model is the same as the Youd et al model. The same reference profile is used (which can be seen in Figure 2-3). A value of 3.0m was determined for the lateral spread parameter T_{15} . As shown in Figure 2-3, the geometry of the site constitutes a ground slope condition with ground slope (i.e. S) equal to 1%. The resulting value of \mathcal{S} for the reference site, as computed from Equation (22), is therefore equal to 6.549.

The lateral spread displacement corresponding to the generic reference site could therefore be obtained from the appropriate map and adjusted in order to provide site-specific lateral spread displacements corresponding to the desired return period. The equation for this site-specific adjustment is given as:

$$[\log D]^{site} = [\log D]^{ref} + \Delta D \quad (25)$$

where $[\log D]^{site}$ is the logarithm of the lateral spread displacement adjusted for site-specific conditions, $[\log D]^{ref}$ is the logarithm of the lateral spread displacement corresponding to the reference site (obtained from the map), and ΔD is the adjustment factor computed by the

engineer. By substituting Equation (20) into Equation (25), the adjustment factor can be written as:

$$\Delta D = (\mathcal{L} - \mathcal{S})^{site} - (\mathcal{L} - \mathcal{S})^{ref} = (\mathcal{L}^{site} - \mathcal{L}^{ref}) + (\mathcal{S}^{ref} - \mathcal{S}^{site}) \quad (26)$$

However, because $\mathcal{L}^{site} = \mathcal{L}^{ref}$, Equation (26) can be simplified as:

$$\Delta D = \mathcal{S}^{ref} - \mathcal{S}^{site} = 6.549 - \mathcal{S}^{site} \quad (27)$$

If Equation (22) is substituted for \mathcal{S} , then Equation (27) can be rewritten as:

$$\Delta D = 6.549 + b_0^{site} + b_{off}^{site} + b_4^{site} \log(W^{site}) + b_5^{site} \log(S^{site}) + 0.558 \log(T_{15}^{site}) \quad (28)$$

where b_o^{site} , b_{off}^{site} , b_4^{site} , and b_5^{site} denote site-specific geometry coefficients dependent on the geometry model (i.e. ground slope or free-face) and are provided in Table 2-4. Parameters with the ‘site’ superscript denote site-specific soil and geometry parameters determined from the site-specific soil information provided by the engineer.

Table 2-4 Site-specific geometry coefficients for computing the adjustment factor, ΔD

Model	b_0^{site}	b_{off}^{site}	b_4^{site}	b_5^{site}
Ground Slope	-6.815	0	0	0.454
Free Face	-6.815	-0.465	0.497	0

Once the reference lateral spread displacement is obtained from the appropriate (i.e. hazard-targeted) map and the adjustment factor is computed using Equation (28) and Table 2-4, the site-specific hazard-targeted lateral spread displacement (in meters) can be computed as:

$$D^{site} = 10^{([\log D]^{ref} + \Delta D)} \quad (29)$$

2.3 Empirical Seismic Slope Stability Models

Probabilistic assessment of earthquake-induced sliding displacements of natural slopes is often based on permanent sliding displacement due to earthquake shaking. Empirical probabilistic seismic slope displacement models developed by Rathje and Saygili (2009) and Bray and Travarasrou (2007) were used to create a numerical tool to compute the full performance-based seismic slope displacement. The capability to evaluate these models in a probabilistic manner was an added to *PBLiquefY*.

2.3.1 Rathje and Saygili (2009) Model

The Rathje and Saygili (2009) model is an update and improvement of the Saygili and Rathje (2008) model. The revised model includes a magnitude term that reduces scatter in the

model, and it also includes an improved estimate of the standard deviation. The Rathje and Saygili (2009) model presents both a scalar and vector models. For the purposes of this study the scalar model is the only one used. The empirical displacement model is based on rigid sliding block displacements computed from recorded horizontal acceleration-time histories. Over 2,000 motions were used, and each was scaled by factors of 1.0, 2.0 and 3.0. Displacements were calculated for k_y values of 0.05, 0.1, 0.2 and 0.3. The proposed model presented in 2009 was the following:

$$\ln D = 4.89 - 4.85 \left(\frac{k_y}{a_{\max}} \right) - 19.64 \left(\frac{k_y}{a_{\max}} \right)^2 + 42.49 \left(\frac{k_y}{a_{\max}} \right)^3 - 29.06 \left(\frac{k_y}{a_{\max}} \right)^4 + 0.72 \ln(a_{\max}) + 0.89(M - 6) \quad (30)$$

where D is the seismic slope displacement in units of cm is, k_y is the yield acceleration and a_{\max} is peak ground surface acceleration both in units of g., and M is the earthquake moment magnitude. The overall standard deviation for this new model is 0.95.

2.3.2 Bray and Travarasrou (2007) Model

The Bray and Travarasrou (2007) model utilizes a nonlinear fully coupled stick-slip sliding block model. The model separates the probability of “zero” displacement from the distribution of “nonzero” displacement, so that very low values do not bias the results. For the Newmark rigid sliding block case ($T_s=0$), the natural logarithm of the seismic displacement can be computed as:

$$\ln(D) = -0.22 - 2.83 \ln(k_y) - 0.333 (\ln(k_y))^2 + 0.566 \ln(k_y) \ln(a_{\max}) + 3.04 \ln(a_{\max}) - 0.244 (\ln(a_{\max}))^2 + 0.278(M - 7) \quad (31)$$

where the standard deviation for this model is 0.67.

The methodology presented by Bray and Travarasrou can be used to calculate the probability of the seismic displacement exceeding a selected threshold of displacement (d) for a specified earthquake scenario and slope properties.

2.3.3 Performance-based Implementation of Seismic Slope Displacement Models

The performance-based application of a seismic slope displacement model involves the incorporation of a probabilistic hazard framework (Rathje and Saygili 2008). A hazard curve showing the mean annual rate of exceeding a seismic slope displacement d^* can be computed as:

$$\lambda_{d^*} = \sum P[D > d^* | GM_i, k_y] \cdot \Delta \lambda_{GM} \quad (32)$$

where $\sum P[D > d^* | GM_i, k_y]$ is the conditional probability of exceeding displacement d^* given a ground motion level i , and $\Delta \lambda_{GM}$ is the incremental mean annual rate of exceedance from the ground motion hazard curve. The sum in the equation represents the integration over all possible

ground motion levels. Because only a single ground motion parameter is used to predict D , this approach is considered a scalar probabilistic assessment.

2.3.4 Simplified Performance-Based Seismic Slope Displacement Procedure

The simplified performance-based seismic slope displacement procedure seeks to approximate displacements calculated by the full-performance based seismic slope displacement procedure described in Section 2.3.3. The models described above will be incorporated in the simplified procedure at specific return periods.

The simplified seismic slope displacement model is derived from the following equation:

$$\ln D^{site} = \ln D^{ref} + \Delta \ln D \quad (33)$$

where D^{site} is the actual performance-based seismic slope displacement at the desired return period, D^{ref} is a reference performance-based seismic slope displacement based on a constant set of reference conditions, and $\Delta \ln D$ is a displacement correction function.

While a series of performance-based analyses can be performed with a constant set of reference conditions to compute $\ln D^{ref}$ at a desired return period across a geographic area, the values of $\ln D^{site}$ and $\Delta \ln D$ are unknown and must be approximated. The value of $\ln D^{site}$ can be approximated with the Rathje and Saygili (2009) model as:

$$\begin{aligned} \ln D^{site} \approx & 4.89 - 4.85 \left(\frac{k_y^{site}}{a_{max}} \right) - 19.64 \left(\frac{k_y^{site}}{a_{max}} \right)^2 + 42.49 \left(\frac{k_y^{site}}{a_{max}} \right)^3 \\ & - 29.06 \left(\frac{k_y^{site}}{a_{max}} \right)^4 + 0.72 \ln(a_{max}) + 0.89(M - 6) \end{aligned} \quad (34)$$

where a_{max} is obtained from the seismic hazard curve for a_{max} at the return period of interest, and k_y^{site} is the site-specific yield acceleration, which is usually estimated using a two-dimensional pseudo-static slope stability analysis.

Using the Bray and Travararou (2007) model, the same approximation is computed as:

$$\begin{aligned} \ln D^{site} \approx & -0.22 - 2.83 \ln(k_y^{site}) - 0.333 \left(\ln(k_y^{site}) \right)^2 + 0.566 \ln(k_y^{site}) \ln(a_{max}) \\ & + 3.04 \ln(a_{max}) - 0.244 \left(\ln(a_{max}) \right)^2 + 0.278(M - 7) \end{aligned} \quad (35)$$

Similarly, the reference seismic slope displacement can be approximated in order to compute $\Delta \ln D$. The reference seismic slope displacement can be approximated using the Rathje and Saygili (2009) model as:

$$\begin{aligned} \ln D^{ref} \approx & 4.89 - 4.85 \left(\frac{k_y^{ref}}{a_{max}^{ref}} \right) - 19.64 \left(\frac{k_y^{ref}}{a_{max}^{ref}} \right)^2 + 42.49 \left(\frac{k_y^{ref}}{a_{max}^{ref}} \right)^3 \\ & - 29.06 \left(\frac{k_y^{ref}}{a_{max}^{ref}} \right)^4 + 0.72 \ln(a_{max}^{ref}) + 0.89(M - 6) \end{aligned} \quad (36)$$

where k_y^{ref} is the constant reference yield acceleration, and a_{max}^{ref} is the peak ground surface acceleration at the return period of interest from the seismic hazard curve corresponding to the reference soil condition.

Using the Bray and Travarasrou (2007) model, the reference seismic slope displacement can be approximated as:

$$\begin{aligned} \ln D^{ref} \approx & -0.22 - 2.83 \ln(k_y^{ref}) - 0.333 \left(\ln(k_y^{ref}) \right)^2 + 0.566 \ln(k_y^{ref}) \ln(a_{max}^{ref}) \\ & + 3.04 \ln(a_{max}^{ref}) - 0.244 \left(\ln(a_{max}^{ref}) \right)^2 + 0.278(M - 7) \end{aligned} \quad (37)$$

With approximated values of $\ln D^{ref}$ and $\ln D^{site}$, we can now approximate $\Delta \ln D$ as:

$$\Delta \ln D = \ln D^{site} - \ln D^{ref} \quad (38)$$

Substituting Equations (34) and (36) into Equation (38), $\Delta \ln D$ for the Rathje and Saygili (2009) model can be represented as:

$$\begin{aligned} (\Delta \ln D)_{rathje} \approx & \frac{4.85}{PGA} \left(\frac{k_y^{ref}}{f_a^{ref}} - \frac{k_y^{site}}{f_a^{site}} \right) + \frac{19.64}{(PGA)^2} \left[\left(\frac{k_y^{ref}}{f_a^{ref}} \right)^2 - \left(\frac{k_y^{site}}{f_a^{site}} \right)^2 \right] \\ & + \frac{42.49}{(PGA)^3} \left[\left(\frac{k_y^{site}}{f_a^{site}} \right)^3 - \left(\frac{k_y^{ref}}{f_a^{ref}} \right)^3 \right] + \frac{29.06}{(PGA)^4} \left[\left(\frac{k_y^{ref}}{f_a^{ref}} \right)^4 - \left(\frac{k_y^{site}}{f_a^{site}} \right)^4 \right] + 0.79 \ln \left(\frac{f_a^{site}}{f_a^{ref}} \right) \end{aligned} \quad (39)$$

where PGA is the hazard-targeted peak ground acceleration corresponding to rock (i.e., $V_{s,30} = 760$ m/s); and f_a^{ref} and f_a^{site} are the reference and site-specific soil amplification factors to account for site response.

Similarly, $\Delta \ln D$ can be approximate for the Bray and Travarasrou (2007) model as:

$$\begin{aligned} (\Delta \ln D)_{bray} = & 2.83 \left[\ln \left(\frac{k_y^{ref}}{f_a^{ref}} \right) - \ln \left(\frac{k_y^{site}}{f_a^{site}} \right) \right] + 0.333 \left[\ln \left(\frac{k_y^{ref}}{f_a^{ref}} \right)^2 - \ln \left(\frac{k_y^{site}}{f_a^{site}} \right)^2 \right] \\ & + 0.566 \ln(PGA) \left[\ln \left(\frac{k_y^{site}}{f_a^{site}} \right) - \ln \left(\frac{k_y^{ref}}{f_a^{ref}} \right) \right] \end{aligned} \quad (40)$$

With this simplified performance-based approach for estimating seismic slope displacements, an engineer can compute uniform hazard estimates of seismic slope displacement at a targeted hazard level in a relatively simple manner. Certain assumptions are needed as inputs such as the yield acceleration for the specific slope using limit equilibrium slope stability methods. It is also required to obtain the probabilistic estimate of PGA from the USGS NSHMP website for rock (i.e., $V_{s,30} = 760$ m/s) at the targeted hazard level. A site-specific soil amplification factor for the ground motion is obtained from either the AASHTO seismic design provisions (based on soil site classification) or from a site-specific site response analysis.

Once approximations of $\Delta \ln D$ are available, site-specific, hazard-targeted estimates of seismic slope displacement can be computed as:

$$D^{site} = \exp[\ln D^{ref} + \Delta \ln D] = (D^{ref}) \exp[\Delta \ln D] \quad (41)$$

where D^{ref} is obtained from the appropriate seismic slope displacement reference parameter map.

2.4 Summary

The derivations of lateral spread displacement and seismic slope displacement models show how to approximate a full performance-based analysis using simple calculations and mapped reference parameters. The simplified lateral spread displacement model is based on the Youd et al. (2002) empirical model while the simplified seismic slope displacement procedure is based on Rathje and Saygili (2009), and Bray and Travararou (2007) seismic slope displacement models.

3.0 VALIDATION OF THE SIMPLIFIED MODELS

3.1 Overview

The effectiveness of the simplified methods depends on how closely they approximate the results of a complete site-specific probabilistic seismic hazard analysis. In order to show that the simplified method is as accurate as expected, the simplified and full performance-based methods will be performed for ten sites throughout the United States. These sites will be evaluated for two different return periods: 475 and 2475 years.

3.1.1 Sites used in the Analysis

The sites chosen for the analysis were selected based on the range of seismicity of each site, as well as their distribution across the United States. Table 3-1 lists the location of these sites as well as their latitudes and longitudes.

Table 3-1 Locations used for the validation of the simplified models

Site	Latitude	Longitude
Butte	46.003	-112.533
Charleston	32.726	-79.931
Eureka	40.802	-124.162
Memphis	35.149	-90.048
Portland	45.523	-122.675
Salt Lake City	40.755	-111.898
San Francisco	37.775	-122.418
San Jose	37.339	-121.893
Santa Monica	34.015	-118.492
Seattle	47.53	-122.3

3.2 Simplified Lateral Spread Displacement Model Validation

To evaluate the site-specific lateral displacement, a soil profile was assumed for each site. These soil parameters are presented in Figure 3-1. Values of 1.0m, 25%, and 1.0mm were computed for the lateral spread parameters T_{15} , F_{15} , and $D50_{15}$, respectively. As shown in Figure 3-1, the geometry of the site constitutes a ground slope condition with ground slope (i.e. S) equal to 1%. The resulting value of \mathcal{S} for the site, as computed from Equation (6), is therefore equal to 9.846 for the Youd et al (2002) model and 6.549 for the Bardet et al (2002) model.

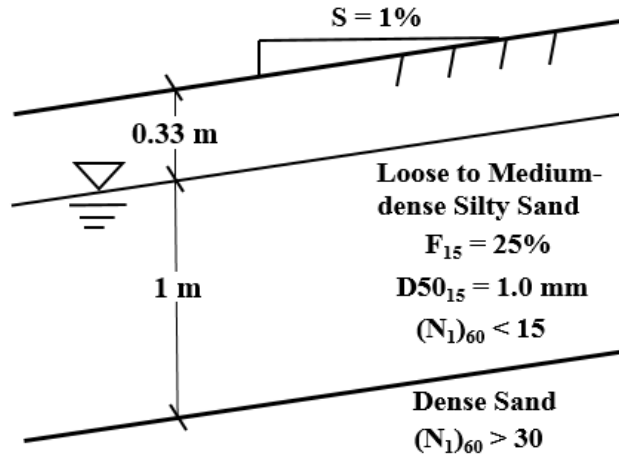


Figure 3-1 Site-specific soil profile used in the simplified lateral spread displacement model validation

3.2.1 EZ-FRISK

To perform the site-specific analysis for both the simplified and full performance-based models, the software EZ-FRISK (Risk Engineering 2013) was utilized. For this analysis, the USGS 2008 seismic source model (Petersen et al. 2008) was used for all locations.

3.2.2 Comparison of Results

Using EZ-FRISK and the soil profile selected for the site specific analysis, the lateral spread displacement was determined for each site using the simplified and full-performance based models. The results of analysis can be seen in Table 3-2 and Table 3-3. As can be seen in Table 3-2, the results of the analysis for the Youd et al (2002) model show that the simplified method falls on average within 3.9% of the values predicted by the full model. The observed discrepancy between the simplified and full performance-based models was no greater than 0.073 m at any site or any return period.

Table 3-2 Lateral spread displacements (m) for the site specific analysis using the two models for the three desired return periods (Youd et al (2002)).

Site	Simplified Model			Full PB Model		
	475 Yrs	1033 Yrs	2475 Yrs	475 Yrs	1033 Yrs	2475 Yrs
Butte	0.001	0.003	0.008	0.001	0.003	0.008
Charleston	0.001	0.017	0.068	0.001	0.015	0.065
Eureka	0.738	2.321	3.737	0.728	2.248	3.724
Memphis	0.003	0.033	0.067	0.003	0.025	0.065
Portland	0.038	0.152	0.333	0.036	0.152	0.334
Salt Lake City	0.162	0.437	0.726	0.167	0.438	0.726
San Francisco	0.744	1.095	1.493	0.745	1.081	1.492
San Jose	0.312	0.574	0.857	0.312	0.574	0.857
Santa Monica	0.171	0.400	0.719	0.172	0.400	0.719
Seattle	0.054	0.162	0.343	0.053	0.162	0.344

Table 3-3 Lateral spread displacements (m) for the site specific analysis using the two models for the three desired return periods (Bardet et al (2002)).

Site	Simplified Model			Full PB Model		
	475 Yrs	1033 Yrs	2475 Yrs	475 Yrs	1033 Yrs	2475 Yrs
Butte	0.006	0.020	0.056	0.008	0.014	0.048
Charleston	0.002	0.069	0.302	0.002	0.063	0.295
Eureka	1.987	7.945	16.036	1.977	7.955	15.555
Memphis	0.010	0.078	0.183	0.009	0.073	0.174
Portland	0.060	0.192	0.430	0.042	0.158	0.408
Salt Lake City	0.366	0.820	1.422	0.360	0.813	1.406
San Francisco	2.875	4.409	6.325	2.862	4.395	6.309
San Jose	1.439	2.705	4.472	1.429	2.689	4.460
Santa Monica	0.596	1.281	2.332	0.588	1.261	2.316
Seattle	0.121	0.349	0.757	0.072	0.260	0.664

For the Bardet et al (2002) model, the comparison between the simplified and full method show relatively close agreement, having only 3.3% error on average. The largest difference between the predicted displacements was no larger than 0.089 m for any location or return period.

Overall, the difference between the simplified and full performance based results for both models were within an acceptable amount of error (defined by this report as 5%). The closeness of the fit is apparent when the results of both analyses are plotted against each other, which can be seen in Figure 3-2 and Figure 3-3 (these are actual displacement values, not averages). The R^2

values for each return period are larger than 0.9995 for both models, indicating that the approximation of the full method is very good. These high R^2 values, as well as the lack of scatter of the results, seem to be too close for a simplified method; however, because this is a mathematically derived relationship it is expected that the results be closely correlated with those of the full probabilistic analysis. If the fit was not so close, then the mathematically derived equation would be suspect.

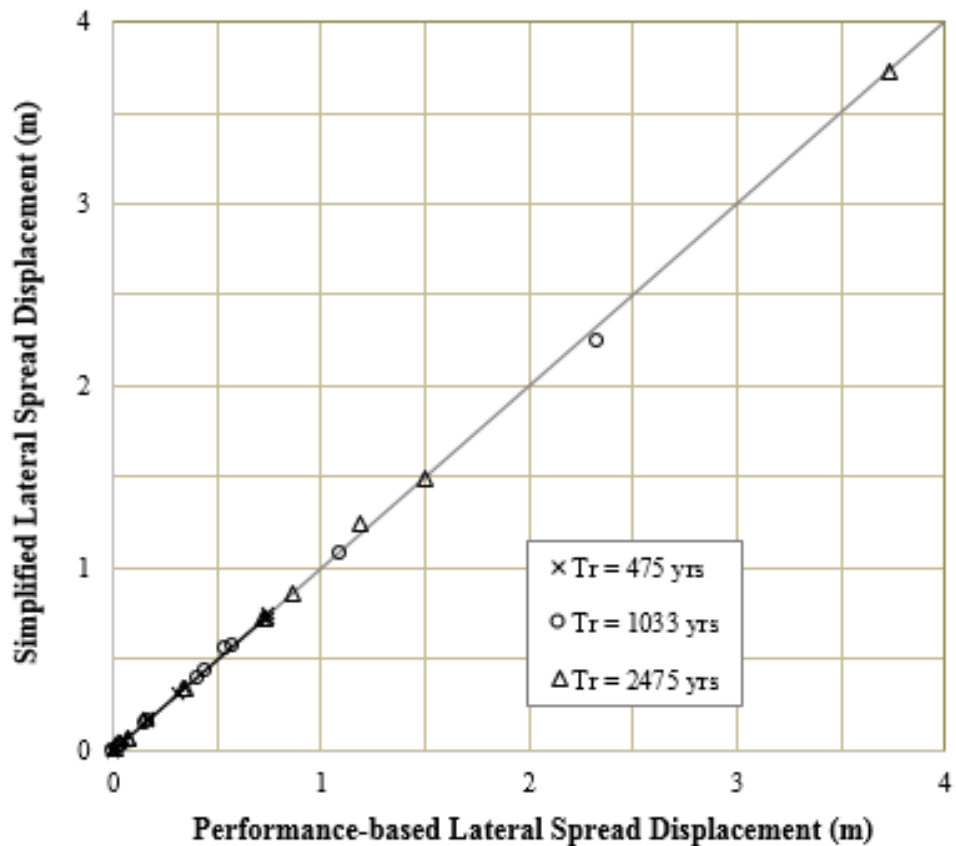


Figure 3-2 Comparison of lateral spread displacements for the simplified and full performance-based models for the Youd et al (2002) model.

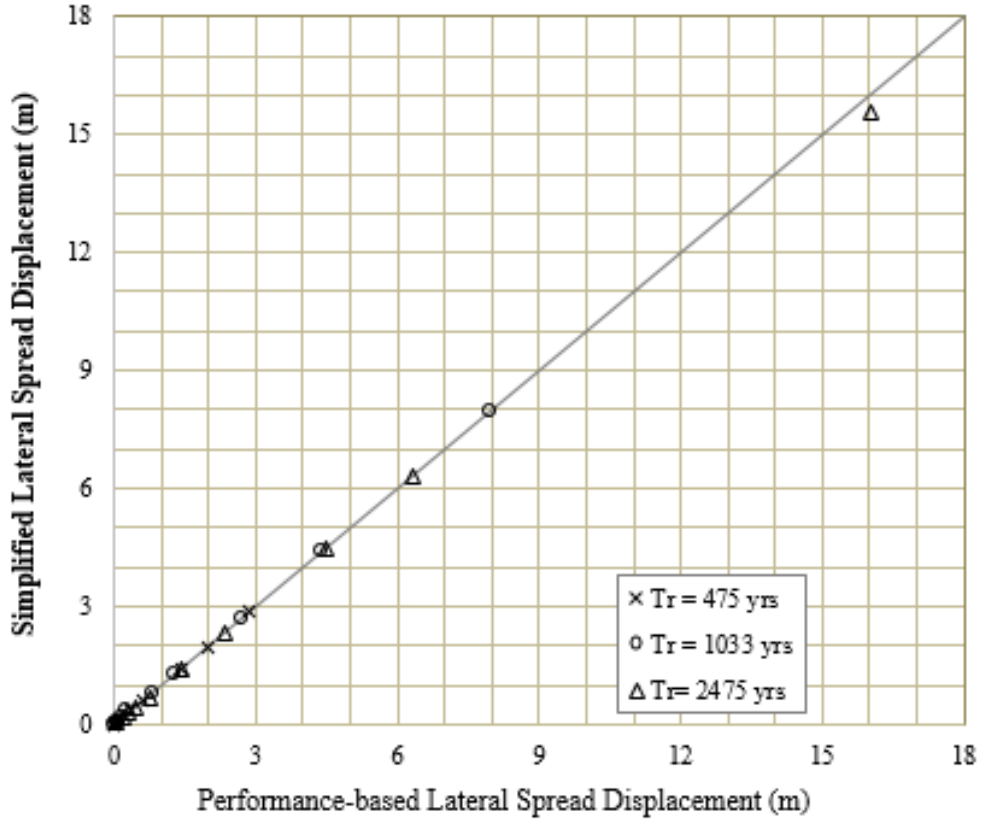


Figure 3-3 Comparison of lateral spread displacements for the simplified and full performance-based models for the Bardet et al (2002) model.

3.3 Validation of the Seismic Slope Stability Models

To evaluate the accuracy of the simplified performance-based procedure for seismic slope displacements, reference parameters of $k_y^{ref} = 0.1g$ and $f_a^{ref} = 1.0$ were selected. Values of k_y^{site} ranging from 0.1g to 0.5g were selected for the “site-specific” site conditions. Values of PGA and mean M were obtained for the ten selected U.S. cities from the 2008 USGS deaggregation for three return periods: 475 years, 1,033 years, and 2,475 years. Values of f_a^{site} were obtained from current AASHTO seismic design provisions using tabulated values of f_{pga} as a function of PGA . Subsequent values of mean M , PGA , and f_{pga} for the three return periods are summarized in Table 3-4 for the ten cities evaluated in this study.

Table 3-4: Summary of Magnitude, PGA and f_a site used for each city used in the validation

Site	Tr = 475			Tr = 1033			Tr = 2475		
	Mean M	PGA	f_a	Mean M	PGA	f_a	Mean M	PGA	f_a
Butte	6.03	0.0834	1.600	6.03	0.1206	1.559	6.05	0.1785	1.443
Charleston	6.61	0.1513	1.497	6.87	0.3680	1.132	7.00	0.7287	1.000
Eureka	7.33	0.6154	1.000	7.40	0.9662	1.000	7.45	1.4004	1.000
Memphis	6.98	0.1604	1.479	7.19	0.3346	1.165	7.24	0.5711	1.000
Portland	7.24	0.1990	1.402	7.29	0.2980	1.204	7.31	0.4366	1.063
Salt Lake City	6.75	0.2126	1.375	6.84	0.4030	1.097	6.90	0.6717	1.000
San Francisco	7.31	0.4394	1.061	7.38	0.5685	1.000	7.44	0.7254	1.000
San Jose	6.66	0.4560	1.044	6.67	0.5627	1.000	6.66	0.6911	1.000
Santa Monica	6.74	0.3852	1.115	6.79	0.5372	1.000	6.84	0.7415	1.000
Seattle	6.75	0.3110	1.189	6.82	0.4444	1.056	6.88	0.6432	1.000

The full performance-based seismic slope displacement equation as described in Section 2.3.3 was implemented in *PBLiquefY* with the reference values described above to compute D^{ref} for the Ten U.S. Cities at the three return periods of interest. Additionally, *PBLiquefY* was used to compute site-specific, full performance-based values of D^{site} using the selected values of k_y^{site} at each of the ten cities for all three return periods. Site-specific values of k_y^{site} were then used to compute simplified approximations of D^{site} using Equations (39), (40), and (41) and the seismic loading values summarized in Table 3-4: Summary of Magnitude, PGA and f_a site used for each city used in the validation

Figure 3-4 and Figure 3-5 below show the comparison of the full and simplified performance-based seismic slope displacement predictions for both the Rathje and Saygili (2009) and Bray and Travarasrou (2007) models, respectively.

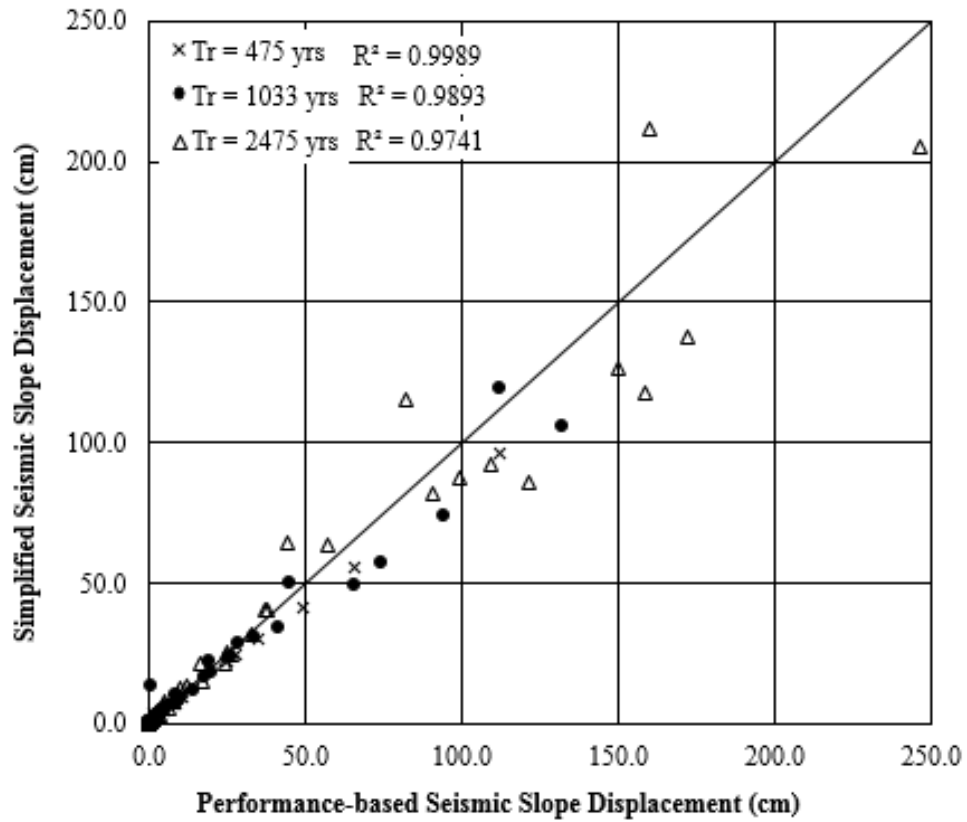


Figure 3-4 Comparison of seismic slope displacements for the simplified and full performance-based models based on Rathje and Saygili (2009)

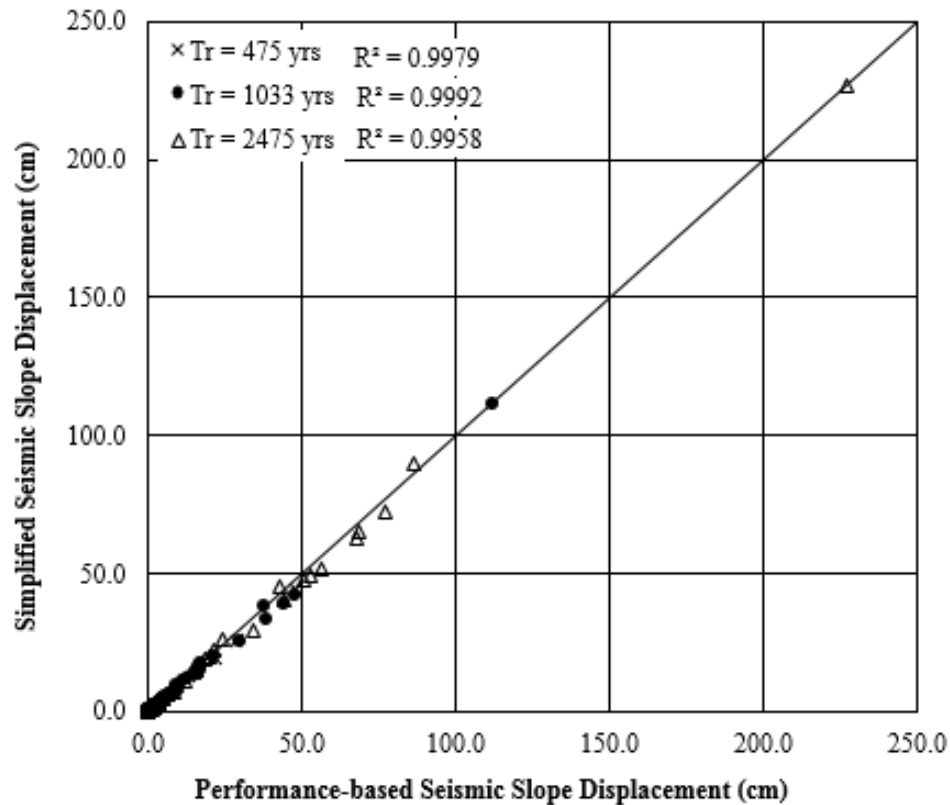


Figure 3-5 Comparison of seismic slope displacements for the simplified and full performance-based models based on Bray and Travararou (2007)

As seen in Figure 3-4 and Figure 3-5, there is generally a good correlation between the full-performance based procedure and the simplified performance-based procedure with both models, although the simplified procedure using the Bray and Travararou (2007) model provides a better approximation of the full performance-based results than the procedure using the Rathje and Saygili (2009) model. The Rathje and Saygili (2009) model incorporates a 4th-order polynomial function of (k_y/PGA) , which can lead to greater discrepancies between the simplified performance-based slope displacements and the full performance-based slope displacements at higher predicted displacements. Nevertheless, relatively high R^2 values indicate that the correlation accounts for nearly all of the variability in the computed response data. The average discrepancy across all return periods and yield accelerations included in this study for the simplified procedure using the Rathje and Saygili (2009) model was 4.9 cm. The average discrepancy for the simplified procedure using the Bray and Travararou (2007) model was 0.8 cm. However, note is that the simplified procedure incorporating the Rathje and Saygili (2009) model accurately and precisely approximates the results of the full performance-based procedure up to predicted displacements of about 50 cm, which is a much greater displacement than what is typically considered acceptable for many engineering applications. For predicted displacements greater than 50 cm, the engineer should interpret the results with caution, understanding that the simplified Rathje and Saygili (2009) results may be imprecise. From these results we can conclude that the simplified procedure for approximating probabilistic seismic slope

displacements will adequately approximate the results of a full performance-based procedure for most practical design applications, particularly if an allowable limit state of 30 cm (i.e., 12 inches) is specified for foundation design.

3.4 Summary

Ten sites throughout the United States were analyzed using both the full and simplified probabilistic procedures for three different return periods: 475, 1033, and 2475 years. Both the simplified lateral spread displacement and simplified seismic slope stability displacement models provided reasonable approximations of their respective full probabilistic methods. When greater than 30 cm of seismic slope displacements were predicted, the simplified procedure with the Rathje and Saygili (2009) model showed more scatter in its ability to approximate the full performance-based procedure. Caution and engineering judgment should be used when such circumstances are encountered in design.

4.0 EVALUATION OF GRID SPACING

4.1 Overview

Because biases due to spacing of grid points in gridded seismic hazard analyses are known to exist, the grid spacing study will evaluate the potential for bias to occur due to grid spacing effects in a gridded probabilistic lateral spread and seismic slope stability hazard assessment. Because the states involved in this study comprise areas of varying seismicity levels, evaluations will be performed in each of the states to assess the optimum grid spacing for development of liquefaction and lateral spread parameter maps in future tasks.

The grid spacing assessment was performed by comparing interpolated results from a simple 4-point grid placed in various parts of the country with site-specific results. The difference between the interpolated and site-specific results was quantified. By minimizing these computed differences, the optimum grid spacing for the liquefaction parameter maps in each state was obtained.

4.2 Grid-Spacing Evaluation

This section will describe the methods used to derive a correlation between optimum grid spacing and *PGA* for simplified performance-based lateral spread and seismic slope stability evaluation. The purpose of this correlation was to provide a simple, readily-available, well-defined set of rules for proper grid spacing across the states of interest. This set of rules is necessary because it is impractical to perform an infinite number of full performance-based analyses to create the liquefaction contour maps. It was necessary to determine a finite number of points to analyze. The set of rules created in this grid spacing study was used to define the optimum number of points which would be feasible to analyze in the amount of time given and would yield an acceptable amount of error due to interpolation between analyzed points.

4.2.1 Methodology

Using a square grid (like the one shown in Figure 4-1) with the city's anchor point as the center of the square, several grid spacings were tested. This preliminary testing process included grid spacings of 1, 2, 4, 8, 16, 25, 35, and 50 km (0.62, 1.24, 2.49, 4.97, 9.94, 15.5, 21.7 and 31.1 mi). Then a full performance-based liquefaction analysis was performed at each corner point and the center anchor point to solve for lateral spread displacement and seismic slope displacement at three return periods (475, 1033, and 2475 years). This process was repeated for each selected city in the study.

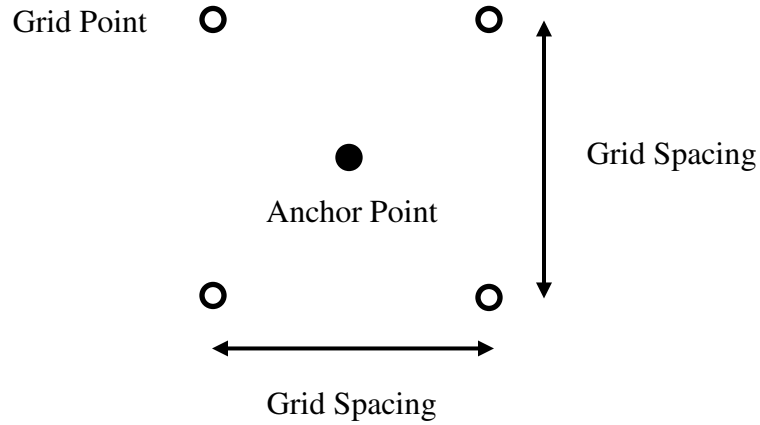


Figure 4-1 Layout of grid points centered on city's anchor point.

Interpolated estimates of the lateral spread displacement and seismic slope displacement hazards at the center point were calculated using the four corner points. These interpolated values were then compared to the full performance-based values (i.e., “true” values) computed at the center points. The difference between the interpolated value and the true value at the center is called the error term. The error terms were normalized to the actual values at the anchor points by calculating the percent error term as follows:

$$PercentError = \frac{|InterpolatedValue - TrueValue|}{TrueValue} \times 100\% \quad (42)$$

The maximum percent error (i.e. the maximum percent error across all return periods for a given anchor point) became the deciding parameter in selecting optimum grid spacing for a given location. The relationship between maximum percent error and grid spacing was analyzed for each city and is discussed in the following section.

It was hypothesized that *PGA* was a major factor in the relationship between grid spacing and maximum percent error. Specifically, it was hypothesized that as *PGA* increases, the optimum grid spacing decreases. To estimate the effect of *PGA* on optimum grid spacing, 35 cities with a wide range of *PGA* values corresponding to $T_R = 2,475$ years were selected for the grid spacing study (see Figure 4-2).

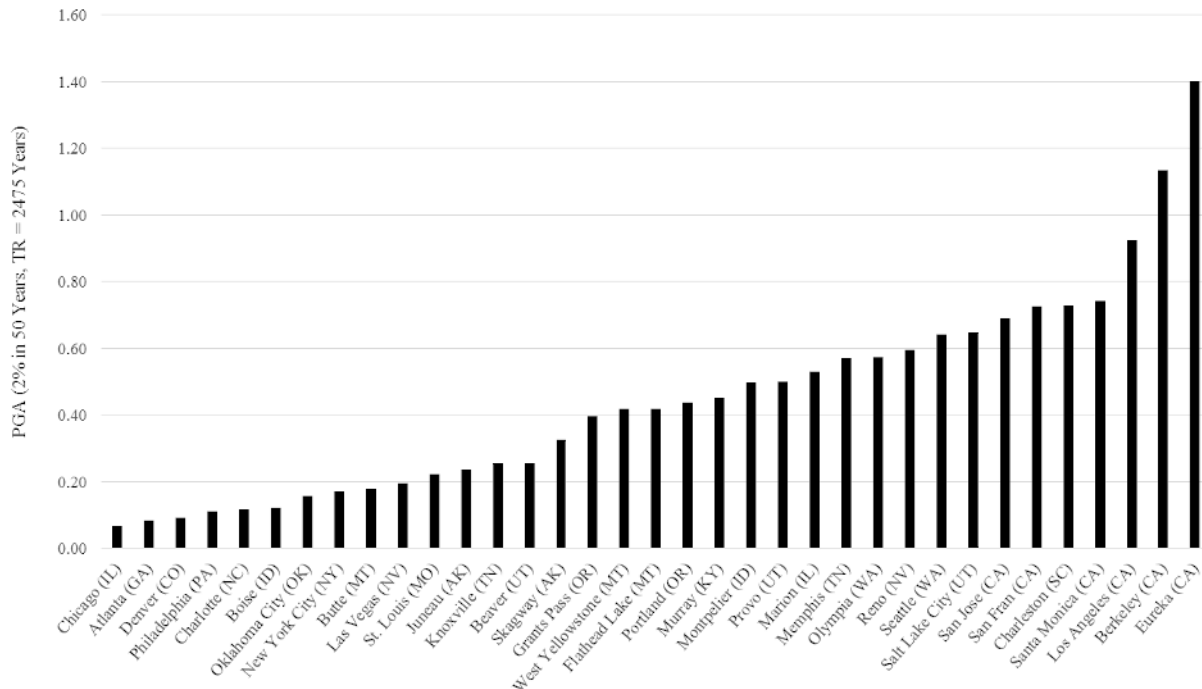


Figure 4-2 Range of *PGA* values for cities included in final grid spacing study.

The desired outcome of the final grid spacing study was to create a correlation between *PGA* and optimum grid spacing in km. An equation for the best-fit trend line alone would not be sufficient, because defining grid points to use in an analysis does not work well with non-integer values for grid spacing and constantly changing distances between points. Therefore, it was necessary to divide the different cities into *PGA* “bins” or defined ranges of values. These bins were determined using the USGS 2008 *PGA* hazard map ($T_r = 2475$ years) as shown in Figure 4-3. The *PGA* hazard map was chosen because it was clear and readily available as a well-documented definition of which areas in the country had significantly different seismicity levels compared to other areas’ seismicity levels. The objective of this study was to determine the optimum grid spacing for each color bin.

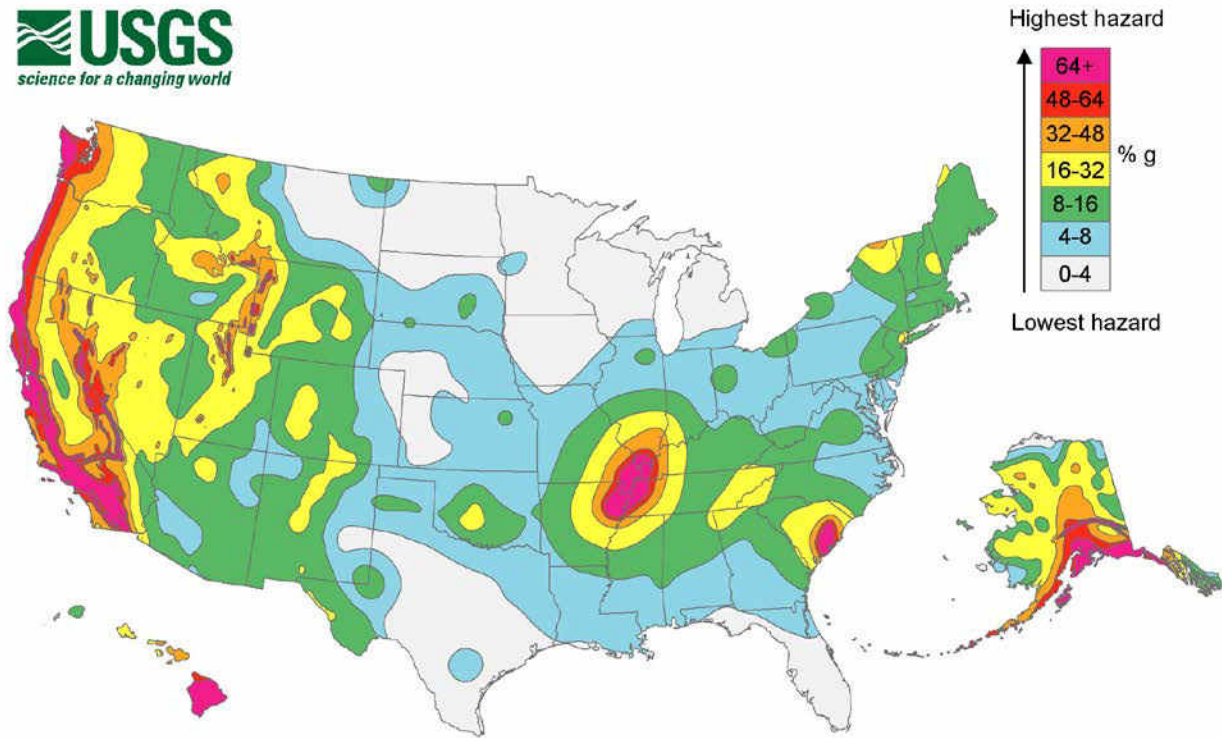


Figure 4-3 USGS 2008 *PGA* hazard map ($T_r = 2475$ years).

As in the preliminary study, a full performance-based analysis was performed at the anchor point of each city and at the corners of the grid surrounding the anchor point. This was repeated for multiple grid spacings until the percent error was within a reasonable amount. It was determined that “optimum grid spacing” would be defined as the smallest grid spacing (i.e. shortest distance between grid points) which yielded a maximum percent error of 5% across all return periods based on the specified parameter.

Grid spacing study results for lateral spread displacement are shown graphically in Figure 4-4. Generally, the trend of the data shows a decreasing required grid spacing with increasing *PGA*. However, the data start to deviate from this trend in areas with $PGA > 0.5$. Some sites like Eureka, CA seemed insensitive to grid spacing entirely, not reaching 5% error even with a grid spacing of 90 km. At the same time, two locations - Reno, NV and Jackson, WY - did not achieve <5% error with any grid spacing, even as small as 1 km.

The atypical behavior observed in predicted lateral spread displacements at Reno and Jackson was examined carefully, and some potentially important observations were made. First, these two sites are located near the edges of the Intermountain Seismic Belt (ISB) of the United States. The ISB is characterized by extensive normal faulting in north-south trending valleys. The 2008 USGS seismic source model (Petersen et al. 2008), which was used in this study, becomes quite complex in these areas as the model transitions from the ISB to other seismic regions characterized by different faulting types, recurrence rates, attenuation relationships, and logic tree weighting factors. Second, the Youd et al (2002) empirical lateral spread model is very sensitive to source-to-site distance at low to medium magnitude events (Franke and Kramer

2014), which are commonly assigned to the individual and gridded seismic sources located near (i.e., < 5km) the Jackson and Reno sites. Therefore, even with a grid spacing as small as 1 km, significant bias was observed when performing simplified performance-based interpolations at these two sites.

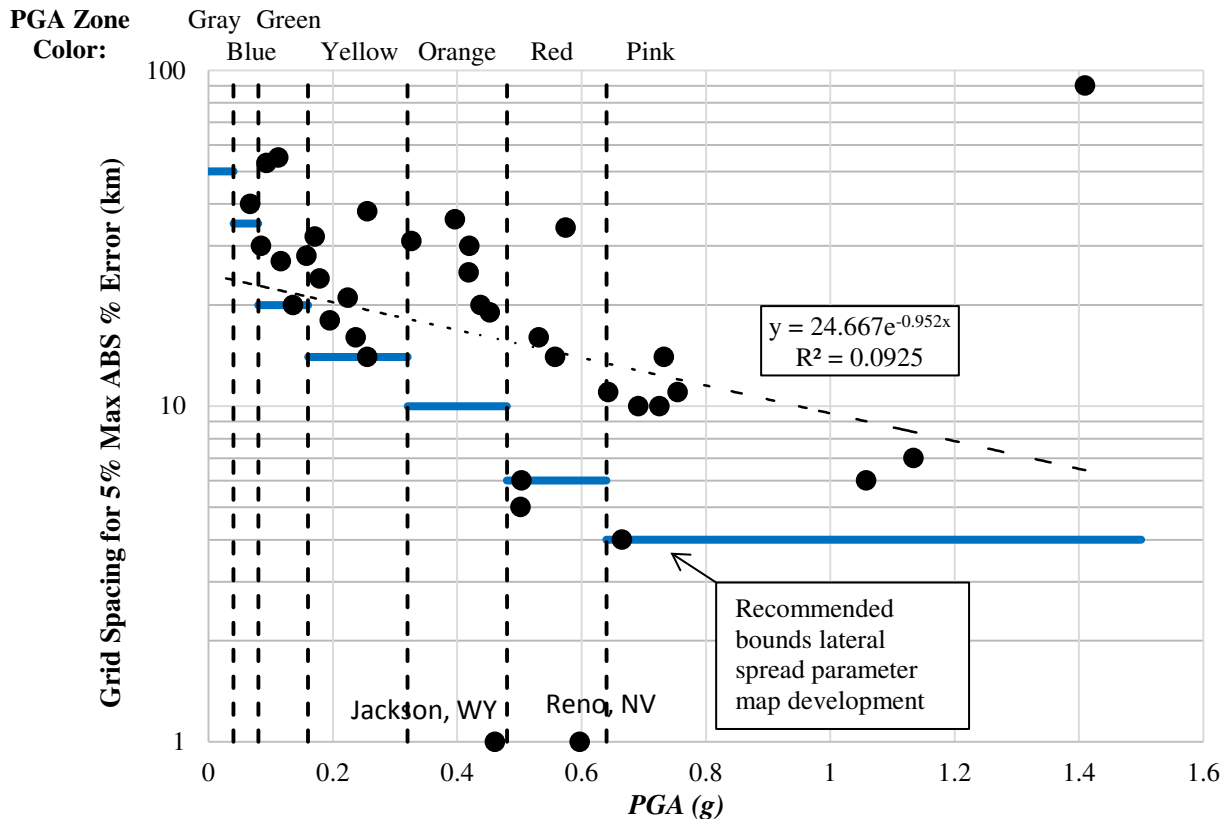


Figure 4-4 Correlation between *PGA* and optimum grid spacing to achieve 5% maximum absolute percent error for predicted lateral spread displacement

Hand-drawn, recommended grid spacings for lateral spread displacement reference parameter maps are summarized in Table 4-1.

Table 4-1 Proposed Grid Spacing for Lateral Spread Displacement Reference Parameter Maps Based on Mapped USGS *PGA*

<i>PGA</i>	Color	Spacing (km)
0 - 0.04	Gray	50
0.04 - 0.08	Blue	35
0.08 - 0.16	Green	20
0.16 - 0.32	Yellow	15
0.32 - 0.48	Orange	10
0.48 - 0.64	Red	6
0.64+	Pink	4

Grid spacing study results for seismic slope stability are presented graphically in Figure 4-5, which shows scatter comparable to that observed with lateral spread displacement. The seismic loading at the different locations seems to be a factor affecting the seismic slope displacement analysis' results. A way to address the uncertainty is with the use of a best fit line to identify a trend in the data's behavior and then draw dashed line just below it as the lower bound to identify the recommended grid spacing for the cities analyzed. The proposed grid spacing for each *PGA* interval was hand drawn with the red lines.

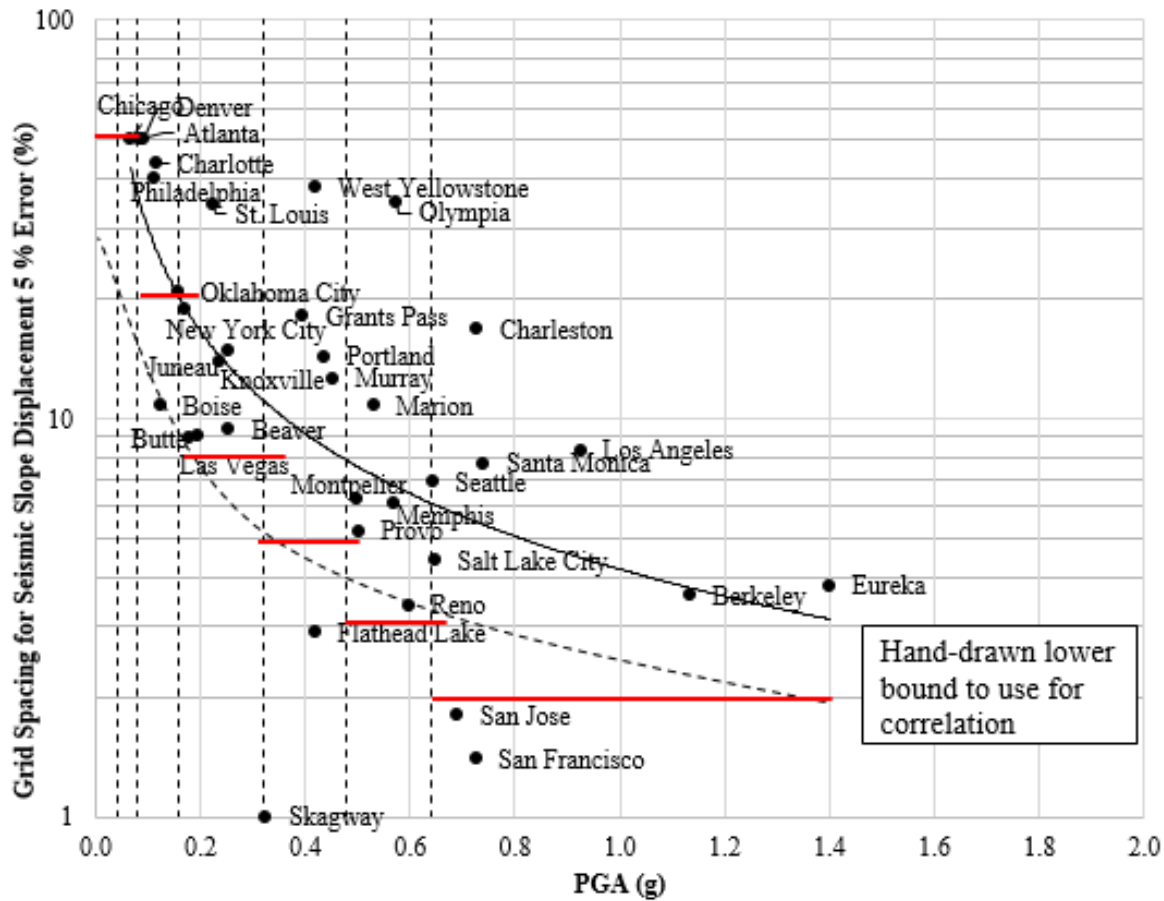


Figure 4-5 Correlation between *PGA* and optimum grid spacing to achieve 5% maximum absolute percent error for predicted seismic slope displacement

Five out of the thirty five cities used in the study did not meet the criteria of 5% error. These cities were Skagway (AK), Flathead (MT), Salt Lake City (UT), San Jose (CA), and San Francisco (CA). After this observation, the absolute difference in centimeters was calculated for these cities. It was observed that if a maximum allowable difference of 5 cm between the actual value and the interpolated value was used instead of a percent error, then less scatter was observed. Therefore, the proposed spacing for these particular cities is shown below in Table 4-2.

Table 4-2 Proposed Grid Spacing for Seismic Slope Displacement Reference Parameter Maps Based on Mapped USGS *PGA*

<i>PGA</i>	Color	Spacing (km)
0 - 0.04	Gray	50
0.04 - 0.08	Blue	50
0.08 - 0.16	Green	20
0.16 - 0.32	Yellow	8
0.32 - 0.48	Orange	5
0.48 - 0.64	Red	3
0.64+	Pink	2

4.3 Summary

Based on the analysis outlined here, the grid spacing necessary to maintain accuracy in the interpolated results was found. The grid spacings should result on average 5% difference between an interpolated value and a full performance-based value for lateral spread displacement, or in an average difference of 5 cm or less between an interpolated value and a full performance-based value for seismic slope displacement. These grid spacings will be very important in creating the grid of points that will be used in the analysis.

5.0 MAP DEVELOPMENT

5.1 Overview

Now that the optimum grid spacing between points has been determined, the grid points used in the analysis need to be determined, then those points need to be analyzed and the hazard parameters calculated. Once the analysis has been conducted for each grid, then those points will be used to create the liquefaction and lateral spread parameter maps for the target return periods.

This process required the use of several specialized software programs. To create the grid spacing and the maps the Graphical Information System (GIS) software ArcMap, developed by ESRI Incorporated, was used extensively. To perform the simplified seismic slope displacement analysis the software PBLiquefy (Franke et al. 2014) was utilized. To perform the simplified lateral spread displacement analysis, the program EZ-FRISK created by Risk Engineering (2013) was used.

5.2 Creating the Grid Points

The process was started by dividing each state into sections based on the USGS 2008 *PGA* hazard map. This was done using GIS shapefiles downloaded from the USGS website representing the 2008 hazard map. Each *PGA* hazard zone was assigned a grid spacing based on the suggested grid spacing from the previous section. Then using ArcMap, a grid of points with latitude and longitude, was generated for each hazard zone at the specified grid spacing. An example of the subdivision and the overall grid of points for Utah can be seen in Figure 5-1.

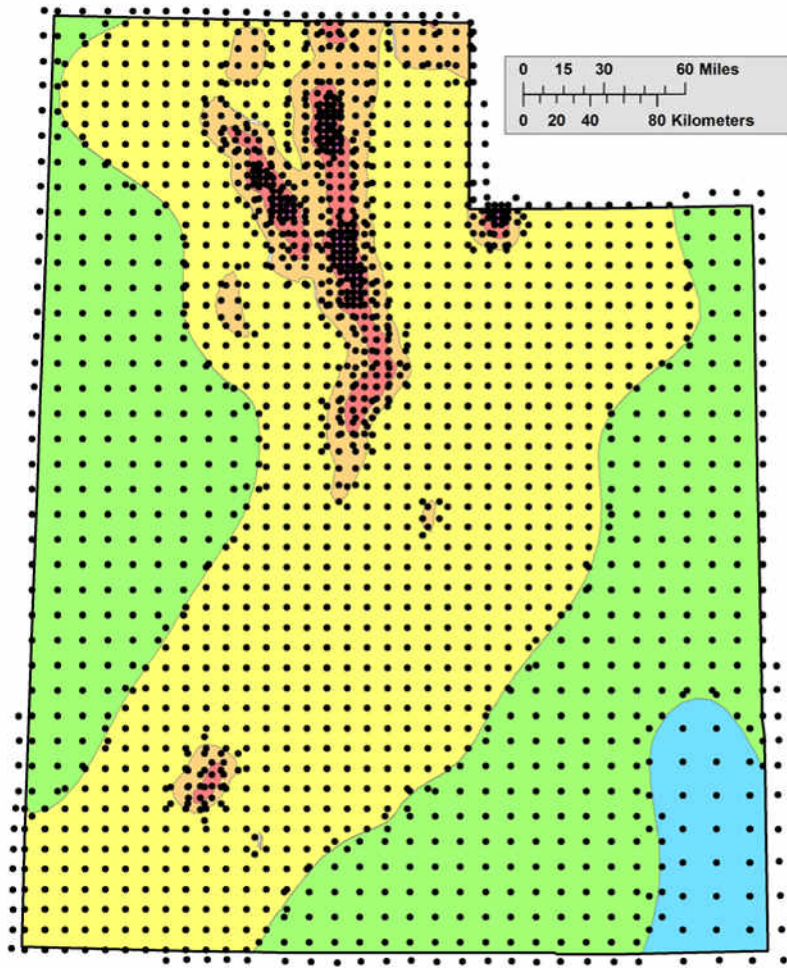


Figure 5-1 Grid points for Utah combined with USGS 2008 PGA hazard map.

5.3 Analysis of the Grid Points

Once the grid points were developed for all the states, the location of each of the points was evaluated for liquefaction and lateral spread hazard using the reference soil profiles discussed in the previous report. Each point was analyzed for the 475, 2475 year return periods. Once all of the points for a particular state were successfully run, the results were compiled and then imported back into ArcMap to begin the process of making the parameter maps.

5.3.1 Analysis of the Lateral Spread Displacement Model Grid Points

Analyzing the grid points in EZ-FRISK requires that a seismic source model be used. The USGS 2008 seismic source model was used to analyze the points in South Carolina, Utah, and Northern California. Only area sources and faults were considered within 300 km of each site, with the exception of subduction zone sources which were considered within 500 km.

5.3.2 Analysis of the Seismic Slope Stability Model Grid Points

The grid points used in the seismic slope displacement method were analyzed using the USGS 2008 Deaggregation for South Carolina, Utah, and Northern California. The process utilized the ability of PBLiquefY to run multiple sites sequentially.

5.4 Creation of the Maps

Once the analyzed grid points were imported back into ArcMap the points needed to be turned into a contour map. This was done by converting the individual points into a surface raster using the Kriging tool. This tool interpolates between each point and makes a surface with a value at every point. In order to ensure that the contours of each state run all the way to the border, the state shape is buffered slightly. The Kriging raster is created based on this buffered shape. Once the Kriging raster is made, the raster surface needs to be converted into a contour.

To make the contour from the Kriging, first the spacing of the contours needs to be determined. It is important that the contour spacing be fine enough that the detail of the map can be read, but far enough apart that the contours can be read. The spacing will vary from map to map based on this process. An example of a Kriging raster and contour for the state of Utah can be seen in Figure 5-2.

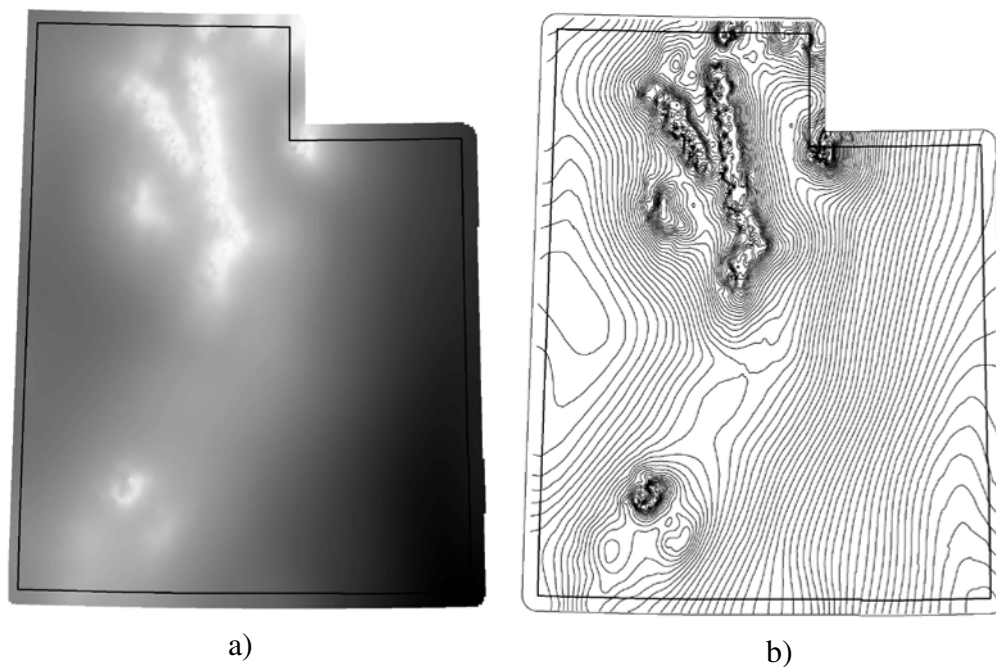
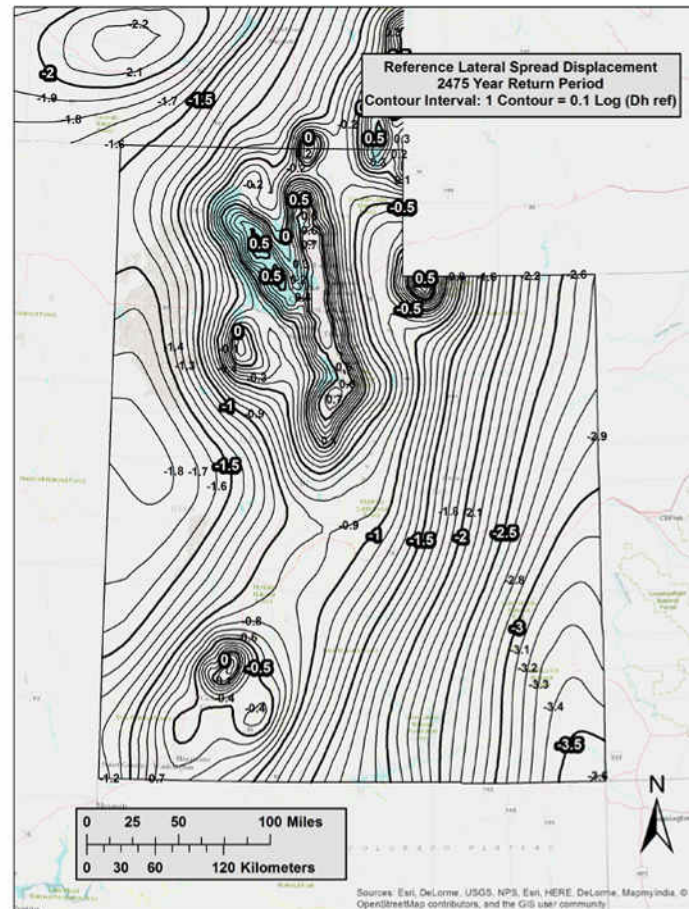


Figure 5-2 a) Kriging raster and b) contours for Utah ($T_r = 2475$ yrs).

Once the proper contour spacing is determined for each map, the contour is labeled and clipped to fit the state shapefile. Then a basemap and reference features are added to provide more detail about the topography to the parameter maps. An example of a completed lateral spread parameter map of D_H^{ref} can be seen in Figure 5-3.

Each model has different parameters represented by the contours on the map. The lateral spread parameter map shows the reference value of displacement, D_H^{ref} as calculated using the Youd et al. (2002) model, and is given in units of Log (meters). The seismic slope displacement map shows the reference value of displacement, D^{ref} as calculated using the Rathje and Saygili (2009) model, and Bray and Travasarou (2007) model. D^{ref} given in centimeters. Careful attention needs to be given to the labeling of each map to ensure that map has the correct parameter and that the reference value used in the later steps of the simplified method are accurately read from the contours.

For this report, maps of D_H^{ref} and D^{ref} were made for each state at the 475 and 2475 year return periods. These maps can be viewed in the Appendix: lateral spread parameter maps in Appendix B and seismic slope displacement parameter maps in Appendix C. The contours were adjusted for each map to make reading it as user friendly as possible.



(PBLiquefy, EZ-FRISK). These points are then imported into ArcMap and converted to a Kriging raster that is then used to create a contour of the reference parameter. Sample maps for the states participating in this research study can be seen in the Appendix.

6.0 COMPARISON OF PROBABILISTIC AND DETERMINISTIC ANALYSES

6.1 Overview

This section provides comparisons between the pseudo-probabilistic, deterministic, and simplified performance-based procedures for lateral spread displacement. The purpose of these comparisons is to identify how the deterministic procedure should be used in the proposed simplified procedure.

6.2 Methodology

Three cities of varying seismicity were selected for the comparison study: San Francisco (high seismicity), Salt Lake City (medium seismicity), and Butte (low seismicity). For each city, three analyses were performed: probabilistic (simplified performance-based procedure developed as part of this research), pseudo-probabilistic (AASHTO), and deterministic. A description of each analysis type is provided below.

6.2.1 Simplified Performance-Based Seismic Hazard Analysis

The simplified performance-based procedures involve retrieving a specified liquefaction hazard parameter from a hazard-targeted map developed using full probabilistic analyses. The probabilistic analyses which created the lateral spread and seismic slope parameter maps involve creating hazard curves which consider all possible combinations of the required seismic hazard analysis variables and their respective likelihoods. Examples of these variables would be: maximum horizontal ground acceleration, a_{max} , moment magnitude, M_w , or site-to-source distance, R .

The parameters used for the comparison of deterministic and simplified methods for this study were: for lateral spread, D_H^{ref} , for seismic slope stability D^{ref} . Each of the parameters were found at the target cities for the 475 and 2475 year return periods.

6.2.1.1 Simplified Lateral Spread Displacements

For the simplified performance-based procedure the appropriate lateral spread parameter map was identified for each site and values of D_H^{ref} were obtained for the necessary return periods. Using a generic soil profile (shown in Figure 6-1), the values of D_H^{ref} were corrected and the D_H^{site} was determined for each city at the targeted return periods. The additional analyses (pseudo-probabilistic and deterministic) for the comparison utilized the same soil profile. This process was previously described in greater detail in the derivation of the simplified procedure.

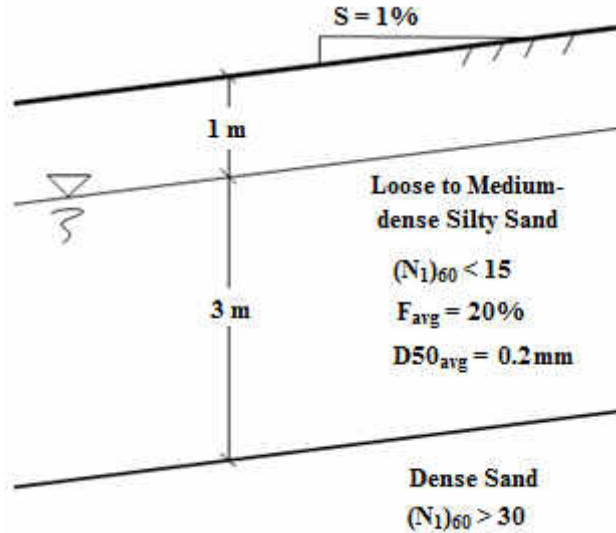


Figure 6-1 Soil profile used for the lateral spread displacement comparison study.

6.2.1.2 Simplified Seismic Slope Displacements

For the simplified performance-based procedure the appropriate seismic slope parameter map was identified for each site and values of D^{ref} were obtained for the necessary return periods. The generic soil profile used AASHTO amplification factors for site class D soils and $k_y = 0.1$ g. The additional analyses (pseudo-probabilistic and deterministic) for the comparison utilized the generic parameters. The simplified performance-based procedure for seismic slope displacement was explained in detail in Section 2.3.4.

6.2.2 Deterministic Procedure

In the deterministic procedure, ground motions are obtained through a Deterministic Seismic Hazard Analysis (DSHA). A DSHA involves deterministically assessing the seismic sources in the nearby region of the site of interest and identifying the source which produces the highest hazard in the area. The software EZ-FRISK was used to identify the top five seismic sources within 200 km for San Francisco and Salt Lake City. The 2008 USGS Seismic Source Model within EZ-FRISK does not include some smaller faults in low seismic regions, such as Butte. Thus, the governing fault for Butte (Rocker Fault) was identified using the USGS quaternary fault database (USGS et al., 2006). In the case of Salt Lake City and San Francisco, EZ-FRISK provided values of M_w , PGA , and R for both the 50th (i.e. median) and 84th (i.e. median + σ) percentiles according using the New Generation Attenuation (NGA) models for the Western United States (Boore and Atkinson, 2008; Campbell and Bozorgnia, 2008; and Chiou and Youngs, 2008) and weighting schemes shown in Table 6-1. For Butte, the 50th and 84th percentile M_w values were estimated using a correlation with surface rupture length developed by Wells and Coppersmith (1994), and PGA was calculated using the same three (NGA) models based on measured dimensions and assumed characteristics of the Rocker Fault. Summaries of the seismic sources considered in this DSHA and details of the Rocker Fault calculations are provided in Tables A.1 and A.2, respectively, in the appendix. Once the model inputs have been determined

through the DSHA they are entered into the respective empirical liquefaction hazard models. A summary of the governing input variables utilized in the deterministic liquefaction initiation and lateral spread displacement models are provided in Table 6-2.

Table 6-1 NGA model weights used in the deterministic procedure.

Attenuation Model	Weight
Boore & Atkinson (2008)	0.333
Campbell & Bozorgnia (2008)	0.333
Chiou & Youngs (2008)	0.333

Table 6-2 Input variables used in the deterministic models (a_{max} calculated using F_{pga} from AASHTO code).

Location	Latitude	Longitude	Distance [km]	Mean M_w	Median (50%)		Median + σ (84%)	
					PGA	a_{max}	PGA	a_{max}
Butte	46.003	-112.533	4.92	6.97	0.5390	0.5390	0.9202	0.9202
Salt Lake City	40.755	-111.898	1.02	7.00	0.5911	0.5911	1.005	1.005
San Francisco	37.775	-122.418	12.4	8.05	0.3175	0.3754	0.5426	0.5426

6.2.2.1 Lateral Spread Displacement

Estimations of lateral spread displacement for the deterministic process were found using the equation from the Youd et al (2002) empirical lateral spread model. The model is a regression based on seismic loading parameters and site specific soil parameters. The seismic loading inputs are shown in Table 6-2, and the site specific soil inputs were drawn from the soil profile seen in Figure 6-1. With these values the lateral spread displacement, D_H , is found using the following equation:

$$\overline{\log D_H} = b_0 + b_1 M + b_2 \log R^* + b_3 R + b_4 \log W + b_5 \log S + b_6 \log T_{15} + b_7 \log (100 - F_{15}) + b_8 \log (D50_{15} + 0.1) \quad (43)$$

where D_H is the median computed permanent lateral spread displacement (m), M is the earthquake moment magnitude, R is the closest horizontal distance from the site to the source (km), W is the free-face ratio (%), S is the ground slope (%), T_{15} is the cumulative thickness (in upper 20 m) of all saturated soil layers with corrected Standard Penetration Test (SPT) blowcounts (i.e., $(N_1)_{60}$) less than 15 blows/foot (m), F_{15} is the average fines content of the soil comprising T_{15} (%), $D50_{15}$ is the average mean grain size of the soil comprising T_{15} (mm), and R^* which is computed as:

$$R^* = R + 10^{0.89M - 5.64} \quad (44)$$

The model coefficients b_0 through b_8 are given in Table 2-1.

6.2.2.2 Seismic Slope Displacement

For the deterministic calculations estimations of seismic slope displacement were found using the equations from Rathje & Saygili (2009) and Bray & Travasarou (2007) seismic slope displacement models. The seismic loading inputs are shown in Table 6-2 and $k_y=0.1$ g was used in both models. D (cm) is found using the following equations, Rathje & Saygili (2009) and Bray & Travasarou (2007) respectively:

$$\ln D = 4.89 - 4.85 \left(\frac{k_y}{a_{\max}} \right) - 19.64 \left(\frac{k_y}{a_{\max}} \right)^2 + 42.49 \left(\frac{k_y}{a_{\max}} \right)^3 - 29.06 \left(\frac{k_y}{a_{\max}} \right)^4 + 0.72 \ln(a_{\max}) + 0.89(M - 6) \quad (45)$$

$$\ln(D) = -0.22 - 2.83 \ln(k_y) - 0.333 \left(\ln(k_y) \right)^2 + 0.566 \ln(k_y) \ln(a_{\max}) + 3.04 \ln(a_{\max}) - 0.244 \left(\ln(a_{\max}) \right)^2 + 0.278(M - 7) \quad (46)$$

6.2.3 Pseudo-probabilistic Seismic Hazard Analysis

In the pseudo-probabilistic procedure, the variables used in the empirical liquefaction hazard models are obtained from a Probabilistic Seismic Hazard Analysis (PSHA). Then these variables are used in the same deterministic procedure outlined previously for both the lateral spread and seismic slope displacements. To find these variables using a PSHA the USGS 2008 interactive deaggregation website (USGS 2008) was utilized. This procedure involved entering the latitude and longitude of the target cities, then selecting the return period for the analysis. Using this tool, the mean magnitude (M_w), peak ground acceleration (PGA) for rock, and source-to-site distance (R) were obtained for a return period of 1,039 years for each city of interest. The resulting values are summarized in Table 6-3.

Table 6-3 Input values found using USGS 2008 Deaggregation ($T_R = 475$ years).

Location	Latitude	Longitude	Distance (km)	Mean M_w	PGA	F_{pga}
Butte	46.003	-112.533	33.3	6.03	0.0834	1.600
Salt Lake City	40.755	-111.898	8.5	6.75	0.2126	1.375
San Francisco	37.775	-122.418	12.9	7.31	0.4394	1.061

Table 6-4 Input values found using USGS 2008 Deaggregation (TR = 2475 years).

Location	Latitude	Longitude	Distance (km)	Mean M_w	PGA	F_{pga}
Butte	46.003	-112.533	33.3	6.2	0.1785	1.443
Salt Lake City	40.755	-111.898	8.5	6.9	0.6717	1.000
San Francisco	37.775	-122.418	12.9	7.44	0.7254	1.000

6.3 Results

Each city was evaluated using the three analysis types discussed previously (probabilistic, pseudo-probabilistic, and deterministic). The following plots allow comparisons between the three methods and help explain the purpose of deterministic analyses within the proposed simplified performance-based procedures.

6.3.1 Empirical Lateral Spread Displacement Model

Once the analysis of the different methods was completed, the data was examined and several charts were created, one for each city. These charts compare, side by side, the results of the simplified, pseudo-probabilistic, and deterministic analyses. These charts can be seen in Figure 6-2, Figure 6-3, and Figure 6-4.

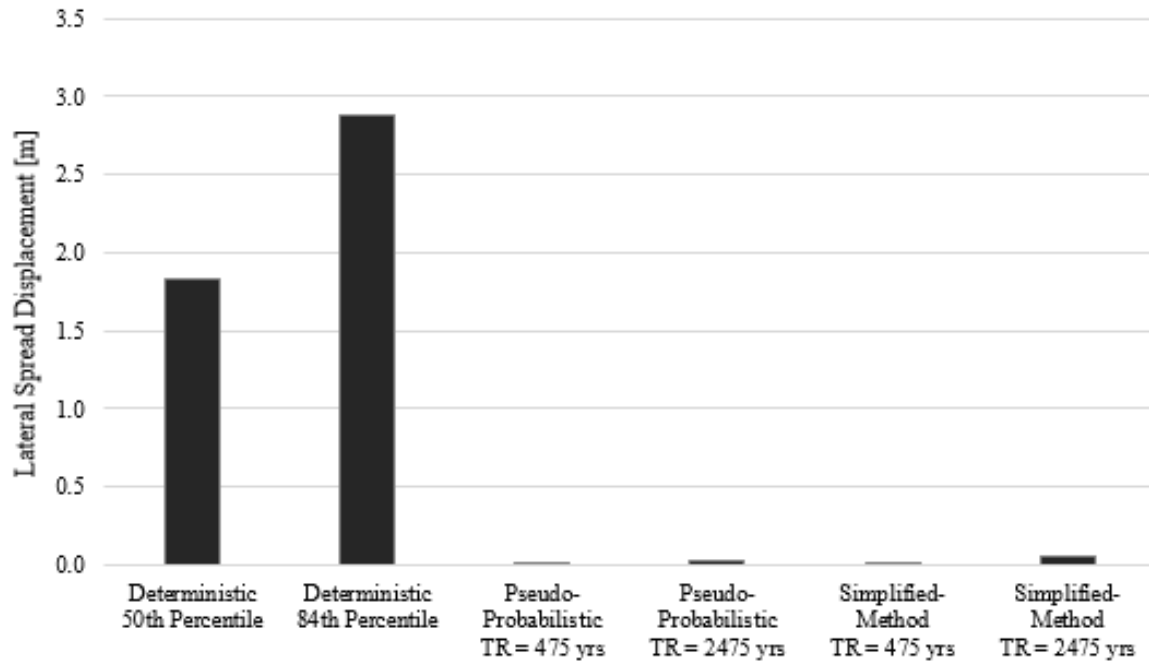


Figure 6-2 Comparison of Deterministic, Pseudo-probabilistic, and Simplified methods for Butte, MT (Latitude 46.033, Longitude -112.533).

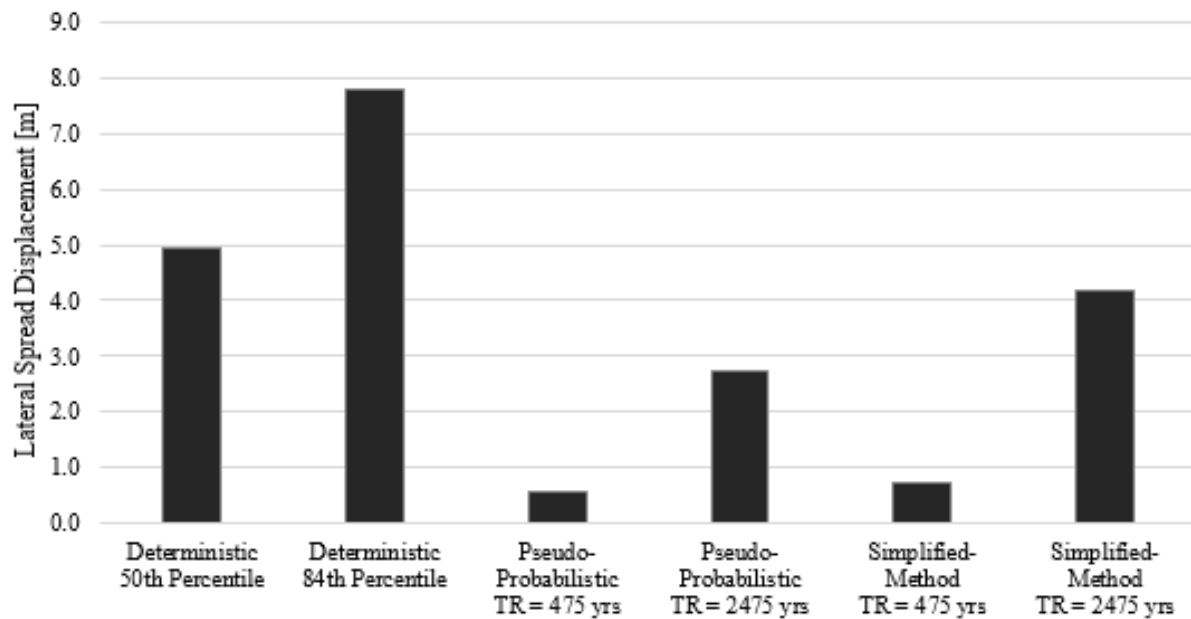


Figure 6-3 Comparison of Deterministic, Pseudo-probabilistic, and Simplified methods for Salt Lake City, UT (Latitude 40.755, Longitude -111.898).

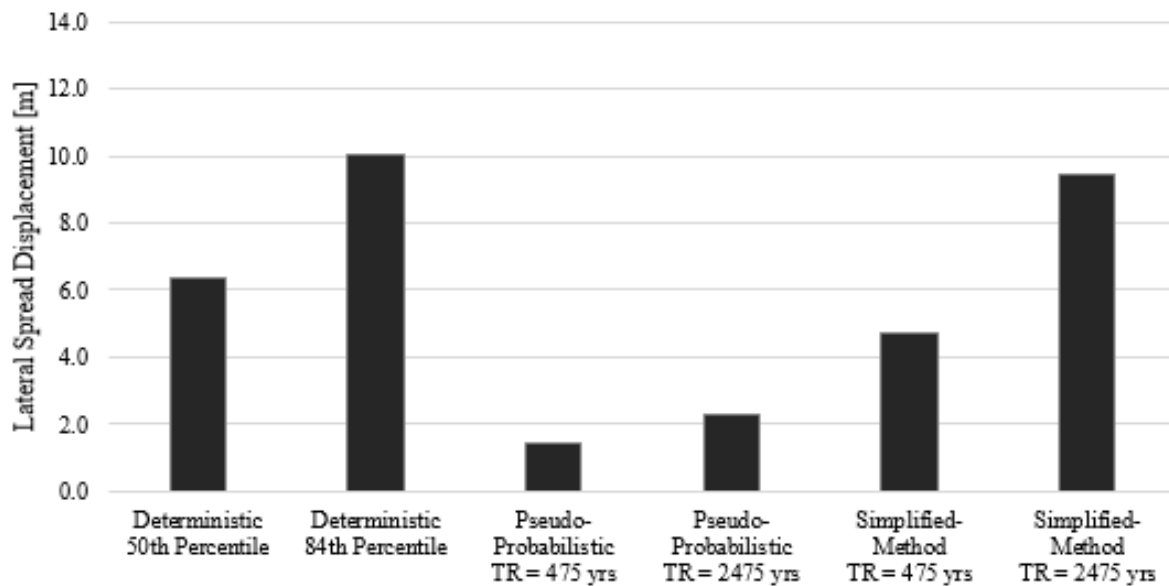


Figure 6-4 Comparison of Deterministic, Pseudo-probabilistic, and Simplified methods for San Francisco, CA (Latitude 37.775, Longitude -122.418).

The different cities are associated with regions of differing seismicity, and the deterministic comparisons with the simplified results yield some interesting conclusions. In the city with low seismicity, Butte seen in Figure 6-2, the deterministic method massively over-predicts the displacements predicted by the simplified and pseudo-probabilistic methods. This result can be attributed to the deterministic procedure not accounting for the likelihood of the Rocker fault rupturing, and predicts a displacement that may have an extremely low probability of occurring. The medium seismicity city, Salt Lake City seen in Figure 6-3, shows as well that the deterministic method predicts displacements higher than the simplified and pseudo-probabilistic procedures. In San Francisco, the high seismicity city, the results are much more similar at the 2475 return period, as can be seen in Figure 6-4. In this area the simplified method for the 2475 year return period predicts a slightly higher displacement than the deterministic mean value. The deterministic 84th percentile still predicts a higher value than the simplified method at the 2475 year return period.

6.3.2 Empirical Seismic Slope Displacement Model

With the completion of the analysis of the different methods described earlier, the data was examined and several charts were created, one for each city. These charts compare, side by side, the results of the simplified, pseudo-probabilistic, and deterministic analyses. These charts can be seen in Figure 6-2, Figure 6-3, and Figure 6-4.

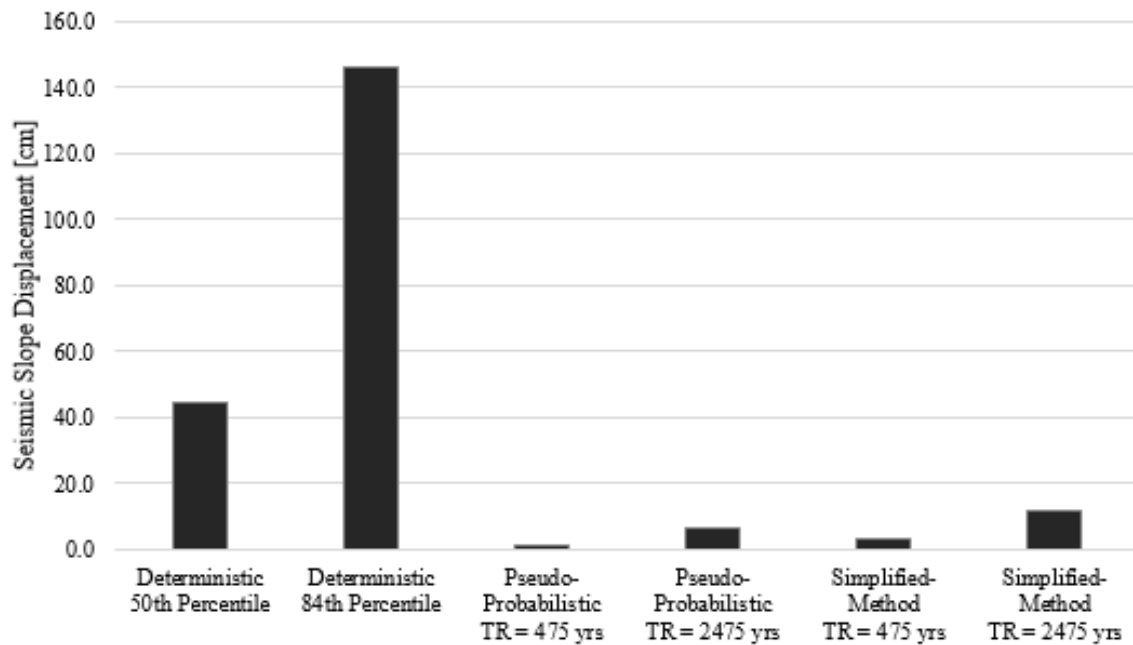


Figure 6-5 Comparison of Deterministic, Pseudo-probabilistic, and Simplified methods for Butte, MT (Latitude 46.033, Longitude -112.533).

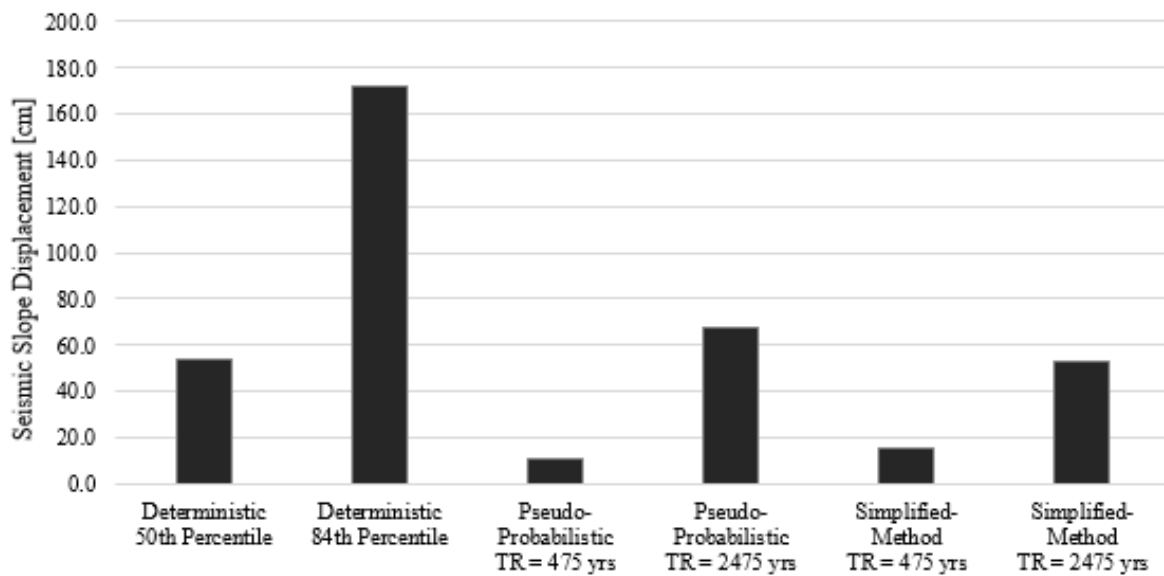


Figure 6-6 Comparison of Deterministic, Pseudo-probabilistic, and Simplified methods for Salt Lake City, UT (Latitude 40.755, Longitude -111.898).

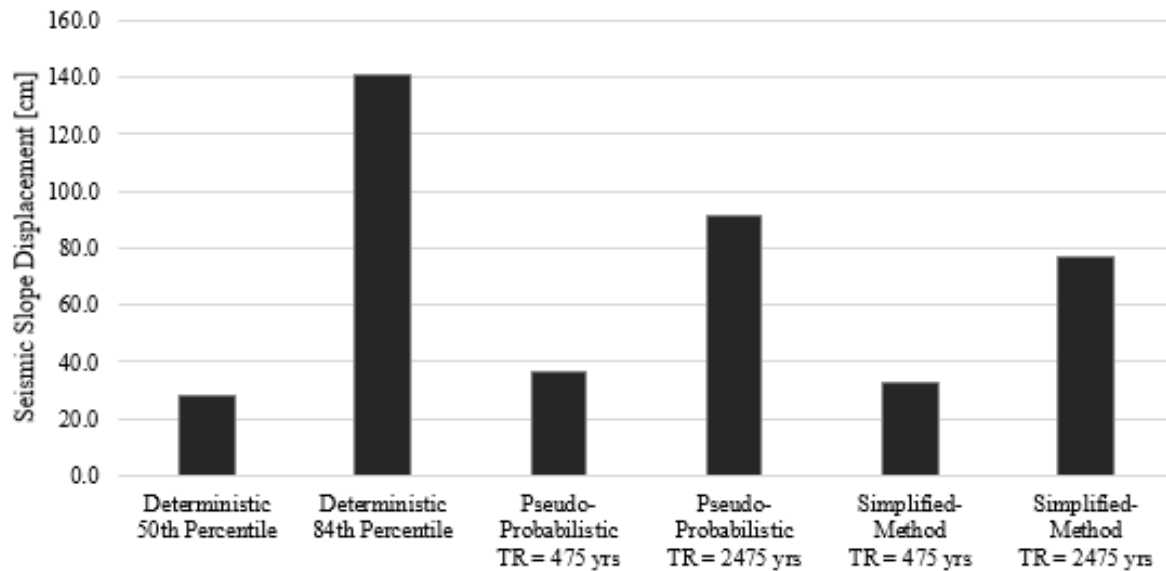


Figure 6-7 Comparison of Deterministic, Pseudo-probabilistic, and Simplified methods for San Francisco, CA (Latitude 37.775, Longitude -122.418).

As observed in the comparison charts for lateral spread displacements, Figure 6-5 for Butte, which is the city of low seismicity in the study showed deterministic values that greatly over-predicting the displacements calculated with the pseudo-probabilistic and simplified methods. Since the deterministic method does not account for the likelihood of the Rocker fault rupturing as explained in the previous section, the displacements calculated with the deterministic method may represent events with a lower probability of occurring. Figure 6-6 shows the results for Salt Lake City with medium seismicity. In this case, the mean deterministic value is very similar to that calculated at the 2475 year return period of the simplified model. The 84th percentile still shows an over-predicted displacements. Lastly, Figure 6-7 shows the results for San Francisco in which the simplified 2475 year return period shows slightly higher displacements than those calculated with the deterministic method, but it is once again over-predicting displacements at the 84th percentile.

6.4 Summary

The results of this study, for both the liquefaction initiation and lateral spread displacement, show that deterministic methods severely over-predicted lateral spread and seismic slope hazard in Butte—an area of low seismicity. The deterministic results also slightly over-predicted lateral spread and seismic slope hazards at high return periods in Salt Lake City—an area of medium seismicity. In San Francisco—an area of high seismicity—the deterministic methods slightly under-predicted liquefaction hazard when considering the 50th percentile ground motions in the deterministic method and the 2,475-year return period in the simplified performance-based procedures. These results suggest that the deterministic results could be used as an upper-bound in areas of high seismicity, but in areas of low seismicity, the deterministic analysis could be optional. Engineers performing analyses in areas of medium to high seismicity could choose to use a deterministic analysis as a “reality check” against the simplified performance-based results. If both deterministic and performance-based methods are considered,

the *lowest* result is the governing value. When deciding whether the deterministic or performance-based results should be accepted, engineers should apply the following rule: the *lowest* value governs.

This rule may seem counter-intuitive, but the idea is not completely foreign—when developing a spectral acceleration design envelope, the lower of the deterministic and probabilistic values is the governing acceleration. If the deterministic value is lower than the performance-based value, the combination of multiple seismic sources in the performance-based analysis may suggest greater lateral spread and seismic slope displacement hazard than would be caused by a single, nearby, governing fault. Therefore, the deterministic analysis provides a type of “reality check” against the performance-based analysis, and the deterministic results should be accepted. If the performance-based value is lower than the deterministic value, the nearby governing fault may have a significantly low likelihood of rupturing and achieving the 50th or 84th percentile ground motions. In this case, the deterministic results could be considered too extreme (especially for some projects which do not need to be designed to withstand such large events). Therefore, the performance-based results should be accepted as a representation of the more *likely* lateral spread and seismic slope displacement hazard.

7.0 CONCLUSIONS

7.1 Summary

The purpose of the research performed was to provide the benefit of the full performance-based probabilistic earthquake hazard analysis, without requiring special software, training, and experience. To accomplish this goal, simplified models of lateral spread and seismic slope displacements were developed that reasonably approximate the results of full performance-based analyses. The objective of this report was to introduce the original models used to determine earthquake hazards (i.e. lateral spread and seismic slope displacements), provide in-depth derivations that demonstrate the development of the simplified methods, validate the simplified models by performing a site-specific analysis for several different sites using the simplified and full models, determine sufficient grid spacings for the development of the liquefaction parameter maps, develop the liquefaction parameter maps for the targeted states at the 475 and 2475 year return periods, compare the results of the simplified methods against deterministic and pseudo-probabilistic procedures, and then introduce a tool for performing the calculations for the simplified methods.

7.2 Findings

7.2.1 Derivation of the Simplified Procedures

The derivations of the simplified liquefaction triggering and lateral spread displacement models show how to approximate a full performance-based analysis using simple calculations and mapped reference parameters. The simplified lateral spread displacement models were based on the Youd et al. (2002) and Bardet et al (2002) empirical models. The simplified seismic slope displacement models were based on the Rathje and Saygili (2009) and Bray and Travararou (2007) empirical models.

7.2.2 Validation of the Simplified Procedures

Ten sites throughout the United States were analyzed using both the full and simplified probabilistic procedures for three different return periods: 475 and 2475 years. Both the simplified liquefaction triggering method and the simplified lateral spread displacement models provided reasonable approximations of their respective full probabilistic methods. This shows that the simplified procedures derived in this report can be used to approximate the results of a full probabilistic procedure without the need for special software, training, and experience.

7.2.3 Evaluation of Grid Spacing

A grid spacing necessary to maintain accuracy in the interpolated results was found for the liquefaction triggering and lateral spread displacement models. These grid spacings resulted on average with a 5% difference between an interpolated value and the result if an analysis were performed at the same site. These grid spacings were very important in creating the grid of points that was used in the analysis.

7.2.4 Map Development

The liquefaction parameter maps were developed for each state by subdividing them into zones and assigning a grid spacing for each zone. The grid points were then generated in ArcMap based on this grid spacing. The points were analyzed using the specified performance-based analytical software (PBLiquefy, EZ-FRISK), then imported into ArcMap and converted to a Kriging raster that is then used to create a contour of the specific reference parameter.

7.2.5 Comparison with Deterministic Procedures

The results of this study show, for the 475 and 2475 year return periods for both the liquefaction initiation and lateral spread displacement, show that deterministic methods severely over-predicted liquefaction hazard in areas of low seismicity. The deterministic results slightly over-predicted liquefaction hazards in areas of medium seismicity. And in areas of high seismicity the deterministic methods slightly under-predicted liquefaction hazard. These results suggest that the deterministic results could be used as an upper-bound in areas of high seismicity, but in areas of low seismicity, the deterministic analysis could be optional. Engineers performing analyses in areas of medium to high seismicity could choose to use a deterministic analysis as a “reality check” against the simplified performance-based results.

REFERENCES

- Bardet, J.P., Tobita, T., Mace, N., and Hu, J. (2002) Regional modeling of liquefaction-induced ground deformation. *Earthquake Spectra*, EERI, 18(1), 19-46.
- Bartlett, S.F., and Youd, T.L. (1995). Empirical prediction of liquefaction-induced lateral spread. *J. Geotech. Eng.*, 121(4), 316-329.
- Bray, J. D., & Travasarou, T. (2007). Simplified procedure for estimating earthquake-induced deviatoric slope displacements. *Journal of Geotechnical and Geoenvironmental Engineering*, 381-392.
- Franke, K.W. and Kramer, S.L. (2014). A procedure for the empirical evaluation of lateral spread displacement hazard curves. *J. Geotech. Geoenviron. Eng.*, ASCE, 140(1), 110-120.
- Franke, K.W., Wright, A.D., and Hatch, C.K. (2014). PBLiquefY: A new analysis tool for the performance-based evaluation of liquefaction triggering. Proceedings, 10th National Conference on Earthquake Engineering, Paper No. 87, EERI, Oakland, CA.
- Kramer, S.L. (2008). Evaluation of liquefaction hazards in Washington State. WSDOT Report WA-RD 668.1, 152 pp.
- Kramer, S.K., Franke, K.W., Huang, Y.-M., and Baska, D. (2007). Performance-based evaluation of lateral spreading displacement. *Proceedings, 4th International Conference on Earthquake Geotechnical Engineering*, Paper No. 1208, Thessaloniki, Greece, June
- Petersen, Mark D., Frankel, Arthur D., Harmsen, Stephen C., Mueller, Charles S., Haller, Kathleen M., Wheeler, Russell L., Wesson, Robert L., Zeng, Yuehua, Boyd, Oliver S., Perkins, David M., Luco, Nicolas, Field, Edward H., Wills, Chris J., and Rukstales, Kenneth S. (2008). Documentation for the 2008 Update of the United States National Seismic Hazard Maps. Open-File Report 2008–1128, United States Geological Survey, Denver, CO: available at website: <http://pubs.usgs.gov/of/2008/1128/>.
- Rathje, E. M., & Saygili, G. (2009, March). Probabilistic Assessment of Earthquake-Induced Sliding Displacements of Natural Slopes. *Bulletin of the New Zealand Society of Earthquake Engineering*, 42(1), 18-27.
- Risk Engineering. (2013). EZ-FRISK, ver. 7.60. Boulder, Colorado.
- USGS. (2008). “USGS 2008 interactive deaggregation.”
<https://geohazards.usgs.gov/deaggint/2008/> (March 26, 2014).
- Youd, T.L., Hansen, C.M., and Bartlett, S.F. (2002). Revised multilinear regression equations for prediction of lateral spread displacement. *J. Geotech. Geoenviron. Eng.*, ASCE, 128(12), 1007-1017.

APPENDIX A: Supplementary Validation Data

Table A. 1 Results from Simplified Seismic Slope Displacement Procedure Based on Rathje & Saygili 2009

	Site	D ^{ref} Rathje & Saygili (cm)			ΔlnD (Rathje & Saygili)			D ^{site} Rathje & Saygili (cm)		
		475 Yrs.	1033 Yrs.	2475 Yrs.	475 Yrs.	1033 Yrs.	2475 Yrs.	475 Yrs.	1033 Yrs.	2475 Yrs.
$k_y^{\text{ref}}=0.1$ $k_y^{\text{site}}=0.1$	Butte	<0.5	<0.5	0.7	15.3	3.3	1.5	0.0	13.8	3.2
	Charleston	<0.5	12.5	81.8	2.0	0.4	0.0	3.6	18.1	81.8
	Eureka	96.0	280.1	670.9	0.0	0.0	0.0	96.0	280.1	670.9
	Memphis	0.5	17.5	92.6	1.8	0.5	0.0	3.0	28.2	92.6
	Portland	2.9	18.5	72.9	1.3	0.6	0.2	11.1	34.3	86.0
	Salt Lake City	2.6	24.0	87.6	1.2	0.3	0.0	8.8	31.2	87.6
	San Francisco	47.6	105.5	205.0	0.2	0.0	0.0	55.8	105.5	205.0
	San Jose	36.7	73.7	137.8	0.1	0.0	0.0	41.1	73.7	137.8
	Santa Monica	22.2	57.2	126.6	0.3	0.0	0.0	30.4	57.2	126.6
	Seattle	12.5	42.7	117.8	0.6	0.1	0.0	21.9	49.4	117.8
$k_y^{\text{ref}}=0.1$ $k_y^{\text{site}}=0.2$	Butte	<0.5	<0.5	0.7	-33.7	-6.1	-1.7	0.0	0.0	0.1
	Charleston	<0.5	12.5	81.8	-2.6	-1.5	-1.2	0.0	2.7	25.6
	Eureka	96.0	280.1	670.9	-1.4	-0.9	-0.5	24.4	119.3	387.1
	Memphis	0.5	17.5	92.6	-2.2	-1.5	-1.5	0.1	3.9	21.3
	Portland	2.9	18.5	72.9	-1.5	-1.5	-1.6	0.7	4.1	15.0
	Salt Lake City	2.6	24.0	87.6	-1.4	-1.5	-1.3	0.6	5.1	24.8
	San Francisco	47.6	105.5	205.0	-1.6	-1.5	-1.2	9.8	24.1	63.8
	San Jose	36.7	73.7	137.8	-1.6	-1.5	-1.2	7.4	16.7	40.5
	Santa Monica	22.2	57.2	126.6	-1.5	-1.5	-1.1	4.8	12.2	40.5
	Seattle	12.5	42.7	117.8	-1.5	-1.6	-1.3	2.8	8.7	31.6
$k_y^{\text{ref}}=0.1$ $k_y^{\text{site}}=0.3$	Butte	<0.5	<0.5	0.7	-347.7	-66.1	-14.1	0.0	0.0	0.0
	Charleston	<0.5	12.5	81.8	-26.2	-3.5	-2.3	0.0	0.4	8.5
	Eureka	96.0	280.1	670.9	-2.6	-1.7	-1.2	7.1	49.7	212.0
	Memphis	0.5	17.5	92.6	-20.9	-3.8	-2.8	0.0	0.4	5.8
	Portland	2.9	18.5	72.9	-9.8	-4.4	-3.2	0.0	0.2	3.0
	Salt Lake City	2.6	24.0	87.6	-8.1	-3.3	-2.4	0.0	0.9	7.8
	San Francisco	47.6	105.5	205.0	-3.2	-2.8	-2.3	2.0	6.5	21.2
	San Jose	36.7	73.7	137.8	-3.1	-2.8	-2.4	1.6	4.5	12.9
	Santa Monica	22.2	57.2	126.6	-3.4	-2.9	-2.2	0.8	3.1	13.7
	Seattle	12.5	42.7	117.8	-4.1	-3.2	-2.5	0.2	1.8	9.6
$k_y^{\text{ref}}=0.1$ $k_y^{\text{site}}=0.4$	Butte	<0.5	<0.5	0.7	-1368.6	-277.9	-60.2	0.0	0.0	0.0
	Charleston	<0.5	12.5	81.8	-112.9	-7.7	-3.3	0.0	0.0	3.2
	Eureka	96.0	280.1	670.9	-3.8	-2.5	-1.8	2.1	22.0	115.5
	Memphis	0.5	17.5	92.6	-90.1	-9.5	-4.2	0.0	0.0	1.4
	Portland	2.9	18.5	72.9	-40.8	-13.1	-5.8	0.0	0.0	0.2
	Salt Lake City	2.6	24.0	87.6	-32.6	-6.5	-3.5	0.0	0.0	2.6
	San Francisco	47.6	105.5	205.0	-5.8	-4.2	-3.3	0.1	1.6	7.8
	San Jose	36.7	73.7	137.8	-5.6	-4.3	-3.4	0.1	1.0	4.5
	Santa Monica	22.2	57.2	126.6	-7.0	-4.5	-3.2	0.0	0.6	5.1
	Seattle	12.5	42.7	117.8	-11.6	-5.7	-3.7	0.0	0.1	3.1
$k_y^{\text{ref}}=0.1$ $k_y^{\text{site}}=0.5$	Butte	<0.5	<0.5	0.7	-3757.7	-798.4	-180.7	0.0	0.0	0.0
	Charleston	<0.5	12.5	81.8	-333.6	-18.8	-4.4	0.0	0.0	1.1
	Eureka	96.0	280.1	670.9	-5.6	-3.3	-2.3	0.3	10.4	64.5
	Memphis	0.5	17.5	92.6	-267.9	-25.1	-6.6	0.0	0.0	0.1
	Portland	2.9	18.5	72.9	-122.8	-36.8	-12.3	0.0	0.0	0.0
	Salt Lake City	2.6	24.0	87.6	-98.0	-14.7	-4.9	0.0	0.0	0.7
	San Francisco	47.6	105.5	205.0	-12.1	-6.7	-4.4	0.0	0.1	2.6
	San Jose	36.7	73.7	137.8	-11.2	-6.8	-4.7	0.0	0.1	1.3
	Santa Monica	22.2	57.2	126.6	-16.6	-7.7	-4.3	0.0	0.0	1.8
	Seattle	12.5	42.7	117.8	-31.9	-11.8	-5.2	0.0	0.0	0.6

Table A. 2 Results from Simplified Seismic Slope Displacement Procedure based on Bray & Travararou 2007

k _y k _y ^s		Site	Latitude	Longitude	Full PB Method Rathje & Saygili			Full PB Method Bray & Travararou		
					D ^{site} (cm)			D ^{site} (cm)		
					475 Yrs	1033 Yrs	2475 Yrs	475 Yrs	1033 Yrs	2475 Yrs
k _y k _y ^s	k _y ^{ref} =0.1 k _y ^{site} =0.1	Butte	46.003	-112.533	<0.5	0.8	3.3	1.0	2.4	5.3
		Charleston	32.726	-79.931	1.4	19.8	90.9	3.1	15.3	50.5
		Eureka	40.802	-124.162	112.4	313.9	759.3	48.2	112.5	227.4
		Memphis	35.149	-90.048	2.6	28.8	109.4	4.2	16.5	44.4
		Portland	45.523	-122.675	11.0	41.5	121.3	8.1	17.3	34.0
		Salt Lake City	40.755	-111.898	7.7	33.6	99.3	7.8	21.7	52.9
		San Francisco	37.775	-122.418	66.0	132.3	246.2	29.3	48.1	76.8
		San Jose	37.339	-121.893	48.9	94.3	172.1	28.4	44.4	67.8
		Santa Monica	34.015	-118.492	35.0	74.5	150.2	21.8	38.5	68.5
		Seattle	47.53	-122.3	24.7	65.9	158.7	15.9	29.8	56.6
k _y k _y ^s	k _y ^{ref} =0.1 k _y ^{site} =0.2	Butte	46.003	-112.533	<0.5	<0.5	<0.5	<0.5	<0.5	1.1
		Charleston	32.726	-79.931	<0.5	2.7	25.1	0.6	3.7	14.9
		Eureka	40.802	-124.162	27.7	112.1	330.0	13.7	37.8	86.5
		Memphis	35.149	-90.048	<0.5	3.7	24.1	0.8	3.9	12.3
		Portland	45.523	-122.675	<0.5	3.9	16.8	1.7	3.9	8.4
		Salt Lake City	40.755	-111.898	<0.5	5.4	26.3	1.7	5.4	15.5
		San Francisco	37.775	-122.418	10.6	25.5	57.0	7.4	12.7	21.7
		San Jose	37.339	-121.893	8.3	17.8	36.9	7.2	11.7	18.9
		Santa Monica	34.015	-118.492	4.9	14.0	38.2	5.3	10.2	20.1
		Seattle	47.53	-122.3	2.6	9.9	33.2	3.7	7.4	15.8
k _y k _y ^s	k _y ^{ref} =0.1 k _y ^{site} =0.3	Butte	46.003	-112.533	<0.5	<0.5	<0.5	<0.5	<0.5	<0.5
		Charleston	32.726	-79.931	<0.5	<0.5	7.9	<0.5	1.4	6.3
		Eureka	40.802	-124.162	7.7	44.9	159.8	5.7	17.3	42.7
		Memphis	35.149	-90.048	<0.5	<0.5	6.3	<0.5	1.5	5.0
		Portland	45.523	-122.675	<0.5	<0.5	2.3	0.6	1.4	3.2
		Salt Lake City	40.755	-111.898	<0.5	0.9	8.1	0.6	2.1	6.5
		San Francisco	37.775	-122.418	1.7	5.8	16.2	2.8	5.1	9.0
		San Jose	37.339	-121.893	1.4	3.9	9.8	2.8	4.7	7.7
		Santa Monica	34.015	-118.492	0.7	3.1	11.8	2.0	4.0	8.5
		Seattle	47.53	-122.3	<0.5	1.5	8.5	1.3	2.9	6.5
k _y k _y ^s	k _y ^{ref} =0.1 k _y ^{site} =0.4	Butte	46.003	-112.533	<0.5	<0.5	<0.5	<0.5	<0.5	<0.5
		Charleston	32.726	-79.931	<0.5	<0.5	2.5	<0.5	0.7	3.2
		Eureka	40.802	-124.162	2.1	19.1	82.4	2.9	9.3	24.2
		Memphis	35.149	-90.048	<0.5	<0.5	1.4	<0.5	0.7	2.5
		Portland	45.523	-122.675	<0.5	<0.5	<0.5	<0.5	0.6	1.5
		Salt Lake City	40.755	-111.898	<0.5	<0.5	2.6	<0.5	1.0	3.3
		San Francisco	37.775	-122.418	<0.5	1.1	4.7	1.3	2.5	4.5
		San Jose	37.339	-121.893	<0.5	0.7	2.6	1.3	2.3	3.9
		Santa Monica	34.015	-118.492	<0.5	0.5	4.0	0.9	2.0	4.3
		Seattle	47.53	-122.3	<0.5	<0.5	2.2	0.6	1.4	3.2
		Butte	46.003	-112.533	<0.5	<0.5	<0.5	<0.5	<0.5	<0.5
		Charleston	32.726	-79.931	<0.5	<0.5	0.6	<0.5	<0.5	1.8

Table A. 3 Results from Full Probabilistic Seismic Slope Displacement Procedure

k _y ^{ref} =0.1 k _y ^{site} =0.5	Memphis	35.149	-90.048	<0.5	<0.5	<0.5	<0.5	<0.5	1.4
	Portland	45.523	-122.675	<0.5	<0.5	<0.5	<0.5	<0.5	0.8
	Salt Lake City	40.755	-111.898	<0.5	<0.5	0.6	<0.5	0.5	1.9
	San Francisco	37.775	-122.418	<0.5	<0.5	1.1	0.7	1.4	2.5
	San Jose	37.339	-121.893	<0.5	<0.5	0.6	0.7	1.2	2.2
	Santa Monica	34.015	-118.492	<0.5	<0.5	1.2	0.5	1.1	2.5
	Seattle	47.53	-122.3	<0.5	<0.5	<0.5	<0.5	0.7	1.8

Table A. 4 Faults Considered in Deterministic Analysis

				Median Acceleration			(Median + 1 St. Dev) Acceleration		
				$T_R = 1033$			$T_R = 1033$		
				PGA	F_{pga}	a_{max}	PGA	F_{pga}	a_{max}
San Francisco	Seismic Source	Dist (km)	Mag						
	1 Northern San Andreas	10.77	8.05	0.3175	1.183	0.3754	0.5426	1.0	0.5426
	2 San Gregorio Connected	16.64	7.5	0.2139	1.372	0.2935	0.3660	1.134	0.4150
	3 Hayward-Rodgers Creek	18.23	7.33	0.1918	1.416	0.2717	0.3282	1.172	0.3846
	4 Mount Diablo Thrust	36.08	6.7	0.1050	1.590	0.1670	0.1811	1.438	0.2604
Salt Lake City	5 Calaveras	34.28	7.03	0.0981	1.6	0.1570	0.1682	1.464	0.2462
	1 Wasatch Fault, SLC Section	1.02	7	0.5911	1.0	0.5911	1.0050	1.0	1.0050
	2 West Valley Fault Zone	2.19	6.48	0.5694	1.0	0.5694	0.9842	1.0	0.9842
	3 Morgan Fault	25.04	6.52	0.0989	1.6	0.1583	0.1713	1.457	0.2497
	4 Great Salt Lake Fault zone, Antelope Section	25.08	6.93	0.1016	1.597	0.1622	0.1742	1.452	0.2529
Butte	5 Oquirrh-Southern, Oquirrh Mountain Fault	30.36	7.17	0.0958	1.6	0.1532	0.1641	1.472	0.2415
	1 Rocker Fault	4.92	6.97	0.5390	1.0	0.5390	0.9202	1.0	0.9202
	2 Georgia Gulch Fault	45.91	6.42	0.0435	1.6	0.0696	0.0754	1.6	0.1206
	3 Helena Valley Fault	75.56	6.6	0.0294	1.6	0.0470	0.0507	1.6	0.0812
	4 Canyon Ferry Fault	81.32	6.92	0.0327	1.6	0.0523	0.0561	1.6	0.0898
	5 Blacktail Fault	84.27	6.94	0.0317	1.6	0.0508	0.0545	1.6	0.0872
	6 Madison Fault	86.51	7.45	0.0420	1.6	0.0671	0.0719	1.6	0.1150

Table A. 5 Characteristics of Rocker Fault (near Butte) and Calculations to Determine PGA and M_w .

* M_w calculated based on

Wells and Coppersmith (1994):

Length = 43 km

(Use "all" slip type, because it's a normal fault and the # of normal events is small)

*PGA calculated based on NGA equations (Linda Al Atik, PEER 2009)

BA08, CB08, and CY08 used with equal weighting

M_w =	6.97	
Dip =	70	degrees
Depth to bottom of rupture =	16	km
R_x =	4.92	km
Z_TOR =	0	km
Width =	17.03	km
R_jb =	0	km
R_rup =	1.68	km
V_s30 =	760	m/s
U =	0	
F_RV =	0	
F_NM =	1	
F_HW =	1	
F_measured =	0	
Z_1 =	DEFAULT	
Z_2.5 =	DEFAULT	
F_AS =	0	
HW Taper =	1	
--> PGA (50%) =	0.5390	g
--> PGA (84%) =	0.9202	g

(Another fault near Butte, has a dip of 70-75 degrees)

(Assumed)

(measured using Google Earth)

(Assumed)

(Assuming the site is on the hanging wall side)

(From NGA spreadsheet)

(From NGA spreadsheet)

APPENDIX B: Sample Lateral Spread Parameter Maps

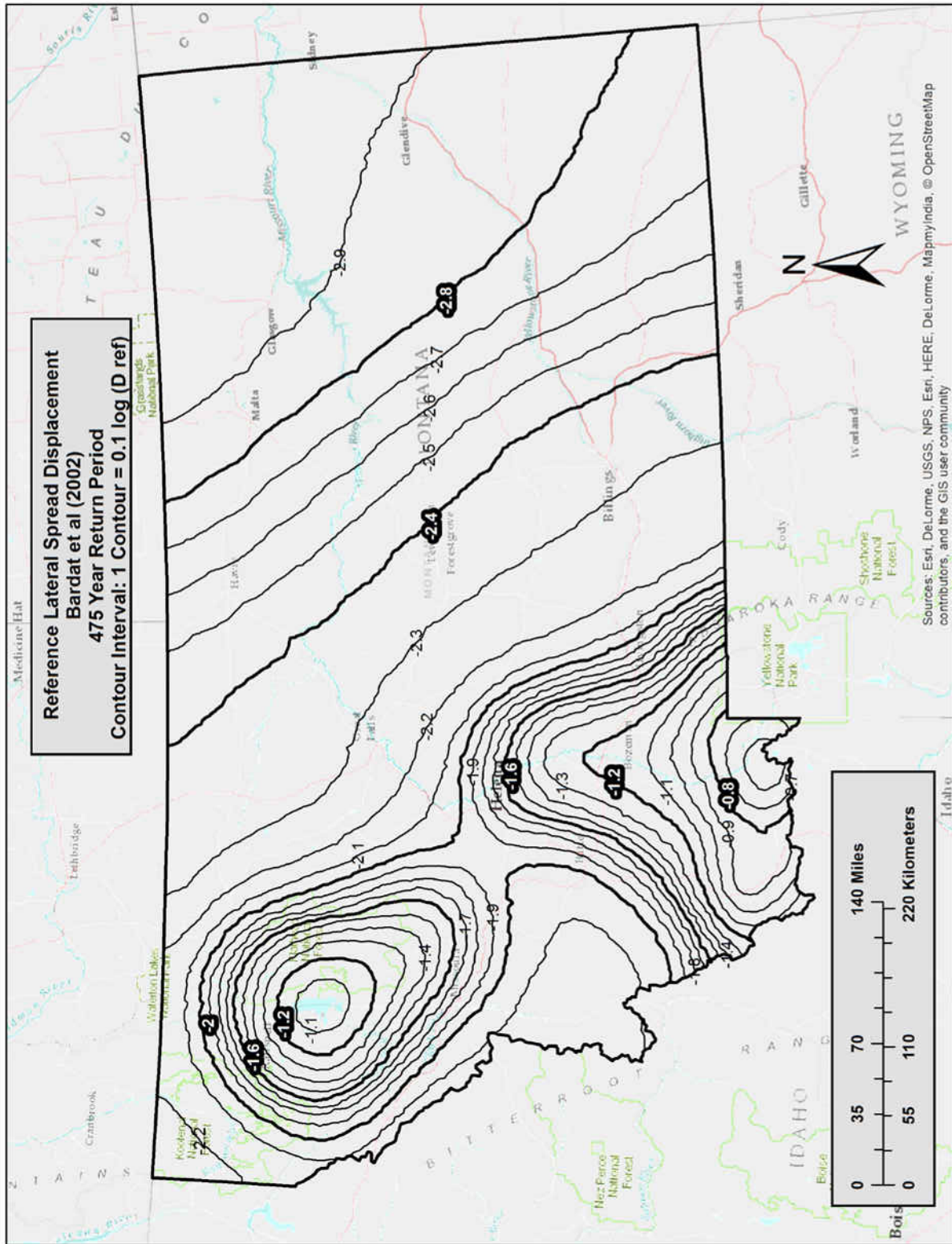


Figure B- 1 Lateral Spread Parameter (D_H^{ref}) Map for Montana (Tr = 475)

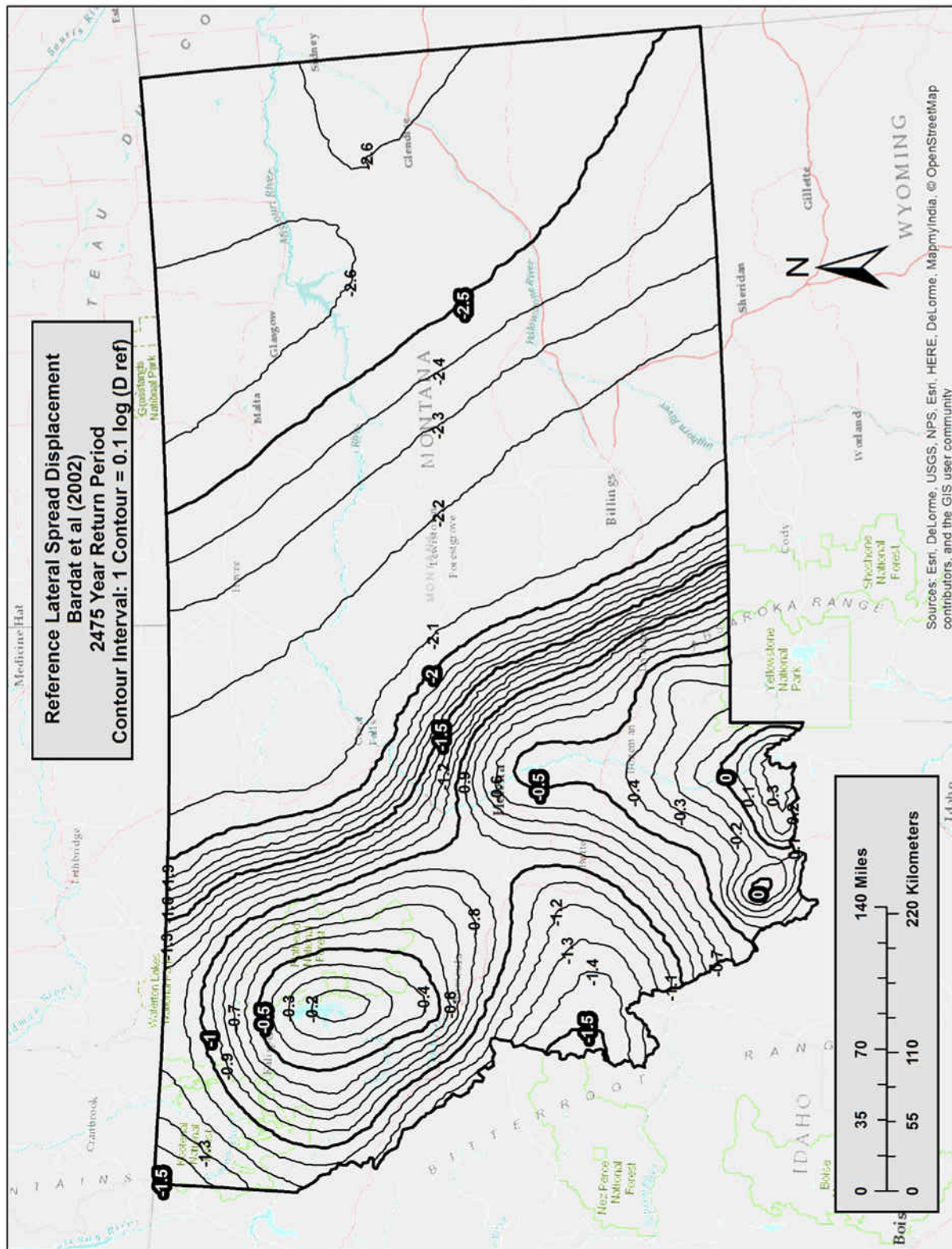
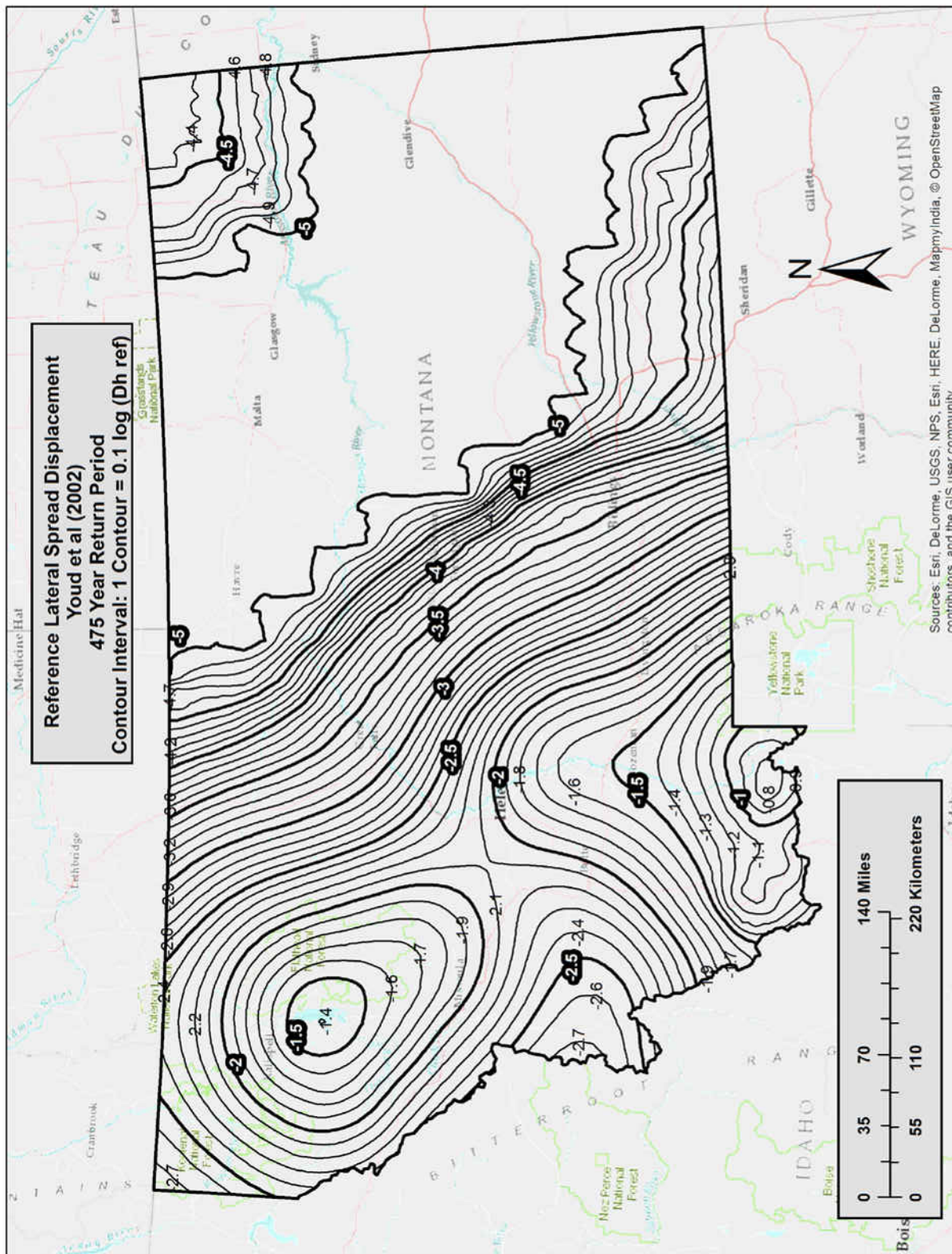


Figure B- 2 Lateral Spread Parameter (D_H^{ref}) Map for Montana ($Tr = 2,475$)



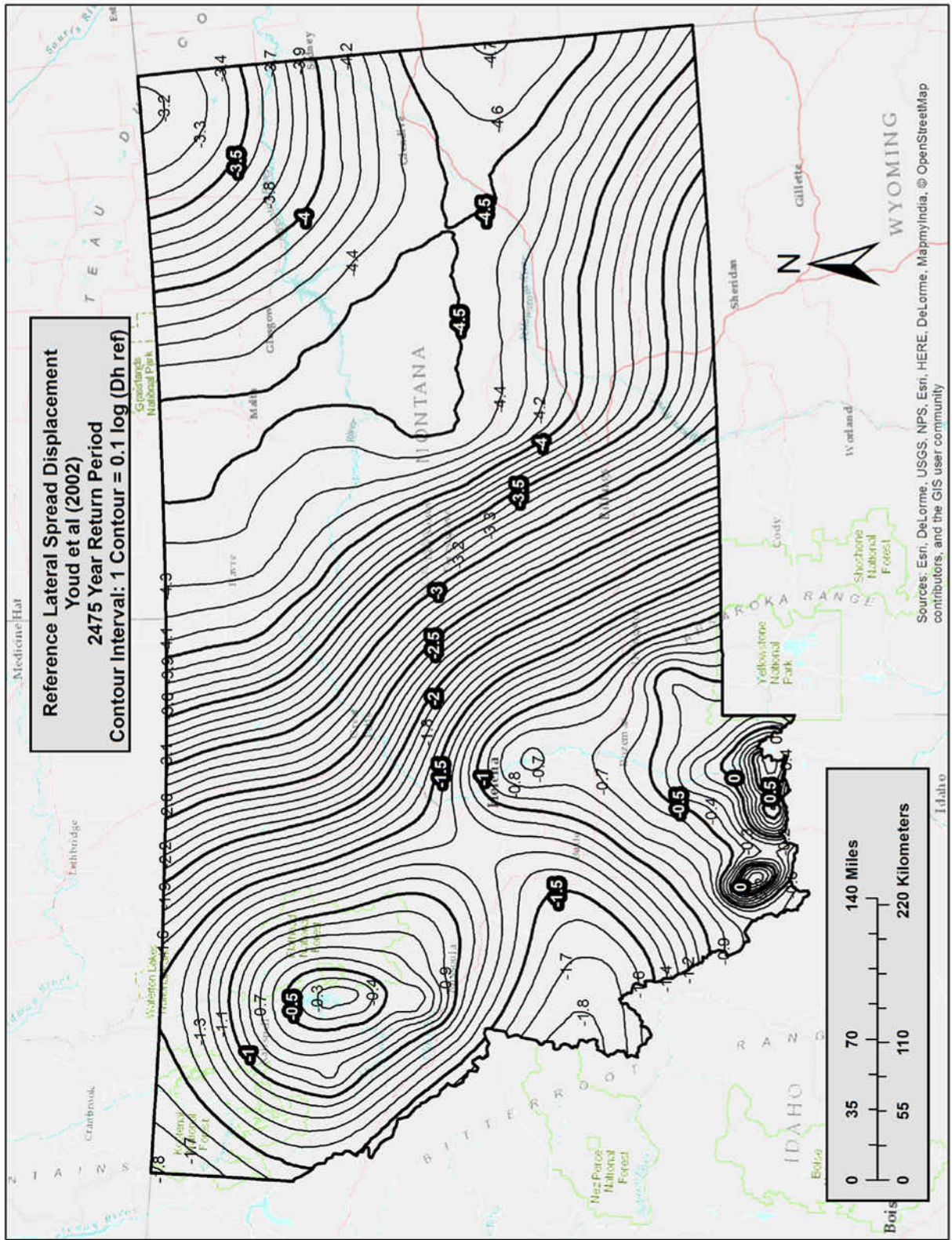


Figure B- 4 Lateral Spread Parameter (D_H^{ref}) Map for Montana ($Tr = 2,475$)

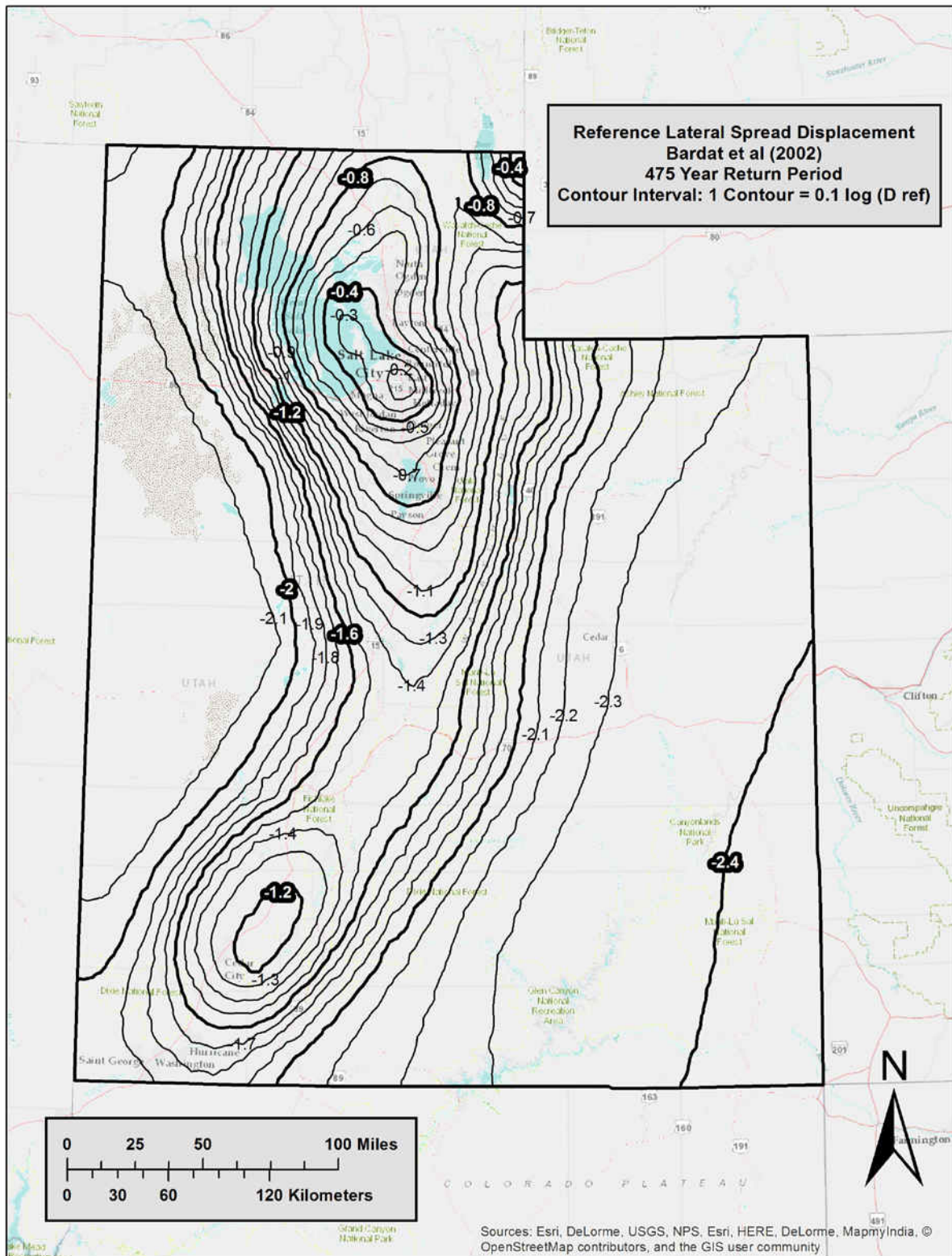


Figure B- 5 Lateral Spread Parameter (D_H^{ref}) Map for Utah ($T_r = 475$)

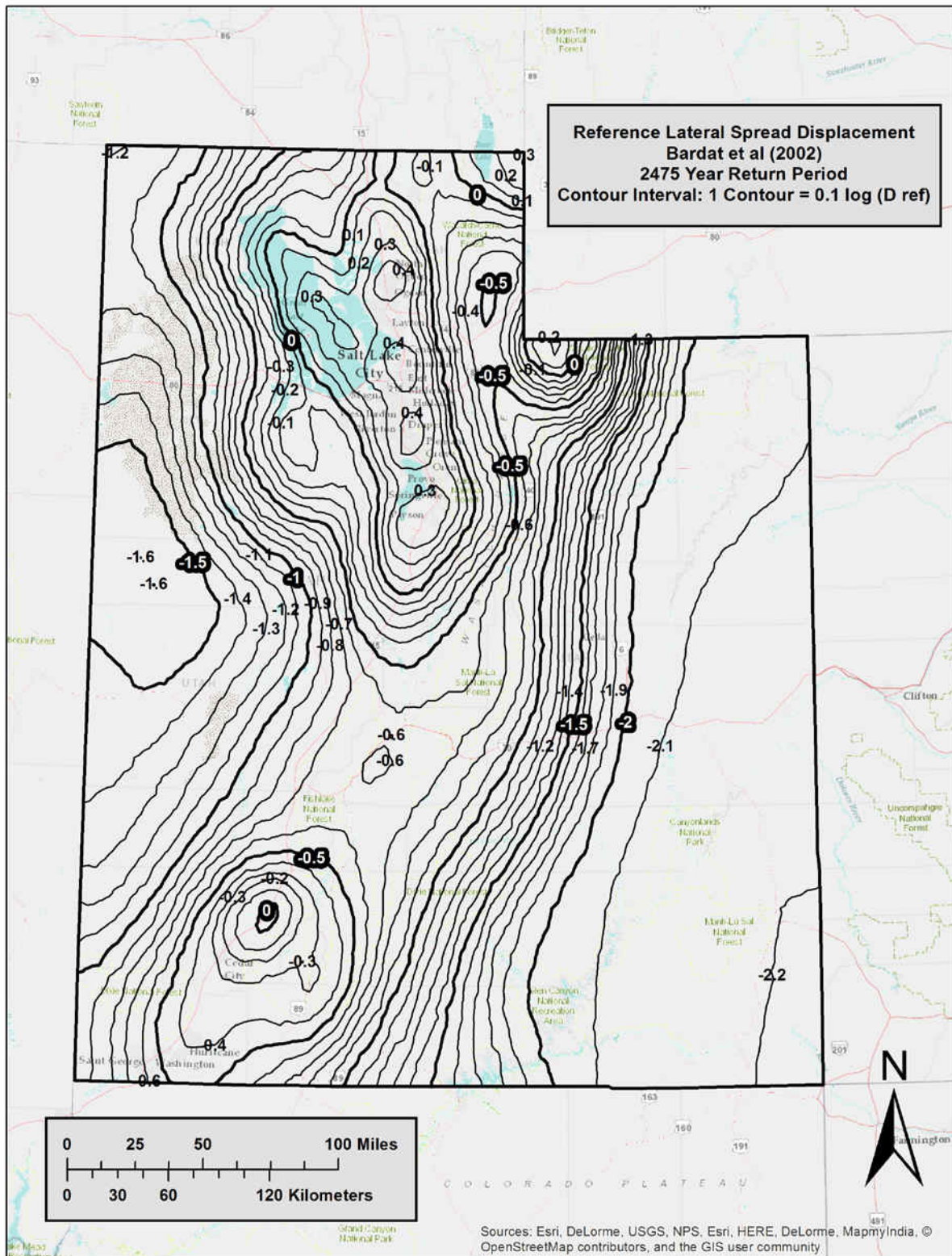


Figure B- 6 Lateral Spread Parameter (D_H^{ref}) Map for Utah ($Tr = 2,475$)

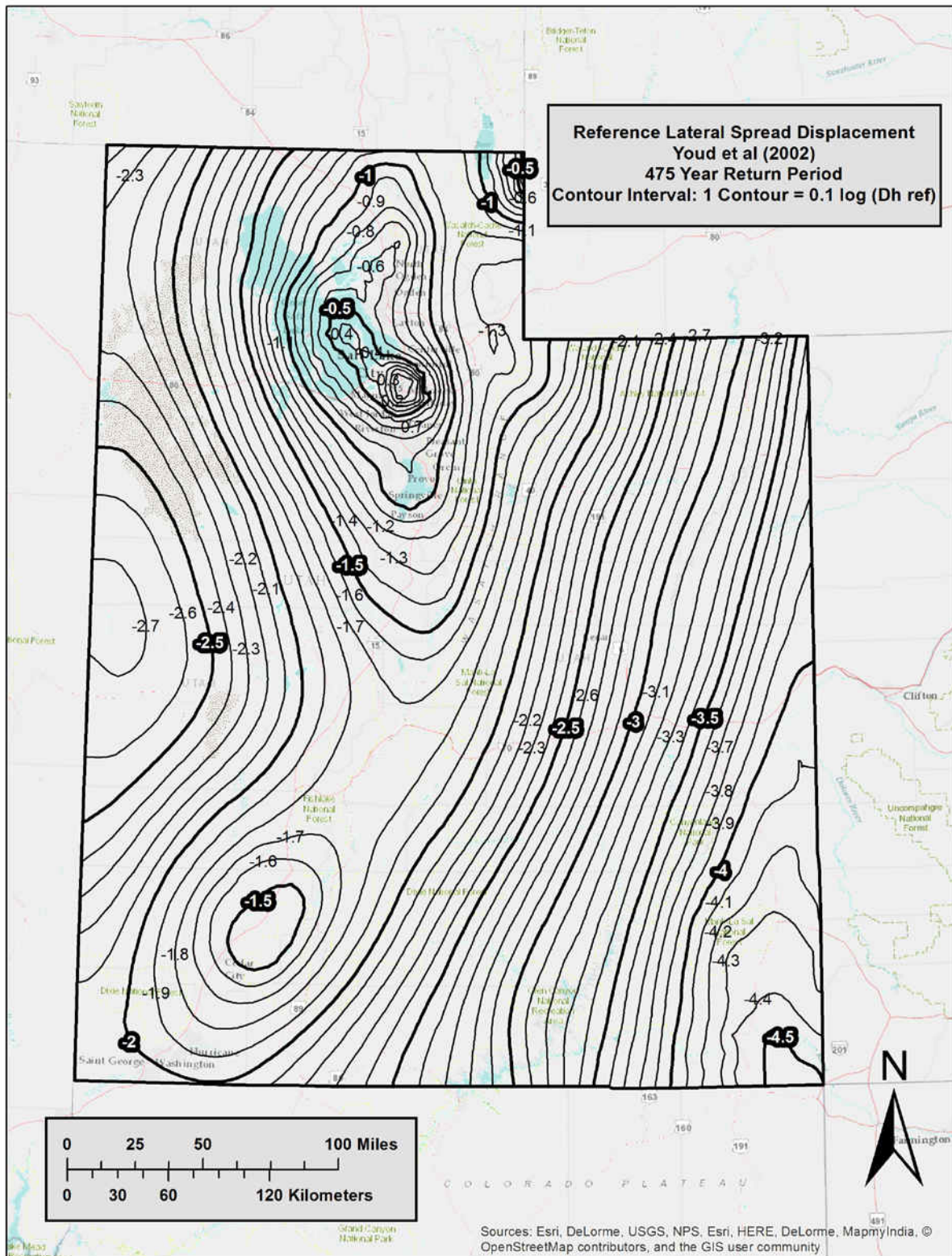


Figure B- 7 Lateral Spread Parameter (D_H^{ref}) Map for Utah ($T_r = 475$)

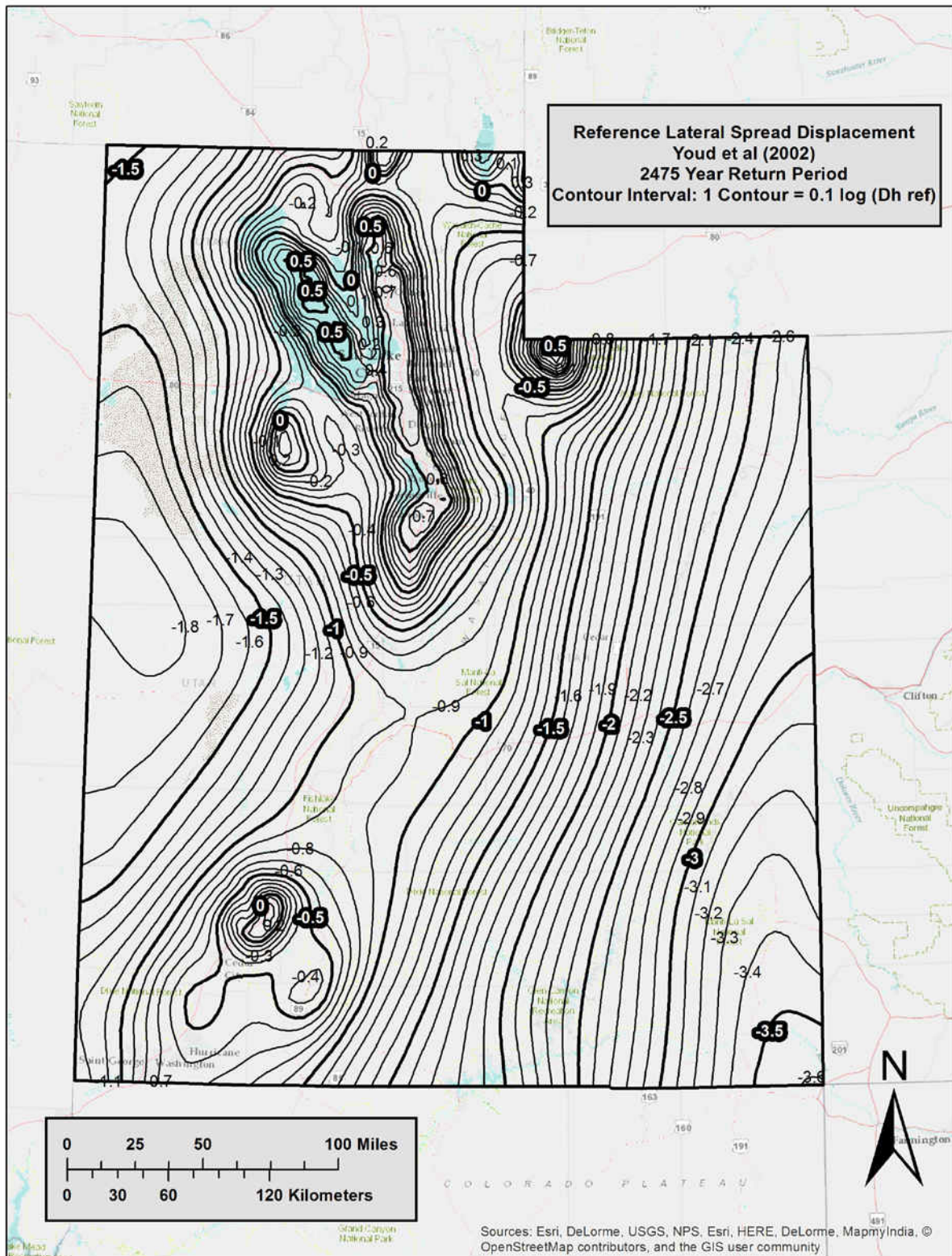


Figure B- 8 Lateral Spread Parameter (D_H^{ref}) Map for Utah ($T_r = 2,475$)

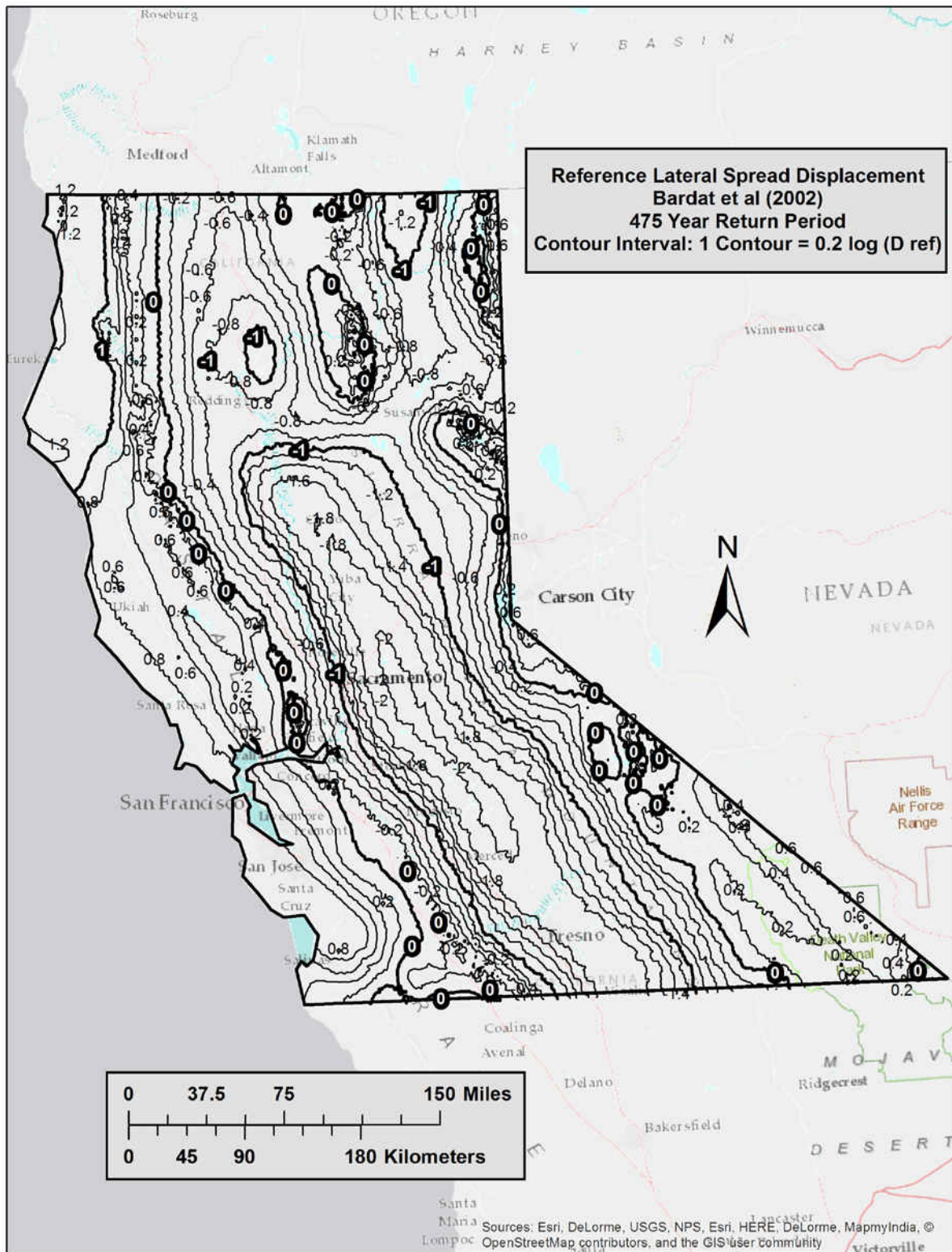


Figure B- 9 Lateral Spread Parameter (D_H^{ref}) Map for Northern California ($T_r = 475$)

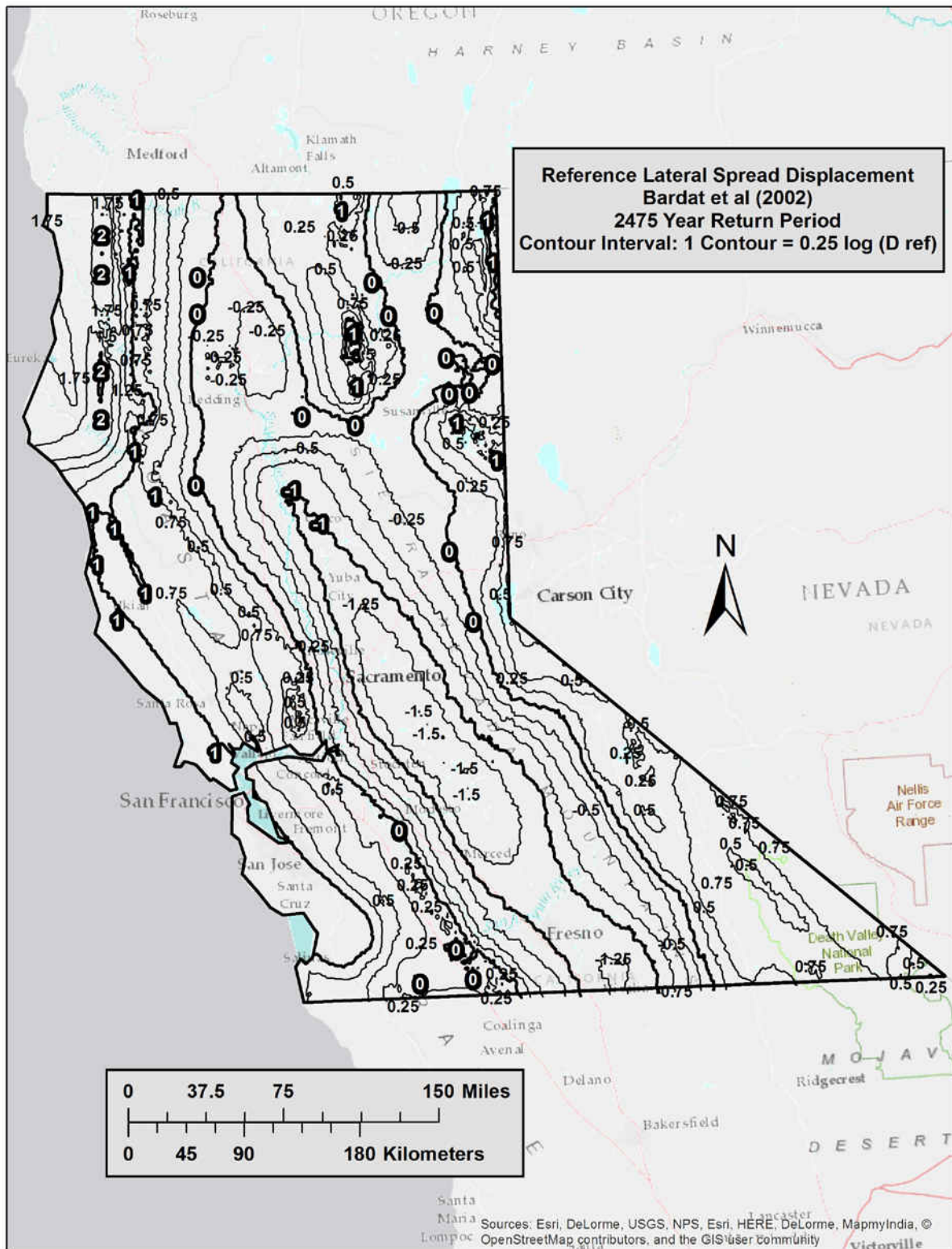


Figure B- 10 Lateral Spread Parameter (D_H^{ref}) Map for Northern California ($T_r = 2,475$)

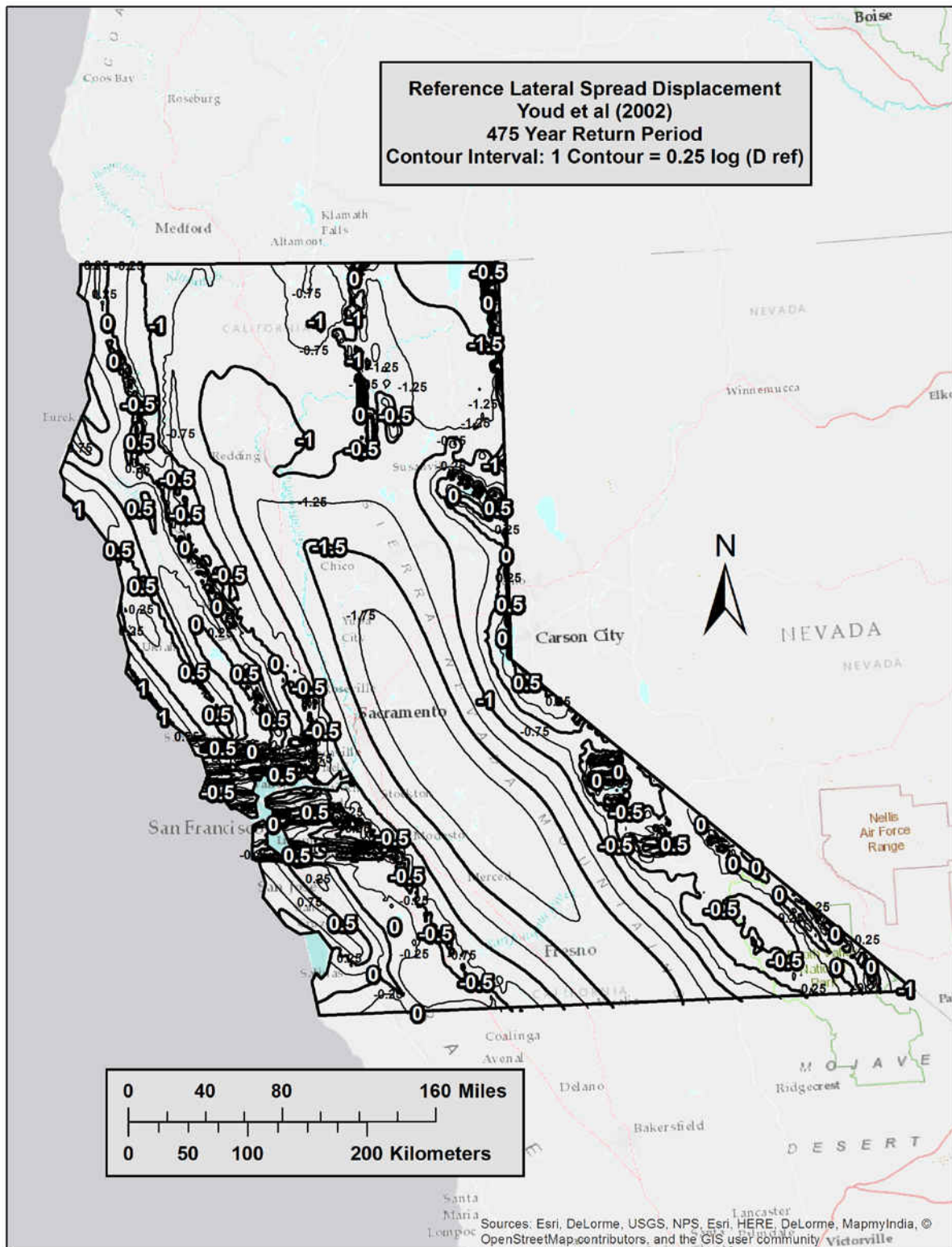
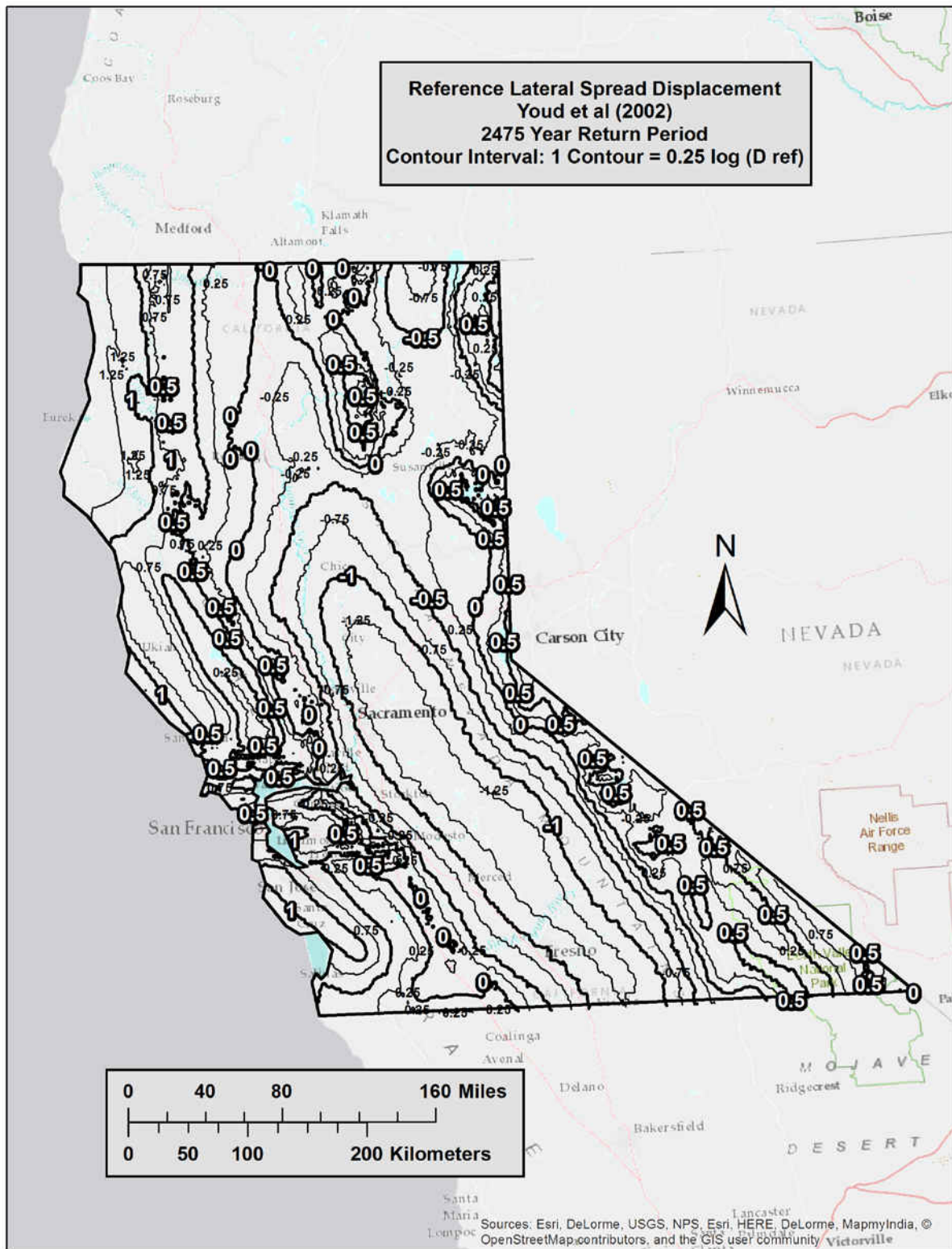


Figure B- 11 Lateral Spread Parameter (D_H^{ref}) Map for Northern California ($T_r = 475$)



APPENDIX C: Sample Seismic Slope Displacement Maps

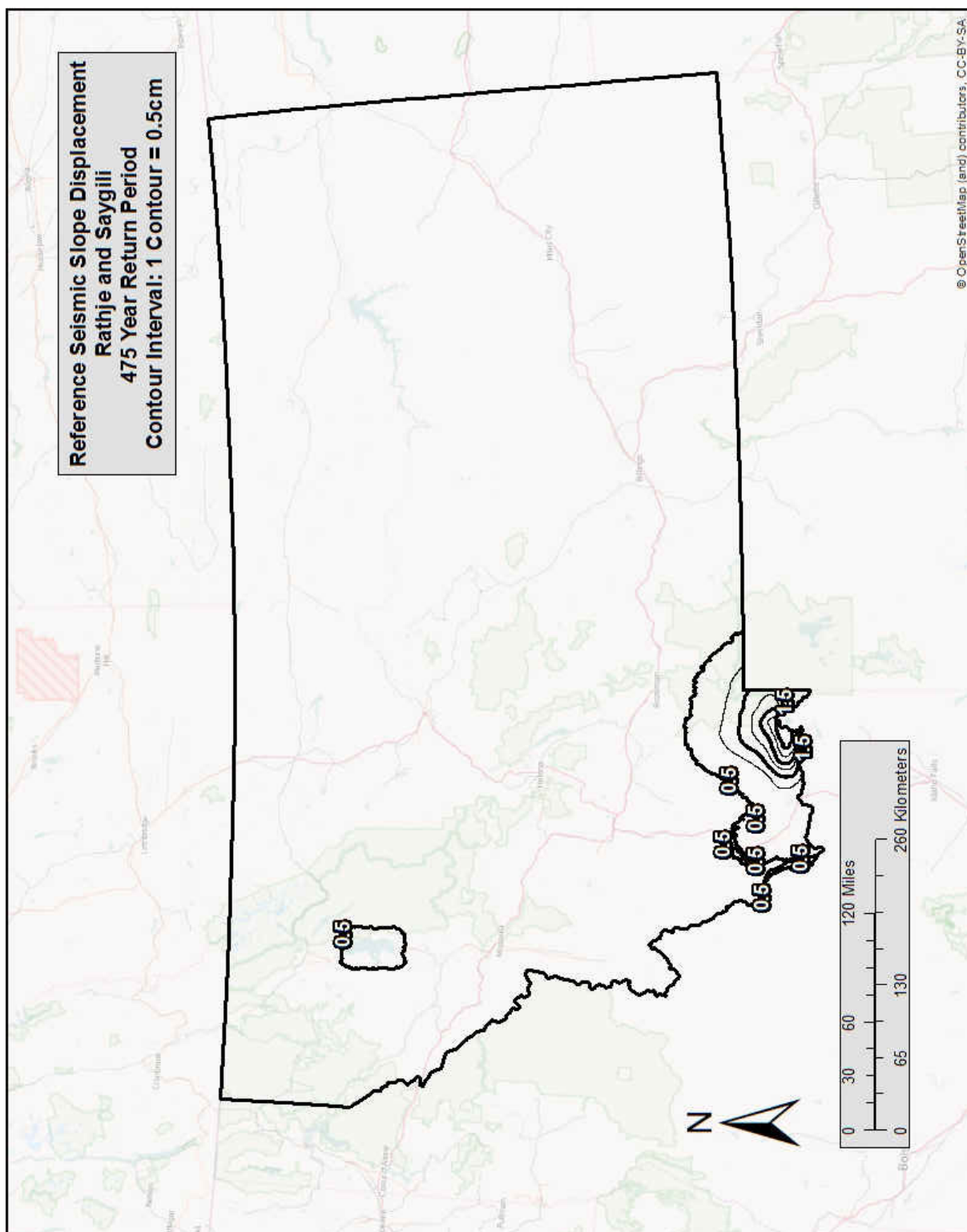


Figure C- 1 Seismic Slope Displacement (D^{ref}) Map for Montana (Tr = 475)

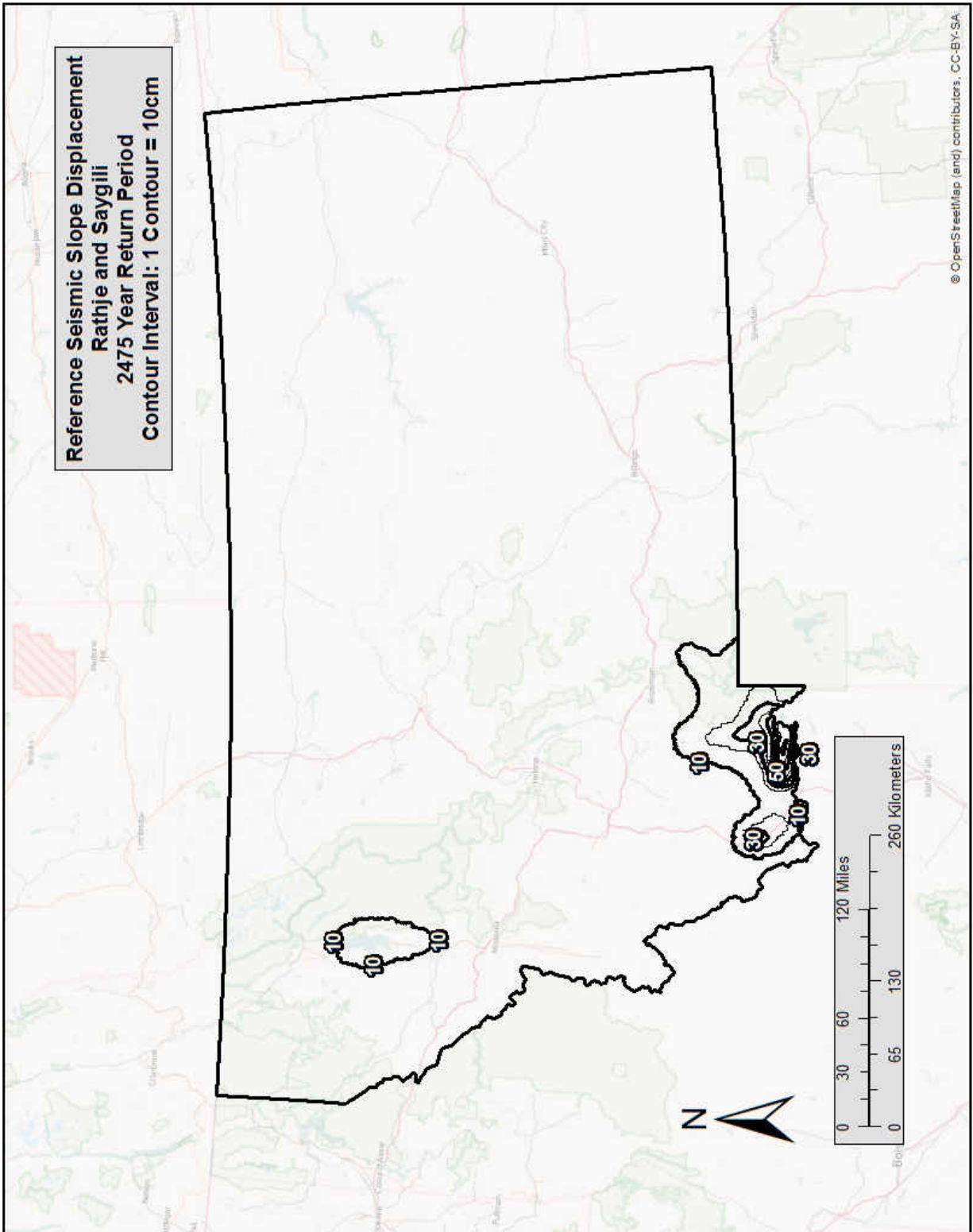


Figure C- 2 Seismic Slope Displacement (D^{ref}) Map for Montana ($Tr = 2,475$)

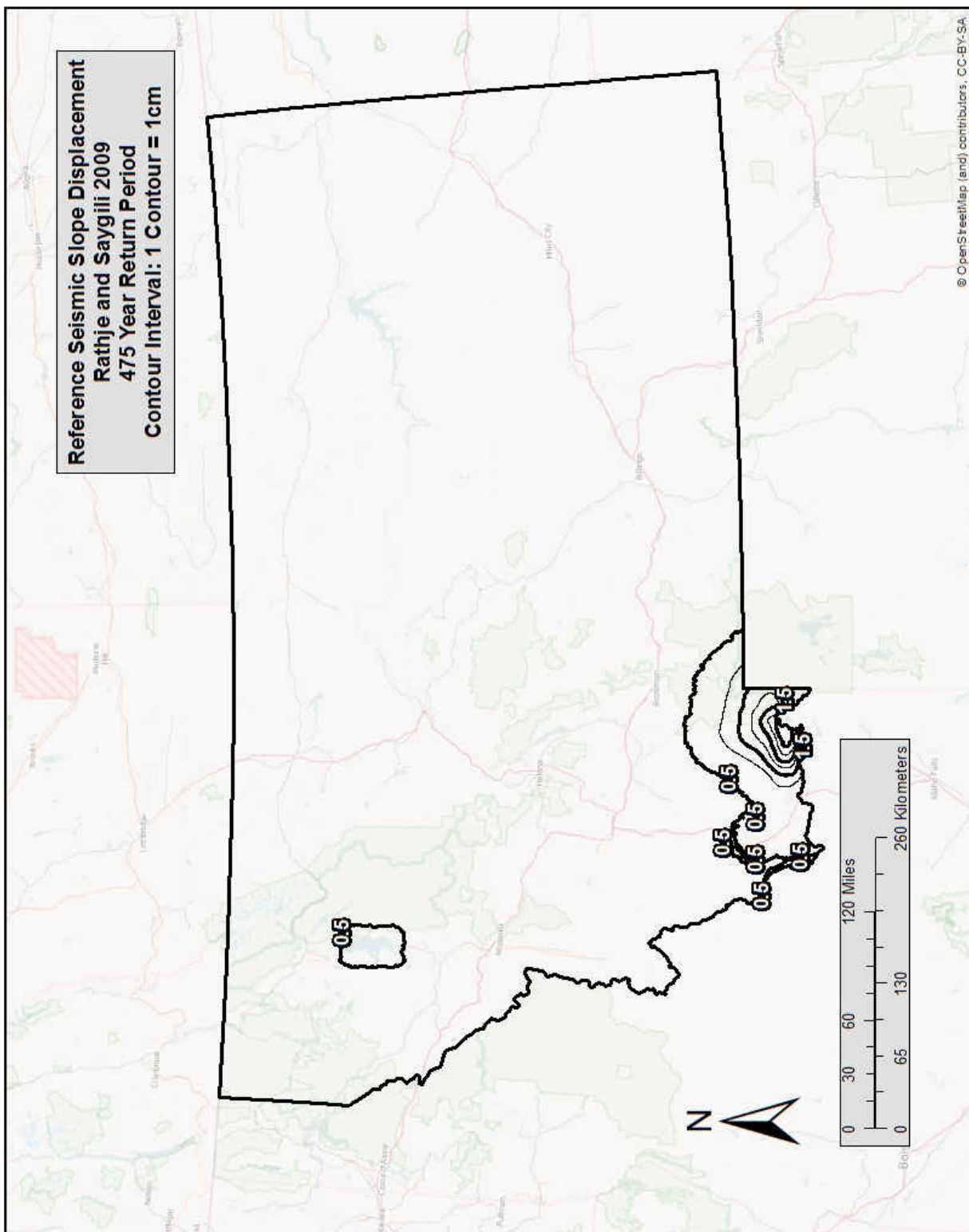


Figure C- 3 Seismic Slope Displacement (D^{ref}) Map for Montana (Tr = 475)

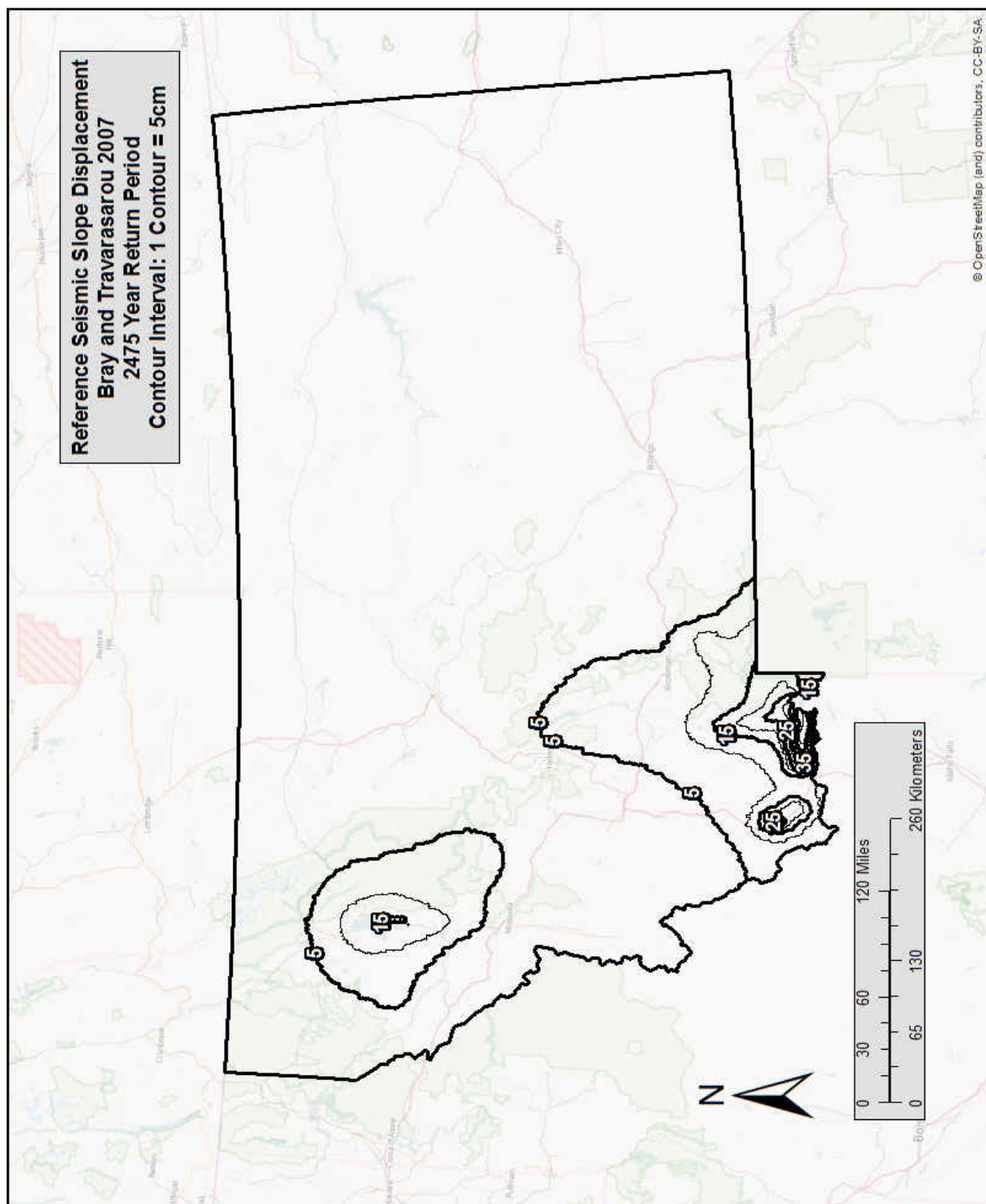


Figure C- 4 Seismic Slope Displacement (D^{ref}) Map for Montana (Tr = 2,475)

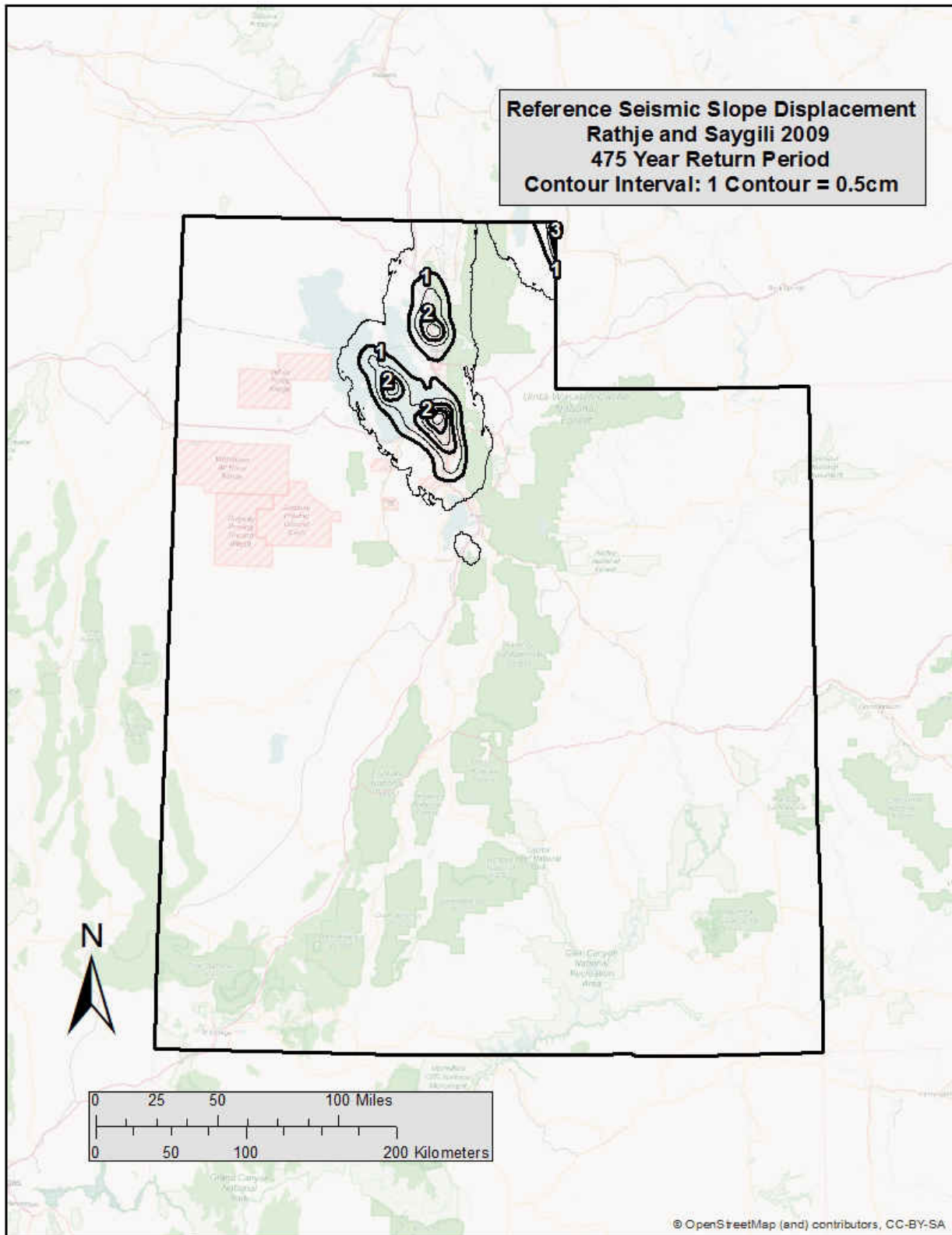
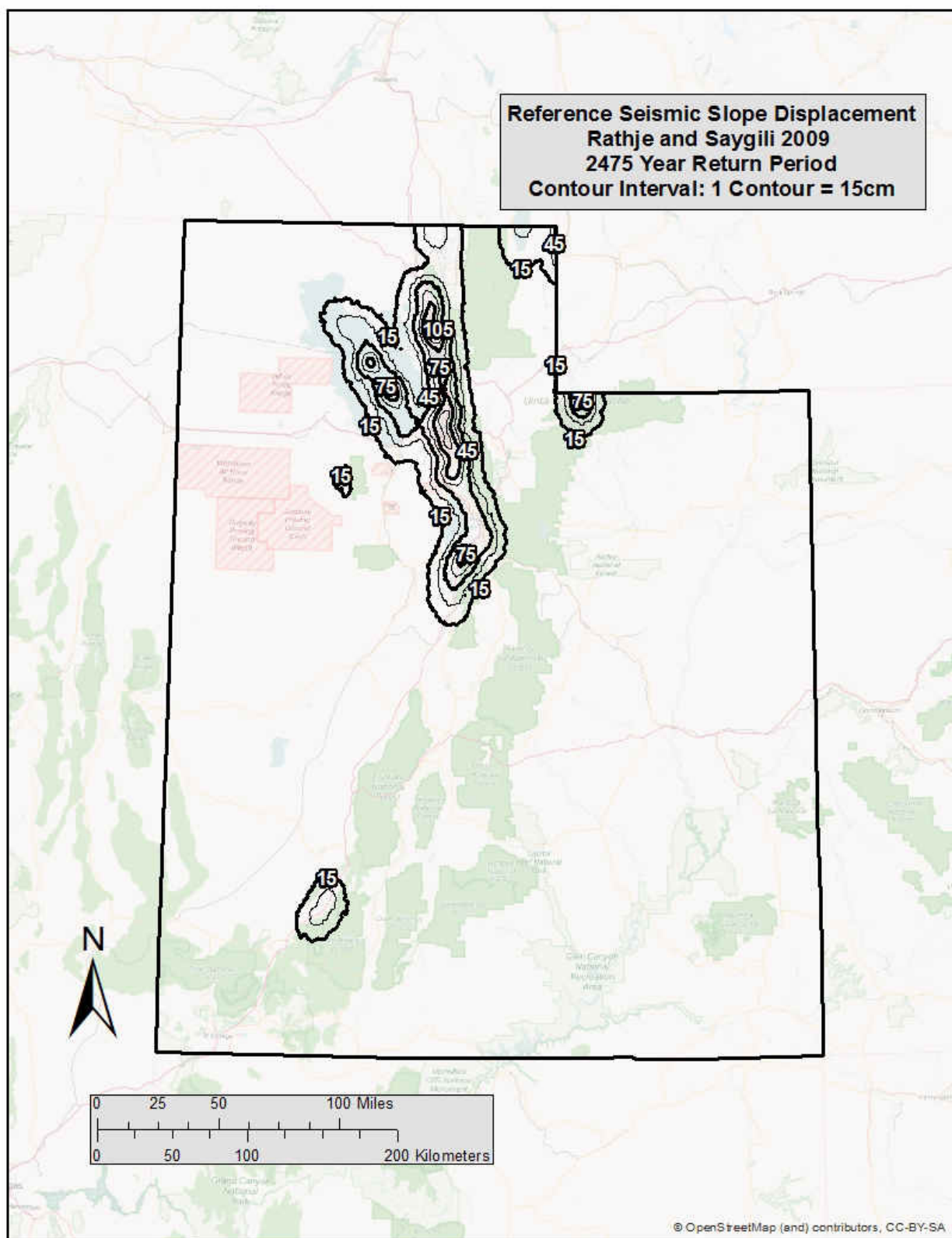


Figure C- 5 Seismic Slope Displacement (D^{ref}) Map for Utah ($Tr = 475$)



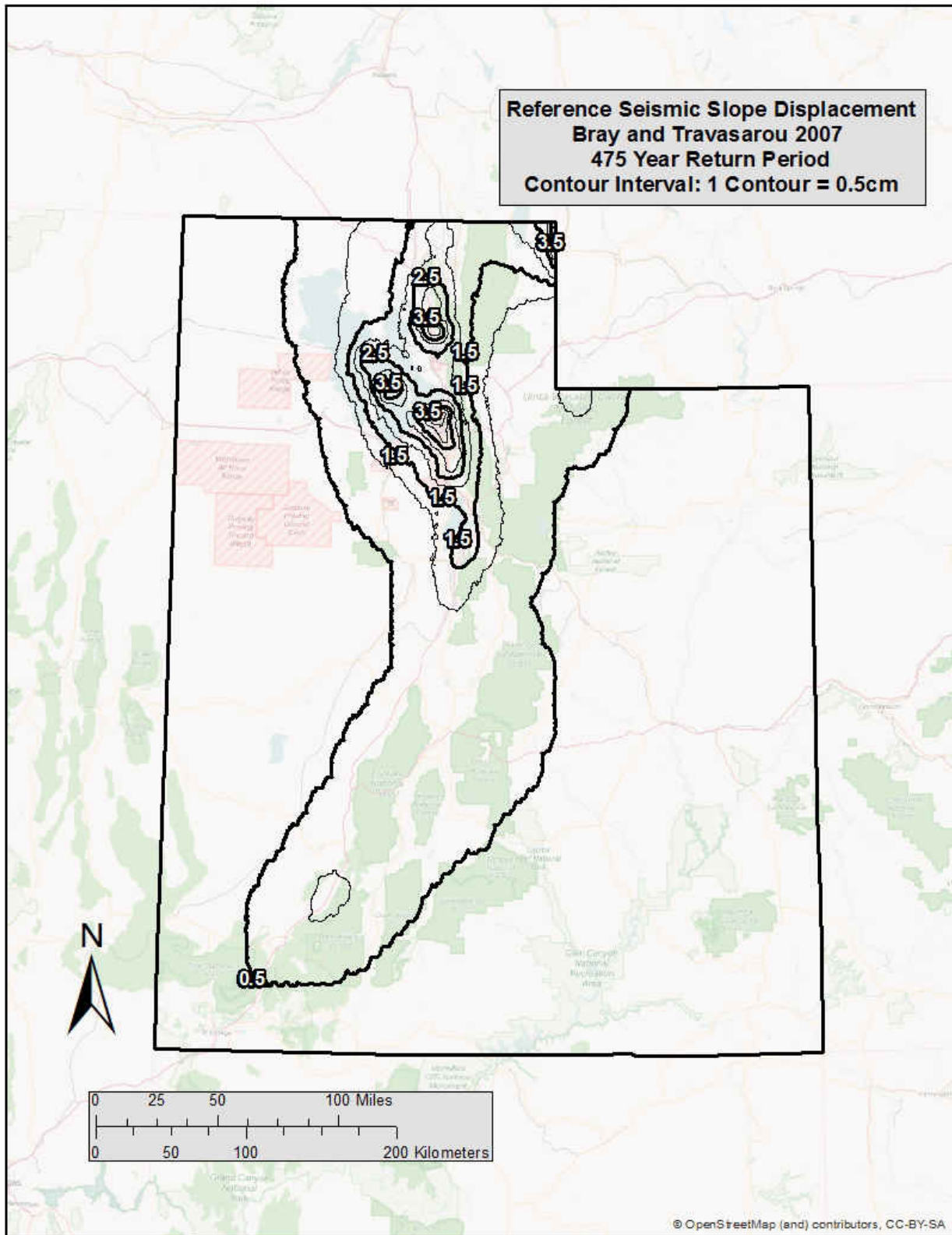


Figure C- 7 Seismic Slope Displacement (D^{ref}) Map for Utah ($Tr = 475$)

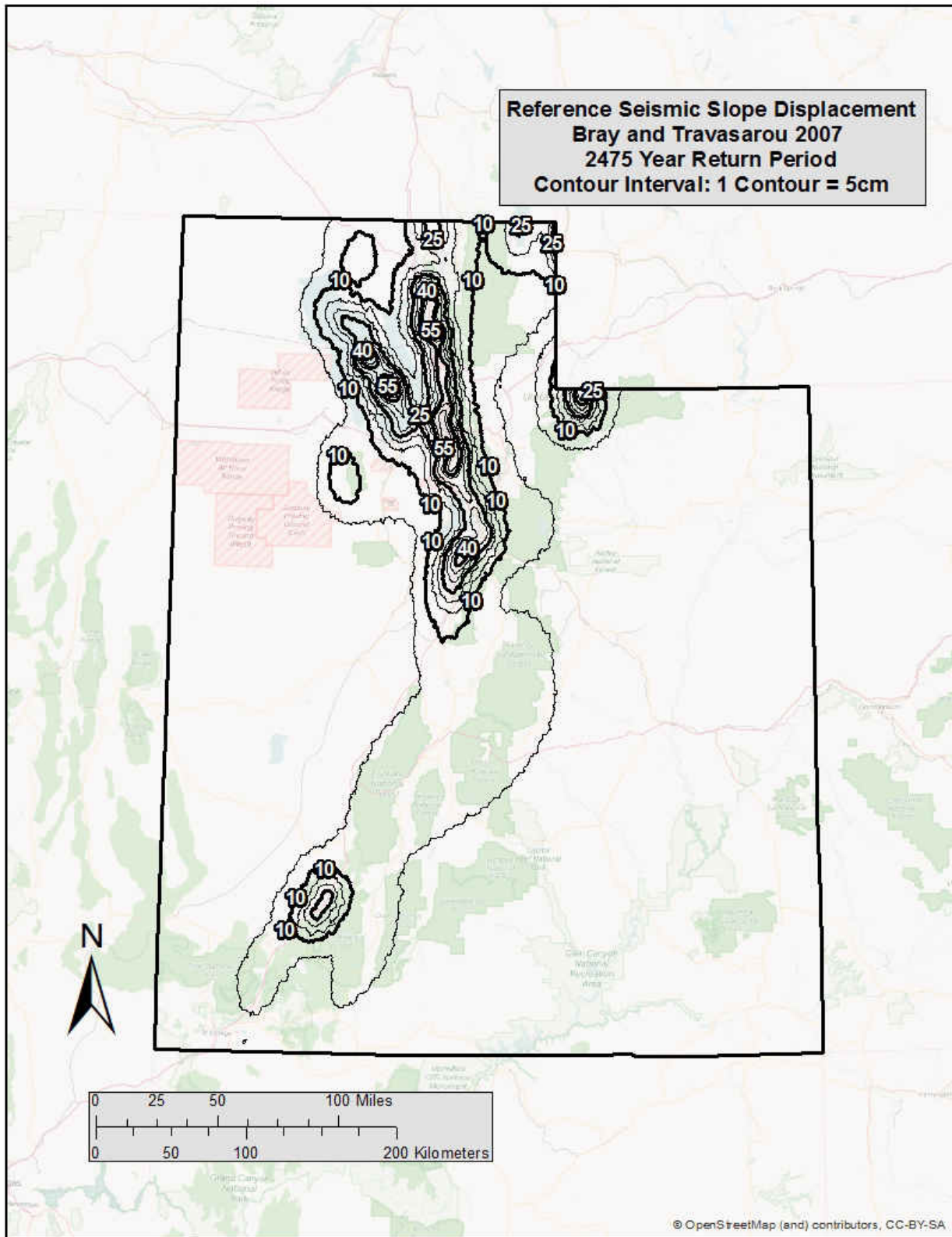


Figure C- 8 Seismic Slope Displacement (D^{ref}) Map for Utah ($Tr = 2,475$)

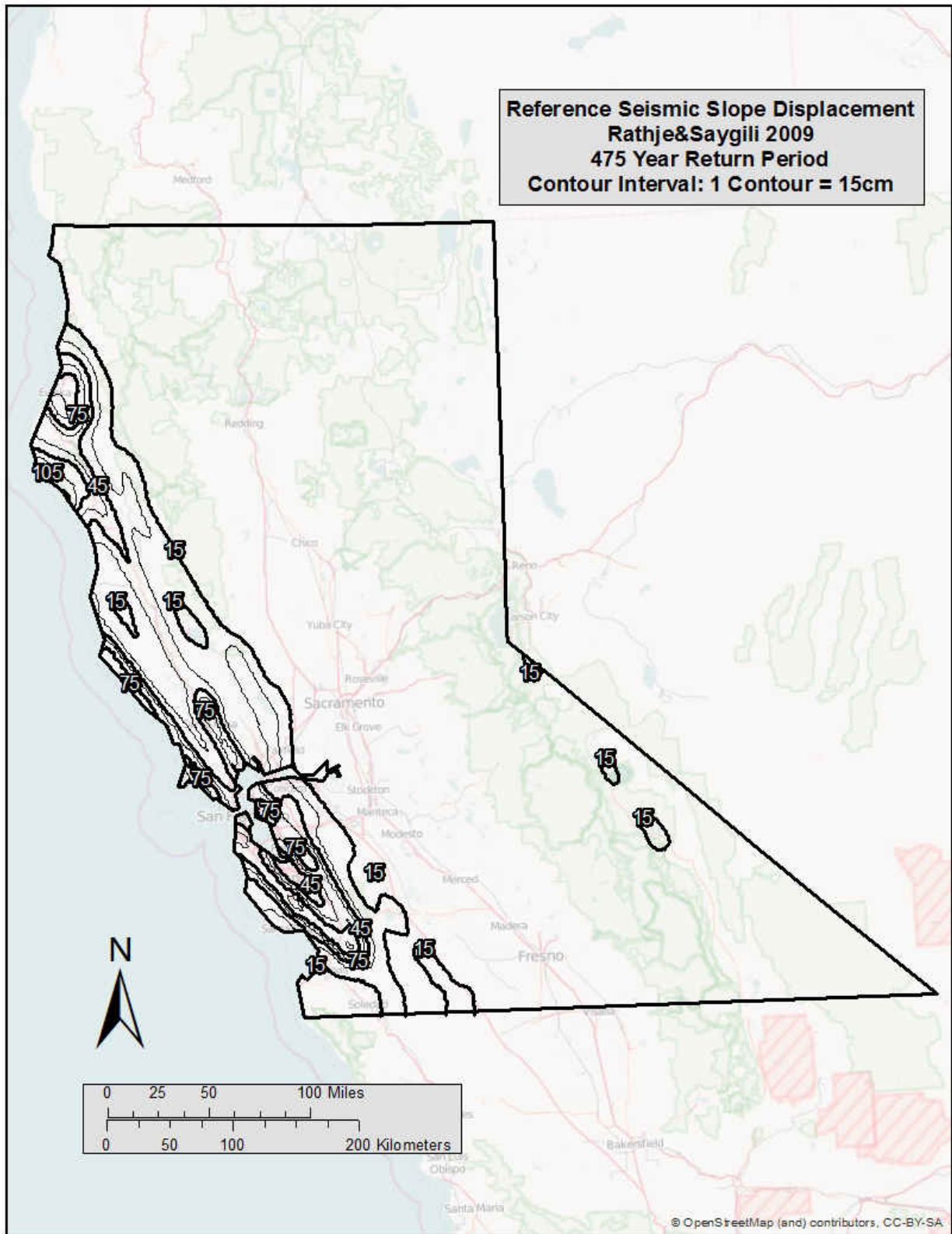


Figure C- 9 Seismic Slope Displacement (D^{ref}) Map for Northern California ($T_r = 475$)

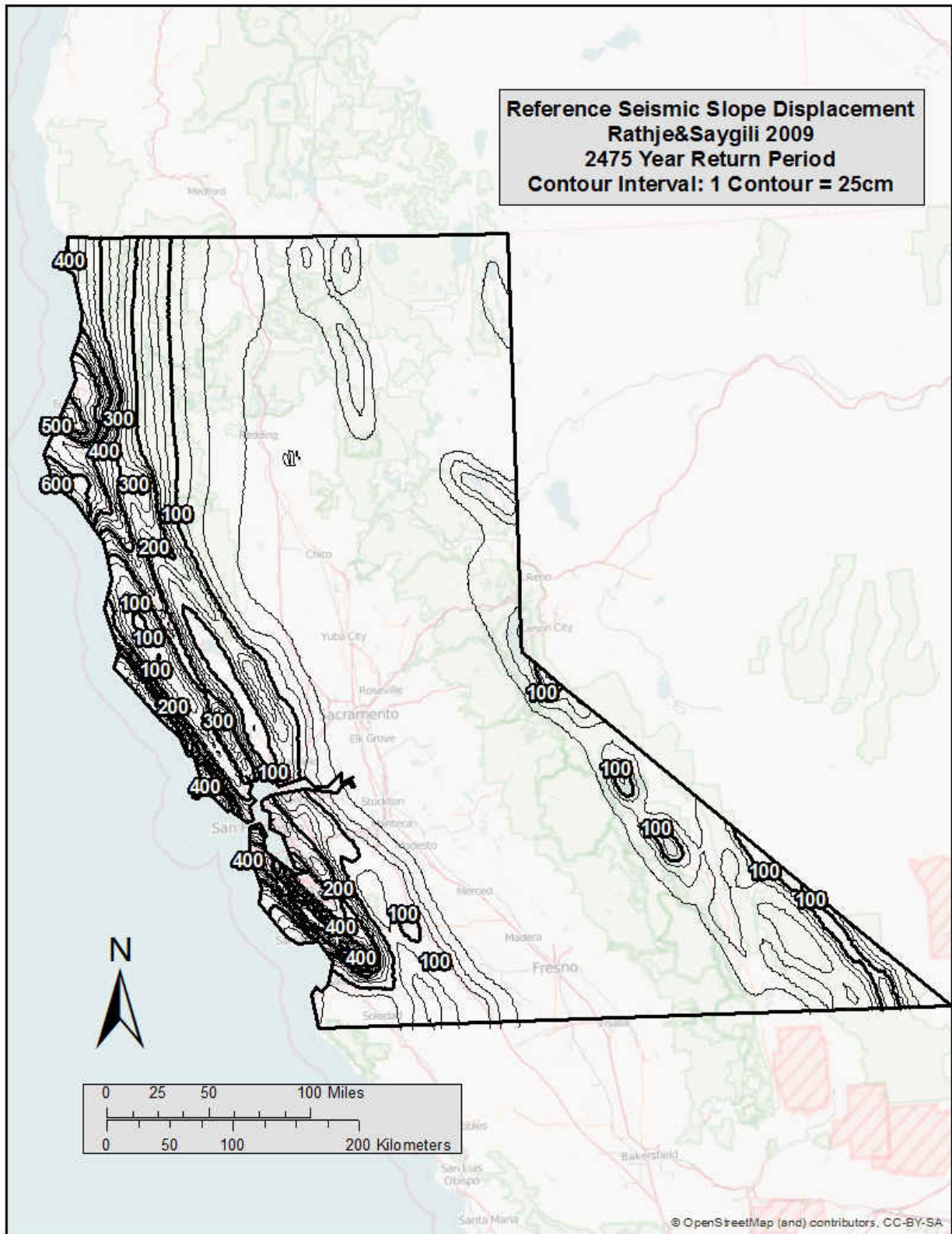


Figure C- 10 Seismic Slope Displacement (D^{ref}) Map for Northern California ($T_r = 2,475$)

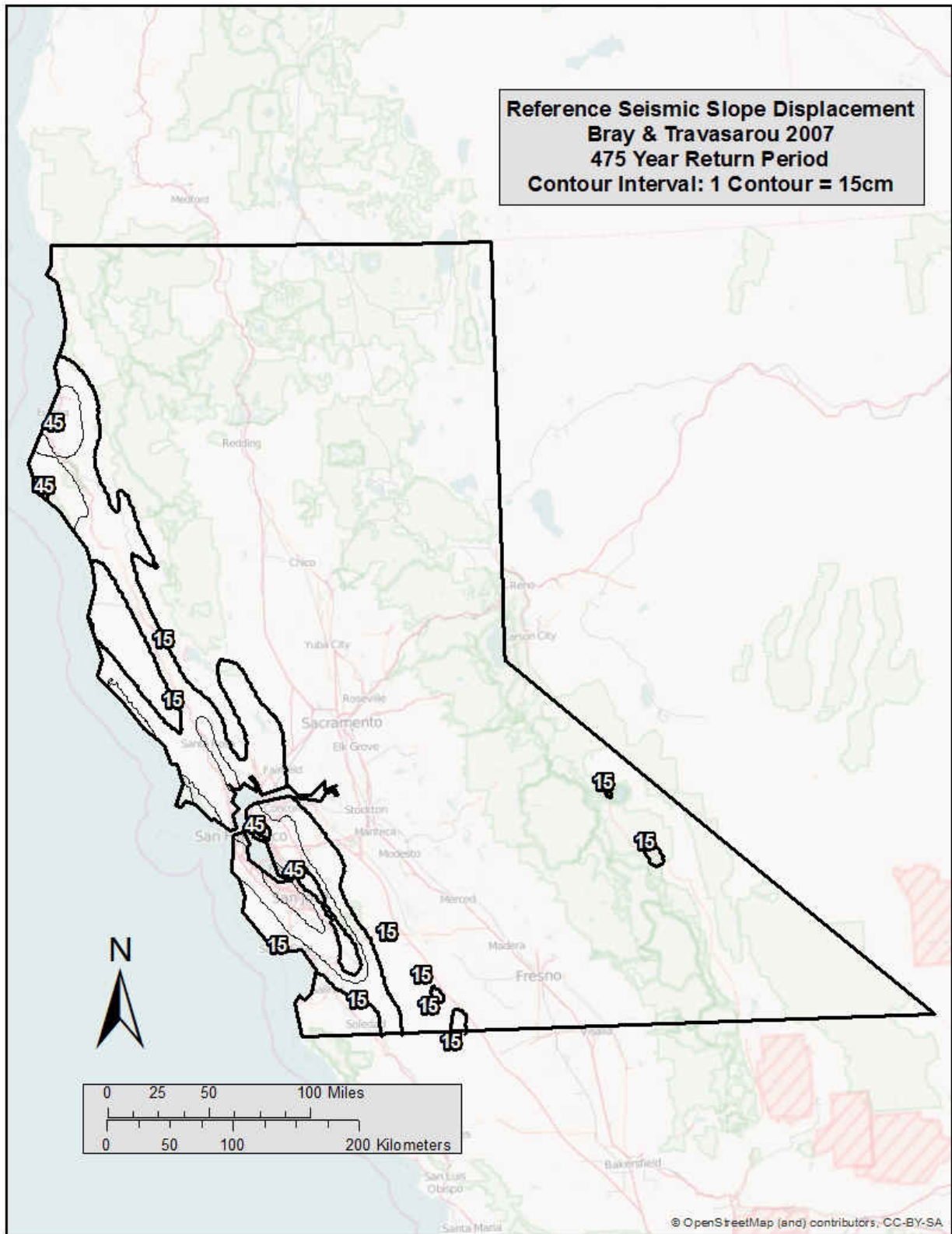


Figure C- 11 Seismic Slope Displacement (D^{ref}) Map for Northern California ($T_r = 475$)

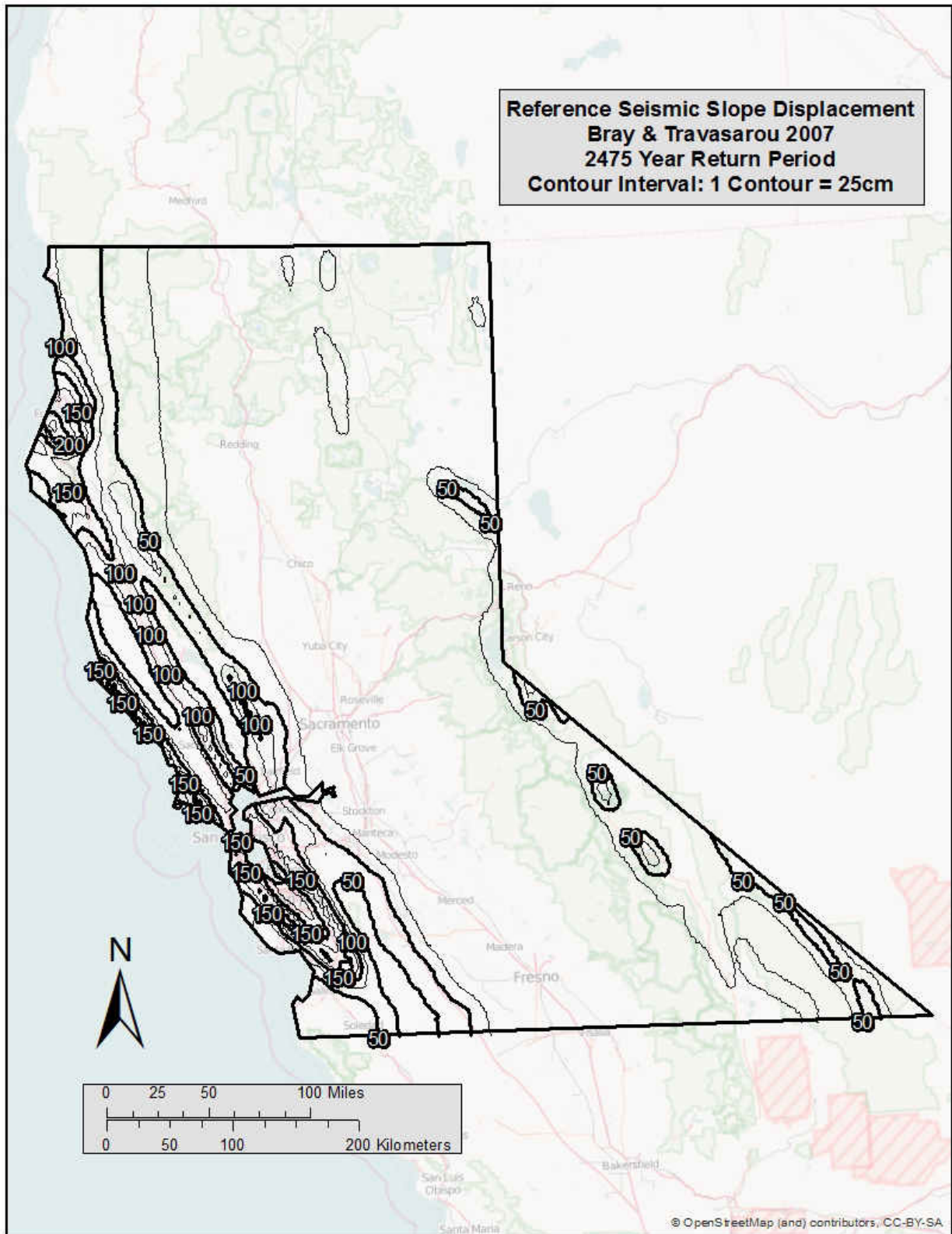


Figure C- 12 Seismic Slope Displacement (D^{ref}) Map for Northern California ($Tr = 2,475$)